PNNL-24683
RPT-IGTP-006 Rev 0

Pacific Northwest
NATIONAL LABORATORY
Proudly Operated by Battelle Since 1965

Technetium, Iodine, and Chromium Adsorption/Desorption K_d Values for Vadose Zone Pore Water, ILAW Glass, and Cast Stone Leachates Contacting an IDF Sand Sequence

GV Last
MMV Snyder
W Um
JR Stephenson
II Leavy
CE Strickland
DH Bacon
NP Qafoku
RJ Serne

November 2015

U.S. DEPARTMENT OF ENERGY

Prepared for the U.S. Department of Energy
under Contract DE-AC05-76RL01830

DISCLAIMER

PACIFIC NORTHWEST NATIONAL LABORATORY
operated by
BATTELLE
for the
UNITED STATES DEPARTMENT OF ENERGY
under Contract DE-AC05-76RL01830

Printed in the United States of America

Available to DOE and DOE contractors from the
Office of Scientific and Technical Information,
P.O. Box 62, Oak Ridge, TN 37831-0062;
ph: (865) 576-8401
fax: (865) 576-5728
email: reports@adonis.osti.gov

Available to the public from the National Technical Information Service
5301 Shawnee Rd., Alexandria, VA 22312
ph: (800) 553-NTIS (6847)
email: orders@ntis.gov <http://www.ntis.gov/about/form.aspx>
Online ordering: http://www.ntis.gov

This document was printed on recycled paper.
(8/2010)

PNNL-24683
RPT-IGTP-006 Rev 0

Technetium, Iodine, and Chromium Adsorption/Desorption K_d Values for Vadose Zone Pore Water, ILAW Glass, and Cast Stone Leachates Contacting an IDF Sand Sequence

GV Last
MMV Snyder
W Um
JR Stephenson
II Leavy
CE Strickland
DH Bacon
NP Qafoku
RJ Serne

November 2015

Prepared for
the U.S. Department of Energy
under Contract DE-AC05-76RL01830

Pacific Northwest National Laboratory
Richland, Washington 99352

Executive Summary

Performance and risk assessments of immobilized low-activity waste (ILAW) at the Integrated Disposal Facility (IDF) have shown that risks to groundwater are quite sensitive to adsorption-desorption interactions occurring in the near- and far-field environment. These interactions between the underlying sediments and the contaminants present in the leachates that descend from the buried glass, secondary waste grouts, and potentially Cast Stone low-activity waste packages have been represented in these assessments using the contaminant distribution coefficient (K_d) construct. Some contaminants (^{99}Tc, ^{129}I, and Cr) present in significant quantities in these wastes have low K_d values and tend to drive risk to public health and the environment. Small changes in the K_d value can cause relatively important changes in transport predictions. Thus, even small uncertainty in the K_d value can result in a relatively large uncertainty in the risk determined through performance assessment modeling.

The purpose of this study is to further reduce the uncertainty in K_d values for ^{99}Tc, iodine (iodide and iodate), and Cr (chromate; CrO_4^{2-}) by conducting systematic adsorption-desorption experiments using actual sand-dominated Hanford formation sediments from beneath the IDF and solutions that closely mimic Hanford vadose zone pore water and leachates from Cast Stone and ILAW glass waste forms.

A total of 24 batch and 16 flow-through column experiments were conducted, yielding 256 K_d measurements for these key contaminants, and contributing to our ability to predict transport from wastes disposed to the IDF. While the batch K_d methodology is not well-suited for measuring K_d values for non-sorbing species (as noted by the U.S. Environmental Protection Agency[1]), the batch K_d results presented here are not wholly inconsistent with the column K_d results, and could be used for sensitivity analyses. Results from the column experiments are consistent with the best estimate and lower range of K_d values reported by Krupka et al. and Cantrell et al.[2,3]

[1] U.S. Environmental Protection Agency. 1999. *Understanding Variation in Partition Coefficient, Kd, Values: Volume I. The Kd Model, Methods of Measurement, and Application of Chemical Reaction Codes.* EPA 402-R-99-004A, U.S. Environmental Protection Agency, Washington, D.C. Prepared by KM Krupka, DI Kaplan, G Whelan, RJ Serne, and SV Mattigod at Pacific Northwest National Laboratory, Richland, Washington.

[2] Krupka KM, RJ Serne, and DI Kaplan. 2004. *Geochemical Data Package for the 2005 Hanford Integrated Disposal Facility Performance Assessment*. PNNL-13037, Rev. 2, Pacific Northwest National Laboratory, Richland, Washington.

[3] Cantrell KJ, JM Zachara, PE Dresel, KM Krupka, and RJ Serne. 2007. *Geochemical Processes Data Package for the Vadose Zone in the Single-Shell Tank Waste Management Areas at the Hanford Site*. PNNL-16663, Pacific Northwest National Laboratory, Richland, Washington.

Acronyms and Abbreviations

BFS	blast furnace slag
BGS	below ground surface
BTC	breakthrough curve
DOE	U.S. Department of Energy
EDS	energy dispersive spectroscopy
eSTOMP	Subsurface Transport Over Multiple Phases (parallel computing version of computer model, designated by "e")
IC	ion chromatography
ICP-MS	inductively coupled plasma-mass spectrometry
ICP-OES	inductively coupled plasma-optical emission spectroscopy
IDF	Integrated Disposal Facility
ILAW	immobilized low-activity waste
K_d	distribution (or partition) coefficient
LAW	low-activity waste
LOI	loss-on-ignition
NIST	National Institute of Standards and Technology
NQA-1	nuclear quality assurance standard published by the American Society of Mechanical Engineers (ASME)
PA	performance assessment
PNNL	Pacific Northwest National Laboratory
PTFE	polytetrafluoroethylene
QA	quality assurance
R&D	research and development
SEM	scanning electron microscopy
SST	single-shell tank
WMA	waste management area
WRPS	Washington River Protection Solutions
WTP	Waste Treatment and Immobilization Plant
WWFTP	WRPS Waste Form Testing Program

Units of Measure

Bar	a unit of pressure equal to 100000 pascal
Bq/L	becquerels per liter
°C	temperature in degrees Celsius
cm	centimeter
d	day
ft	foot
g	gram
g/mol	grams per mole
keV	thousands of electronvolts
L	liter
m	meter
M	molarity, mole/liter
m^2/g	square meters per gram
mCi/mL	millicuries per milliliter
meq	milliequivalents
mg	milligram
mg/L	milligrams per liter
mL	milliliter
mL/g	milliliters per gram
mm	millimeter
mM	millimole
mol	mole
mol/L	moles per liter
mS/cm	millisievert
mV	millivolt
pCi/mL	picocuries per milliliter
pH	the logarithm of the reciprocal of hydrogen ion concentration in gram atoms per liter, used to express the acidity or alkalinity of a solution on a scale of 0 to 14, where less than 7 represents acidity, 7 neutrality, and more than 7 alkalinity
ppb	parts per billion
ppm	parts per million
s	second
S	siemens
wt%	weight percent
µ	micro (prefix, 10^{-6})
µg/g	micrograms per gram

µg/L	micrograms per liter
µg/mL	micrograms per milliliter
µm	micrometer
µS/cm	microsieverts per centimeter

Acknowledgements

The authors thank Dave Swanberg at Washington River Protection Solutions for project funding and programmatic guidance.

The authors are especially indebted to Dr. Kirk Cantrell, who developed the scope of work, Test Plans, and Test Instructions and led this work throughout fiscal years 2014 and 2015 up until his retirement in May 2015.

We would also like to thank Steven Baum, Ray Clayton, Cristian Iovin, Eirik Krogstad, and Odeta Qafoku for their contributions to the laboratory and analytical work; Keith Geiszler, Amanda Lawter, Ben Williams, and Renee Russell for data reviews; Jim Neeway, Gary Smith, and Bill Dey for their independent technical reviews; and Matt Wilburn for editorial review and document production.

Contents

Figures

Tables

1.0 Introduction

The Hanford Site, in south-central Washington State, holds approximately 56 million gallons of radioactive waste in 177 underground storage tanks generated by over four decades of nuclear fuel processing to produce plutonium for the nation's nuclear weapons arsenal. The U.S. Department of Energy (DOE) is proceeding with plans to retrieve the waste from the tanks, separate the low-activity waste (LAW) fraction from the high-level waste fraction, and immobilize both fractions separately in glass, in preparation for final disposal.

The relatively small volume of immobilized high-level waste will be stored on the Hanford Site until a federal geologic repository is selected for final disposal. However, the much larger volume of immobilized low-activity waste (ILAW) glass will be buried in a near-surface disposal system, known as the Integrated Disposal Facility (IDF), in the 200 East Area. It is projected that over 200,000 m^3 (7 million ft^3) of waste with significant inventory of long-lived radionuclides will be disposed in the IDF.

The variety of wastes planned for disposal in the IDF is documented in the *Final Tank Closure and Waste Management Environmental Impact Statement for the Hanford Site* (DOE 2012). This includes ILAW glass, secondary wastes (e.g., Cast Stone), wastes generated during Tank Farm operations to retrieve and deliver the waste to the Hanford Waste Treatment and Immobilization Plant (WTP), and other Hanford wastes such as immobilized waste (grout) from the Effluent Treatment Facility and spent melters from the WTP.

Prior to receiving a disposal authorization statement, DOE must prepare a performance assessment (PA) for the IDF (DOE O 435.1; DOE M 435.1-1). The PA provides key information for development of specific waste acceptance criteria for the IDF and a waste incidental to reprocessing determination for the ILAW. The IDF PA must be a rigorous analysis using best available data and appropriate tools (computational models) to demonstrate that performance standards for the disposal facility will be met over the period of compliance, considering all agreed-upon exposure scenarios. The IDF PA will undergo review by the Low-Level Waste Federal Review Group and the U.S. Nuclear Regulatory Commission.

Past ILAW and IDF facility performance and risk assessments (Mann et al. 1998, 2001, 2003a, 2003b; and the 2005 IDF PA, which was drafted but not released) have shown that risks to groundwater are quite sensitive to adsorption-desorption interactions. Adsorption-desorption interactions between the underlying sediments and the contaminants present in the leachates that descend from the buried glass, secondary waste grout, and potentially Cast Stone waste packages containing solidified LAW are often represented in these assessments using the contaminant distribution coefficient (K_d) construct.[1]

[1] The K_d parameter, is assumed to represent a reversible and equilibrium ratio of the mass of a contaminant bound to the solid geomedia (e.g., sediment) divided by the equilibrium concentration of the contaminant in the solution (e.g., pore water) in contact with the geomedia. The K_d parameter has units of volume/mass, typically mL/g. The classical (and rigorous) usage of the K_d parameter requires that the sorbing constituent be at such low concentrations that the adsorption isotherm is linear and reversible and that the system is at equilibrium (steady state conditions for the amount of constituent in solution and adsorbed onto the solid). In reality, the K_d values generated in laboratory experiments are empirical ratios of the amount of contaminant associated with the solid phase of interest (per gram) divided by concentration (mass/mL) of the contaminant in the associated solution at some contact time that hopefully represents enough time to approach equilibrium. For more information, see EPA (1999).

Several contaminants present in significant quantities in wastes that will be disposed at the IDF adsorb relatively weakly to sediments under typical Hanford environmental conditions and thus have been assigned relatively low K_d values. These contaminants (^{99}Tc, ^{129}I, and Cr) tend to drive risk to public health and the environment. For contaminants with low K_d values, small changes in the K_d value can cause relatively large changes in the retardation factor. This means that a small uncertainty in the K_d value can result in a relatively large uncertainty in the risk determined through PA modeling.

Additionally, past K_d measurements for iodine (I) on Hanford sediments were made using I only in the form of iodide (I^-). This is because I^- is thought to be the thermodynamically stable form of I in Hanford groundwater. However, Xu et al. (2014) recently found that I occurs predominantly as iodate species (IO_3^-) in Hanford groundwater, suggesting that the thermodynamic data are incorrect or that the Hanford subsurface is not at equilibrium for I. Regardless, these findings suggest that additional adsorption studies are needed for the iodate species interacting with the sediments surrounding and below the buried waste forms.

1.1 Purpose

The purpose of this study is to reduce the uncertainty in the K_d values for key contaminants of concern, ^{99}Tc, iodine (iodide and iodate), and Cr (chromate; CrO_4^{2-}), by conducting systematic adsorption-desorption experiments using actual IDF sediments and solutions that closely mimic Hanford vadose zone pore water and leachates from Cast Stone and ILAW glass waste forms.

1.2 Objective

The objective of this study is to develop a set of adsorption/desorption K_d values for Tc as $^{99}TcO_4^-$, iodine as both I^- and IO_3^-, and Cr as CrO_4^{2-} under conditions relevant to sand-dominated Hanford formation sediments beneath the IDF, using simulated ILAW glass and Cast Stone leachates, and uncontaminated vadose zone pore water. The adsorption/desorption data presented in this report do not apply to the waste form environment itself. Contaminant release data from the waste forms themselves (LAW glass, supplemental Cast Stone, and cement-encapsulated secondary wastes and engineered waste packages) are being developed and documented in separate waste form data packages, which may or may not use the K_d construct to quantify contaminant release.

1.3 Report Contents and Organization

This report is organized into six sections. Section 1 describes the purpose and key objective of the sorption-desorption experiments conducted for this study. Section 2 reviews past IDF-relevant laboratory sorption-desorption testing and past geochemical data tabulations used for Hanford Site PAs and risk assessments. Section 3 describes the methods and materials used in the sorption-desorption experiments and Section 4 presents the results. Section 5 summarizes the key K_d measurement results and discusses their implications. Section 6 provides a list of references cited throughout the report.

1.4 Quality Assurance

This work was conducted with funding from Washington River Protection Solutions (WRPS) under contract 36437-161, *ILAW Glass Testing for Disposal at IDF*. The work was conducted as part of Pacific Northwest National Laboratory (PNNL) Project 66309, ILAW Glass Testing for Disposal at IDF.

All research and development (R&D) work at PNNL is performed in accordance with PNNL's laboratory-level Quality Management Program, which is based on a graded application of NQA-1-2000, *Quality Assurance Requirements for Nuclear Facility Applications*, to R&D activities. In addition to the PNNL-wide quality assurance (QA) controls, the QA controls of the WRPS Waste Form Testing Program (WWFTP) QA program were also implemented for the work. The WWFTP QA program consists of the WWFTP Quality Assurance Plan (QA-WWFTP-001) and associated QA-NSLW-numbered procedures that provide detailed instructions for implementing NQA-1 requirements for R&D work. The WWFTP QA program is based on the requirements of NQA-1-2008, *Quality Assurance Requirements for Nuclear Facility Applications*, and NQA-1a-2009, *Addenda to ASME NQA-1-2008 Quality Assurance Requirements for Nuclear Facility Applications*, graded on the approach presented in NQA-1-2008, Part IV, Subpart 4.2, "Guidance on Graded Application of Quality Assurance (QA) for Nuclear-Related Research and Development."

Performance of the FY 2015 sorption/desorption tests and preparation of this report were assigned the technology level "Applied Research" and were conducted in accordance with procedure QA-NSLW-1102, *Scientific Investigation for Applied Research*. All staff members contributing to the work have technical expertise in the subject matter and received QA training prior to performing quality-affecting work. The Applied Research technology level provides adequate controls to ensure that the activities were performed correctly. Use of both the PNNL-wide and WWFTP QA controls ensured that all client QA expectations were addressed in performing the work.

2.0 Background

Understanding the interactions among components released from the waste forms disposed in the IDF, the disposal system components, and the near-field natural environment is key to understanding the fate and transport of risk-driving contaminants and developing a scientifically defensible K_d data set for the IDF PA.

2.1 Conceptual Model of Vadose Zone Transport

Last et al. (2006) present an overview of the conceptual understanding of the geologic, hydraulic, and geochemical controls on contaminant movement through the vadose zone at the Hanford Site, and some of the approaches for representing these controls in numerical assessments. The previous IDF and ILAW as well as most other performance and risks assessments on the Hanford Site have approximated the interaction between dissolved contaminants and vadose zone sediment using the linear sorption isotherm model, represented by contaminant distribution coefficients (K_d). These sorption-desorption parameters can be used to quantitate the interactions of dissolved risk-driving contaminants with the near-field disposal system components (waste forms, corroded canisters, other leachates, backfill, liners, etc.) and subsurface Hanford Site sediments (both in the vadose zone and aquifer).

2.2 Previous Studies

Sorption-desorption parameters to support the ILAW and IDF PAs have been the subject of numerous previous studies since 1995. These studies (summarized in the following sections) were conducted to improve the technical defensibility of the PAs for the disposal of wastes in the IDF.

2.2.1 Distribution Coefficient Values Describing Iodine, Neptunium, Selenium, Technetium, and Uranium Sorption to Hanford Sediments

The first study directly related to assembling geochemical information, especially K_d values, to support ILAW/IDF PAs was documented by Kaplan and Serne (1995). That study provided 1) a review of the key geochemical processes affecting radionuclide migration through the near- and far-field at the proposed Hanford ILAW disposal facility, now called the IDF; 2) a summary of available information and data on geochemical interactions between Hanford subsurface waters, Hanford sediments, and radionuclides; 3) a strategy and rationale for generating additional data; and 4) recommendations on data collection methods. Particular attention was directed at understanding the important factors for unsaturated, alkaline, high carbonate, low organic matter subsurface environments, typical of the Hanford Site for the radionuclides I, Np, Se, Tc, and U (the five radionuclides thought at the time to be the greatest risk drivers for the groundwater pathway).

The K_d tabulation in Kaplan and Serne (1995) used available Hanford Site-specific data where available and suggested that the range in K_d values for iodine was 0.04 to 18 mL/g and for technetium the range was 0 to 1.3 mL/g for solutions with compositions similar to groundwater or dilute liquid wastes with near-neutral pH. Based on the Hanford Site data, albeit not for sediments or solutions directly relevant to the IDF site, Kaplan and Serne (1995) recommended that the most probable range in K_d values for both iodine and technetium would be 0 to 0.8 mL/g. They further suggested that the very limited

amount of available Hanford Site-specific flow-through column sorption tests showed negligible to negative adsorption (anion exclusion) for technetium and two of the available column test breakthrough results (Gee and Campbell 1980) calculated iodine K_d values of 0.04 and 0.06 mL/g for solutions spiked with 20 ppb stable iodide and carrier-free ^{125}I. When only carrier-free ^{125}I was present in the simulated groundwaters, ^{125}I in the effluents never reached a $C/C_{(0)}$ value of 0.5, the "breakthrough" value used to calculate K_d values. Further, Gee and Campbell (1980) found that iodide batch K_d values for sorption onto a Hanford Site surface sediment (< 2 mm size fraction used) dominated by sand was quite sensitive to the starting iodide concentration spiked into simulated groundwaters. When carrier-free ^{125}I alone (at 2 pCi/mL) was spiked into the groundwaters, the observed K_d values after 7-d contact periods and a 30:1 solution-to-sediment ratio ranged from 4 to 18 mL/g. The carrier-free ^{125}I was quantified by gamma counting the 27 keV X-ray using a 5-in NaI well detector. Based on the vendor's specifications of the ^{125}I being carrier free, the iodide mass concentration of this 2 pCi/mL solution was only 2 parts per trillion. When a small amount of stable iodide in the range of 5 to 20 parts per billion (µg/L) was added along with the carrier-free ^{125}I to the simulated groundwaters, the iodide K_d values decreased to 0.05 to 0.08 mL/g. Both the batch and column results for ^{125}I suggest the "massless" carrier-free data are biased by some loss of activity from the solution phase during contact with sediments that is not occurring when small concentrations of stable iodide are also present.

Kaplan and Serne (1995) particularly noted that anion exclusion could make anionic species such as iodide, iodate, and pertechnetate travel through the subsurface at a rate slightly greater than the water advecting through the sediments. In the only unsaturated flow-through column study using Hanford Site sediments and groundwater (Gee and Campbell 1980), pertechnetate exhibited breakthrough (C/C_0 =0.5) at 0.95 pore volumes compared to the conservative tracer, tritium, which showed a breakthrough at 1.02 pore volumes. Thus, pertechnetate may have travelled through the sediment column 5% faster than tritium.

A principal recommendation in Kaplan and Serne 1995 was to use laboratory-scale flow-through column breakthrough adsorption testing to best evaluate the migration of low-adsorbing radionuclides rather than batch K_d methods. They also discuss other geochemical reactions (e.g., solubility-precipitation, colloid facilitated migration, and redox) that impact contaminant migration in the subsurface and acknowledge that empirical batch and flow-through column breakthrough tests are too empirically based to elucidate all potential controlling mechanisms. Empirical approaches such as these two were defended by Kaplan and Serne (1995) because they felt that 1) mechanistic studies could not be completed in a realistic time frame for all key contaminants given time and resource constraints and 2) the empirically derived K_d data could be easily accommodated in the computer PA codes available at the time.

2.2.2 Radionuclide Adsorption Distribution Coefficients Measured in Hanford Sediments for the Low-Level Waste Performance Assessment Project

Kaplan et al. (1996) described the results of batch adsorption tests using Hanford Site sediments. At the time, IDF site-specific sediments were not available. Three Hanford formation sediments from 200 West Area and one from 200 East Area were used in the tests. The test solution consisted of uncontaminated groundwater from well 699-S3-25 spiked with contaminants of interest. The batch K_d tests used a solution-to-sediment ratio of 2 mL to 1 g. The sediments were pre-equilibrated at least three times with unspiked groundwater until the pH was stable at the groundwater's natural value. A fresh

aliquot of contaminant-spiked groundwater was then contacted with the sediment for up to 1 month. In separate tests for each of the four sediments (using the < 2 mm size fraction), individual contaminants were spiked into aliquots of the groundwater. Carrier-free ^{125}I and ^{99}Tc were among the contaminants studied. After centrifugation and filtration, the contaminants in the filtrate were measured using liquid scintillation counting (LSC) and compared with control samples (spiked groundwater only). Other control samples were sediment in contact with unspiked groundwater to make sure no "contaminants" leached out of the sediments (this was only relevant for uranium studies).

The ^{99}Tc batch studies were conducted with spiked groundwater concentrations of 0.3 to 100 μCi/L (0.02 to 5.9 ppm mass concentration). Contact time was fixed at 30 days. For the sediment most similar to the sand-dominated IDF sediments, the observed K_d did not vary with starting Tc concentration. The average ^{99}Tc K_d was -0.02 ± 0.05 mL/g. For the groundwater spiked with 100 μCi/L ^{99}Tc, the K_d as a function of contact time slowly increased from -0.18 to +0.11 mL/g as contact time increased from 7 to 398 days. Kaplan et al. (1996) concluded that 1) a small degree of anion exclusion occurred in the batch tests, creating the slightly negative K_d values (on the order of -0.1 mL/g), and thus such negative K_d values are not solely the result of experimental error; and 2) the ^{99}Tc K_d values appear to increase with long contact times such that the best estimate for future IDF PA predictions should use 0 ± 0.1 mL/g values.

Iodide batch K_d tests were performed with the groundwater spiked with 100 uCi/L carrier-free ^{125}I (90 ppb mass concentration) and with contact times varying from 7 to ~340 days. Key conclusions were that 1) iodide did absorb to the sediments; and 2) the amount of iodide that sorbed (or at least was no longer found in solution) increased with time. The mean iodide K_d value for the batch tests using three sediments for the four contact times of 7, 200, ~265, and ~340 days was 3.8 ± 1.0 mL/g with a range of 0.07 to 9.8 mL/g. The process that caused the increased K_d with contact time was not known, but it was speculated that the cause could have been microbiological activity in the long-term batch tests. A similar hypothesis had been offered in Gee and Campbell (1980) for flow-through column tests that had sediment-packed columns used repeatedly after loading pulses of spiked simulated groundwater followed by flushing until no contaminant was present. Then a different contaminant was spiked into synthetic groundwater and a pulse (several pore volumes) was loaded and then flushed with unspiked solution. By the end of several months of testing there were visual signs of organic matter staining on the sides of the column walls.

Kaplan et al. (1996) suggested that because the iodide K_d clearly increased with contact time and because contact times for leachates from the waste forms disposed in the IDF with Hanford formation sediments would be long, that past iodide adsorption tests using at most a 30-day contact time might underestimate iodide sorption. Thus, they recommended an iodide K_d equal to 3 mL/g.

In retrospect, we now question whether the use of carrier-free ^{125}I with infinitesimal mass might have led to loss of ^{125}I by volatilization. As noted by Gee and Campbell (1980), when 5 to 20 ppb of stable iodide was added along with the carrier-free ^{125}I, ^{125}I adsorption was dramatically reduced. The calculated mass of iodide in carrier-free ^{125}I present at the start of the batch testing at 100 uCi/L is 90 ppb, but after 360 days of decay (6 half lives) in the long-term batch experiments would be only 1.4 ppb. Thus, perhaps the use of carrier-free ^{125}I without any stable iodide mass was causing artifacts in the iodide adsorption tests where only ^{125}I was present.

2.2.3 Effects of High pH and High Ionic Strength Groundwater on Iodide, Pertechnetate, and Selenite Sorption to Hanford Sediments

It is expected that the leachate from the glass waste forms and supplemental waste grout used for the ILAW will have high-pH and high ionic-strength properties. Thus, Kaplan et al. (1998a) performed batch sorption experiments on a Hanford sediment contacted with groundwater that had ionic strength and pH varied in separate tests. Generally, as the ionic strength increases, adsorption of cationic and anionic contaminants decreases because there is greater competition for adsorption sites and the activity of the sorbed species decreases. However, high ionic strengths can occasionally have the opposite effect (i.e., as the ionic strength increases, solute interactions with the solid phase also increase [Stumm and Morgan 1981]). Kaplan et al. (1998a) found that selenium and technetium K_d values increased as ionic strength increased. This most likely occurred because the higher ionic strength caused the double layer around the sediment particles to collapse, permitting greater interaction between anions in solution with the charged mineral surfaces, and decreasing anion exclusion from the mineral surfaces.

Kaplan et al. (1998a) conducted their batch sorption experiments with a 200 Area sediment (from trench AE-3) that was previously characterized (Kaplan et al. 1996). Trench AE-3 sediment has the texture of a silty loam. The mineralogy of the clay-size fraction is dominated by smectite, illite, and vermiculite. X-ray diffraction analysis of the samples revealed that the carbonate phase was dominated by calcite. The hydrous iron oxide concentration of this sediment was between 0.2% to 0.5% (wt) amorphous Fe_2O_3. The groundwater was taken from well 699-S3-25 and was then augmented with NaOH for the pH tests and $NaClO_4$ additions for the ionic-strength experiments. The NaOH additions in the pH experiment were expected to change the ionic strength and pH of the solutions, whereas the $NaC1O_4$ additions were expected to change only the ionic strength, not the pH, of the solutions. The pH effects tests measured K_d values for pertechnetate, iodide, and selenate. The ionic strength tests measured K_d values for pertechnetate and selenite. The effect of $NaC1O_4$ concentration on I^- adsorption was not evaluated because ClO_4 would oxidize the I^- to iodate.

Analysis for ^{99}Tc was by LSC, using a quench-calibrated Wallac®141 5 LSC and Packard® Opti-fluorm LSC cocktail. Analyses for ^{75}Se and ^{125}I were by gamma energy analysis using a Wallac 1480 Wizard 3-in. NaI automatic gamma detector.

The sediment was first pre-equilibrated with the uncontaminated groundwater. This was accomplished by adding groundwater to the sediments, shaking the suspensions overnight, centrifuging, pouring off the supernatant, and then measuring the pH of the supernatant. This was repeated until the pH of the groundwater did not change before and after contact with the sediment, usually three washes.

Radionuclide spikes were added to uncontaminated Hanford Site groundwater and then the spiked groundwaters were placed on a platform shaker for 7 days, a period selected to ensure that steady-state conditions were achieved. These solutions were then passed through a 0.20-µm filter, and the filtrates were analyzed for pH, electrical conductivity, and total dissolved radionuclide activity.

A 20-mL aliquot of the filtered radionuclide solutions was then added to 10 g of pre-equilibrated sediment; solid-to-solution ratio 1:2. The radionuclide/groundwater/sediment suspensions were placed on a slow-moving platform shaker for 14 days. This duration was selected to ensure that the system was in a steady state. Preliminary experiments showed that I^- sorption to trench AE-3 sediment remained constant between 2 and 14 days (Kaplan et al. 1996). The suspensions were centrifuged and the supernatants were

then passed through 0.20-µm filters. Radionuclide activity, pH, and electrical conductivity of the filtrates were measured. Three or four replicates of each batch test were used. Table 2.1 shows the measured K_d values.

Table 2.1. K_d Results from Kaplan et al. (1998a) as a Function of Ionic Strength and pH

$NaClO_4$ added (M) / Calculated Ionic Strength (mM)	pH	EC (mS/cm)	TcO_4^- Kd (mL/g)	I^- Kd (mL/g)
0.05 / 47	7.74	9.06	-0.16 ± 0.04	NA
0.10 / 85	7.76	10.94	-0.13± 0.00	NA
0.50 / 262	7.73	11.05	-0.28 ± 0.01	NA
1.00 / 536	7.7	>20	3.94 ± 0.99	NA
pH varied by adding NaOH				
0 / 6	8.1	0.66	NA	0.22 ± 0.01
0 / 8	9.9	0.79	NA	0.01 ± 0.01
0 / 8	10.2	0.79	NA	-0.02 ± 0.02
0 / 17	11.0	1.15	NA	-0.04 ± 0.02
0 / 26	11.9	3.46	NA	0.01 ± 0.01
0 / 6	8.1	0.59	-0.02 ± 0.01	NA
0 / 8	9.9	0.7	1.04 ± 0.06	NA
0 / 8	10.2	0.7	1.05 ± 0.02	NA
0 / 17	11.0	1.13	1.07 ± 0.05	NA
0 / 26	11.9	6.14	1.07 ± 0.03	NA

NA = not applicable
Note that the pH and EC values were measured on batch test effluents collected at the end of a 14-d contact time.

Over the increase in ionic strength, Tc K_d values increased non-systematically from -0.16 to 3.94 mL/g. The cause of this increase in K_d values perhaps is that the higher ionic strength caused the double layer around the sediment particles to decrease, thereby permitting greater TcO_4^- interaction with the mineral surfaces. Hanford Site sediments have few positively charged sorption sites at pH 7 to 8 or higher; however, these few sites may play an important role, especially at the extremely low TcO_4^- and I^- concentrations (on the order of 10^{-10} M) used in these tests and expected in leachate emanating from breached repositories.

As the pH increased from 8.1 (background) to 11.9, I^- K_d values non-systematicallydecreased from 0.22 to 0.01 mL/g. This pH trend is consistent with the geochemical rule-of-thumb that anion sorption decreases as the pH increases. The reason for this trend is that as the pH increases, the extent of negative surface charge increases on the sediment as a result of increased concentration of OH^- on the mineral surface. This trend was not observed with TcO_4^- K_d values. Instead, as the pH increased from 8.1 to 11.9, the TcO_4^- K_d values non-systematically increased from -0.02 to 1.07 mL/g. The cause for this unexpected but very consistent trend is not known, but perhaps is related to the collapse of the double layer electrostatic charge field around sediment particles.

Kaplan et al. (1998a) concluded that TcO_4^- K_d values for sediments in the near field are likely to be >0 mL/g, and perhaps conservatively set at 0.2 to 0.6 mL/g. They also found that I^- adsorption on near-field sediments was influenced by high pH and high ionic strength conditions, and that conservative

iodide K_d values for solutions with background pH (~8) and higher ionic strength (above 80 mM, less than two times background) should be 0.5 mL/g.

2.2.4 Radionuclide Distribution Coefficients for Sediments Collected from the IDF Site

Kaplan et al. (1998b) measured distribution coefficients (K_d) for a number of radionuclides using IDF-specific sediments to support the 1998 ILAW PA. They reported over 360 distribution coefficients (K_d) for radionuclides (including iodine [as iodide, I^-] and technetium) that were measured using 20 different sediment samples from three stratigraphic layers within the sandy sequence of the Hanford formation (identified by Reidel et al. [1998]) encountered in borehole 299-E17-21. They used Hanford groundwater from well 699-S3-25, with a measured pH of 8.4, for the adsorption tests. K_d measurements were made following the batch procedure described in Relyea et al. (1980), using oven-dried sediments, preequilibrated in Hanford groundwater. The sediment-to-liquid ratio used for the I and Tc experiments was 1 g of sediment to 2 mL of Hanford groundwater, spiked with 15 mCi/mL ^{125}I (as $^{125}I^-$) or 10 mCi/mL ^{99}Tc[1], and placed on a platform shaker for 14 days. Their conservative and best estimate K_d values for iodine and technetium are reproduced in Table 2.2.

Kaplan et al. (1998b) found that iodine K_d values measured in borehole 299-E17-21 were appreciably less than the previously estimated iodine K_d values measured on a variety of Hanford Site sediments using neutral to high pH solutions (0.7 to 15 mL/g, with 3.1 mL/g average, reported by Kaplan and Serne [1995]). They noted that these differences underscore the importance of basing K_d estimates on measurements using IDF site-specific sediments. Some of the differences in iodide K_d values found in Kaplan et al. (1998b) versus past iodide K_c estimates are likely because previous sediments studied had a finer grain texture and because previous studies used different contacting solutions with different macro constituent and iodide concentrations as well as different contact times and solid-to-solution ratios. All of these variables have been shown to influence the measured K_d values for some contaminants. No detailed study of the impact of these parameters has been performed for iodide sorption onto Hanford Site sediments.

Table 2.2. Range, Conservative and Best Estimates of K_d Values from Kaplan et al. (1998b)

	Layer 3 (5 to 58 ft BGS), and Layer 2 (58 to 163 ft BGS)			Layer 1 (163 to 247 ft BGS)		
Radionuclide	K_d Range (mL/g)	Conservative K_d (mL/g)	Best Estimate K_d (mL/g)	K_d Range (mL/g)	Conservative K_d (mL/g)	Best Estimate K_d (mL/g)
I (as I^-)	-0.03 to 0.12	0	0 ± 0	-0.01 to 0.13	0	0.1 ± 0.1
^{99}Tc	-0.04 to 0.00	0.0	0 ± 0	-0.03 to 0.01	0.0	0 ± 0

BGS = below ground surface.
Stratigraphic layers are those identified by Reidel et al. (1998).
Conservative estimates were based on the minimum value and best estimates were based on the median ± standard deviation.

[1] Kaplan et al. (1998b) in Table 2 state that the spike solution activity was 15 mCi/mL for ^{125}I and 10 mCi/mL for ^{99}Tc, but these values are not realistic. Either the authors reported the activity in the radioactive stock solutions from which a small volume was pipetted into the groundwater or the values might be in µCi/mL. We suspect the former is correct and that the authors did not report the actual starting activity in the spiked groundwater.

2.2.5 The Influence of Glass Leachate on the Hydraulic, Physical, Mineralogical, and Sorptive Properties of Hanford Sediment

Kaplan et al. (2003) studied the effects of high pH/high ionic strength solutions contacting a Hanford Site sediment and quartz minerals. Under chemical conditions approaching the most caustic glass leachate conditions predicted in the near field of the IDF disposal site, approximated by 0.3 M NaOH, significant changes in mineralogy were observed. The clay minerals of the Hanford sediment (Warden silt loam) evidenced the greatest dissolution, thereby increasing the relative proportions of the more resistant minerals (e.g., quartz, feldspar, and calcite) in the remaining sediment mass. Some re-precipitation of solids (mostly amorphous gels) was observed after caustic solution contact with both the Warden silt loam and quartz solids; these precipitates increased the moisture retention of both solids, likely because of water retained within the gel coatings. The hydraulic conductivities were slightly lower, but because of experimental artifacts, these reductions should not be considered significant.[1]

Thus, there does not seem to be large differences in the hydraulic properties of the quartz sand or Warden silt loam soil after 192 days of contact with caustic fluids similar to glass leachate. The long-term projected impact of the increased moisture retention has not been evaluated, but likely will not invalidate past simplified performance projections. Despite the fact that some clay minerals, such as smectites and kaolinite, almost totally dissolved within a year of contact with 3.0 M NaOH (and by inference after longer time frames for 0.3 M NaOH, a more realistic surrogate for ILAW glass leachate), other sorbing minerals such as illite and chlorite do not appreciably react. In caustic solutions, there was no appreciable adsorption for the three anions I^-, SeO_4^{2-}, or TcO_4^-. Because a majority of the dissolution and precipitation occurred within 7 days of contact with the caustic solution, future research on the dissolution aspects of caustic attack can be conducted over shorter durations, but the subsequent re-precipitation processes and the re-incorporation of trace contaminants into secondary minerals and gels appear to occur over periods that do not reach steady state within 1 year.

In summary, these studies showed that under chemical conditions approaching the most caustic glass leachate conditions predicted in the near field of the IDF disposal site, approximated by 0.3 M NaOH, significant changes in mineralogy were observed. The clay minerals evidenced the greatest dissolution, thereby increasing the relative proportions of the more resistant minerals (e.g., quartz, feldspar, and calcite) in the remaining mass. Some re-precipitation of solids (mostly amorphous gels) was observed; these precipitates increased the moisture retention in both the quartz and Warden soil, likely because of water retained within the gel coatings. The hydraulic conductivities were slightly lower, but because of experimental artifacts, these reductions should not be considered significant. Neither iodide (I^-), selenate (SeO_4^{2-}), nor pertechnetate (TcO_4^-) sorbed appreciably to soils treated with and contacting NaOH solutions used to simulate glass leachates.

2.2.6 Geochemistry of Samples from Borehole C3177 (299-E24-21)

Horton et al. (2003) described the physical and geochemical properties for six large composite samples and six discrete depth samples from the second ILAW borehole C3177. The composite samples

[1] It is not clear if the decreased hydraulic conductivity was caused by reaction with the caustic solution or by compaction from centrifugation during measurement of moisture retention. It was discovered that use of an unsaturated flow apparatus to measure moisture retention compacted the solids before making the hydraulic conductivity measurements.

were made so that large volumes of well-characterized material would be available for future geochemical studies.

Of most interest to the current study is the composite sample C3177-215, which was used in the K_d experiments. This sample is a composite of sediments from a depth interval of 215 to 234 ft from well 299-E24-21 (C3177). Horton et al. (2003) classified this sample as a gravelly sand, consisting of 22.94 wt% gravel, 73.12 wt% sand, 3.20 wt% silt, and 0.74 wt% clay. The bulk sediment composition for discrete sediment samples used in the composite sample is shown in Table 2.3. Semi-quantitative X-ray diffraction results are shown in Table 2.4 and Table 2.5. Horton et al. (2003) reported surface area values for three aliquots of the bulk sediment (sample C3177-215) as 7.51, 7.92, and 15.58 m^2/g, and for two measurements on the clay-size fraction as 52.2 and 58.5 m^2/g. Table 2.6 shows the analytical results for 1:1 water extracts for both composite sample C3177-215 and discrete sample C3177-223.5 (collected from a depth of 223.5 ft). Horton et al. (2003) also calculated the cation exchange capacity; Figure 2.1 presents these results as a function of depth, showing the locations of samples relevant to composite sample C3177-215.

Table 2.3. Bulk Sediment Composition of Selected Sediment Samples from Borehole C3177 (from Horton et al. 2003)

Analyte	C3177-215	C3177-223.5
Loss-on-ignition, LOI (bound water content), wt%	1.76	2.11
Major element oxides (wt%)		
SiO_2	64.92	67.06
Al_2O_3	13.65	13.54
TiO_2	1.118	0.940
Fe_2O_3	7.68	6.67
MnO	0.114	0.100
CaO	5.15	4.52
MgO	2.62	2.24
K_2O	2.00	2.16
Na_2O	3.31	3.25
P_2O_5	0.219	0.194
Trace elements (µg/g)		
Ni	19	20
Cr	43	41
Sc	27	21
V	174	132
Ba	767	821
Rb	56	66
Sr	401	403
Zr	140	134
Y	28	22
Nb	11.2	10.8
Ga	19	17
Cu	27	28
Zn	78	67
Pb	9	10
La	19	36
Ce	37	38
Th	6	2
Total (wt%)	103.351	101.044
Carbon (wt%)		
Total Carbon	0.11	0.14
Inorganic Carbon	0.07	0.10
Equivalent $CaCO_3$	0.58	0.83
Organic Carbon by difference	0.04	0.04

Table 2.4. Semi-quantitative X-ray Diffraction Results of Selected Samples from Borehole C3177 (from Horton et al. 2003)

Mineral Phase (wt%)	C3177-215	C3177-223.5
Quartz	26	33
Amphibole	3	4
Plagioclase	40	34
K-spar	18	18
Mica	11	8
Chlorite	3	3
Goodness of fit(a)	0.73	0.56

(a) Values closest to 1.0 represent ideal refinement.

Table 2.5. Semi-quantitative X-ray Diffraction Results of Clay Minerals Separated from Selected Samples from Borehole C3177 (from Horton et al. 2003)

Mineral Phase (wt%)	**C3177-215**	**C3177-223.5**
Smectite	30	NA
Illite	46	NA
Chlorite	20	NA
Kaolinite	4	NA

NA = not analyzed

Table 2.6. Concentrations in 1:1 Water Extracts (from Horton et al. 2003)

Analyte	C3177-215	C3177-223.5
Alkalinity (mg $CaCO_3$/L)	43.68	-
pH	7.54	7.66
Electrical Conductivity (µS/cm)	199	184
Dilution Corrected Electrical Conductivity (µS/cm)	9,142	8,305
Major Metals (µg/L), values in parentheses are less than limit of quantitation		
Al	43	(22)
Ca	11,995	10,702
Fe	20	15
K	5,341	4,775
Mg	3,985	3,665
Na	15,349	15,105
S	17,154	13,975
Si	9,748	9,892
Major cations (µg/mL)		
Al	0.058 / 0.050	0.082 / 0.109
Ca	13.547 / 16.330	12.766 / 11.475
Fe	0.136 / 0.037	0.072 / 0.104
K	6.123 / 6.409	6.354 / 6.006
Mg	4.719 / 5.719	4.326 / 3.988
Na	17.106 / 15.868	16.429 / 14.841
S	18.399 / 21.575	14.015 / 13.965
Si	8.105 / 8.539	8.345 / 8.076
Anions (µg/mL)		
Nitrate	61.53	82.59
Chloride	63.55	79.41
Sulfate	2,594.81	2,096.41
Phosphate	11.03	10.83
Fluoride	18.60	15.97

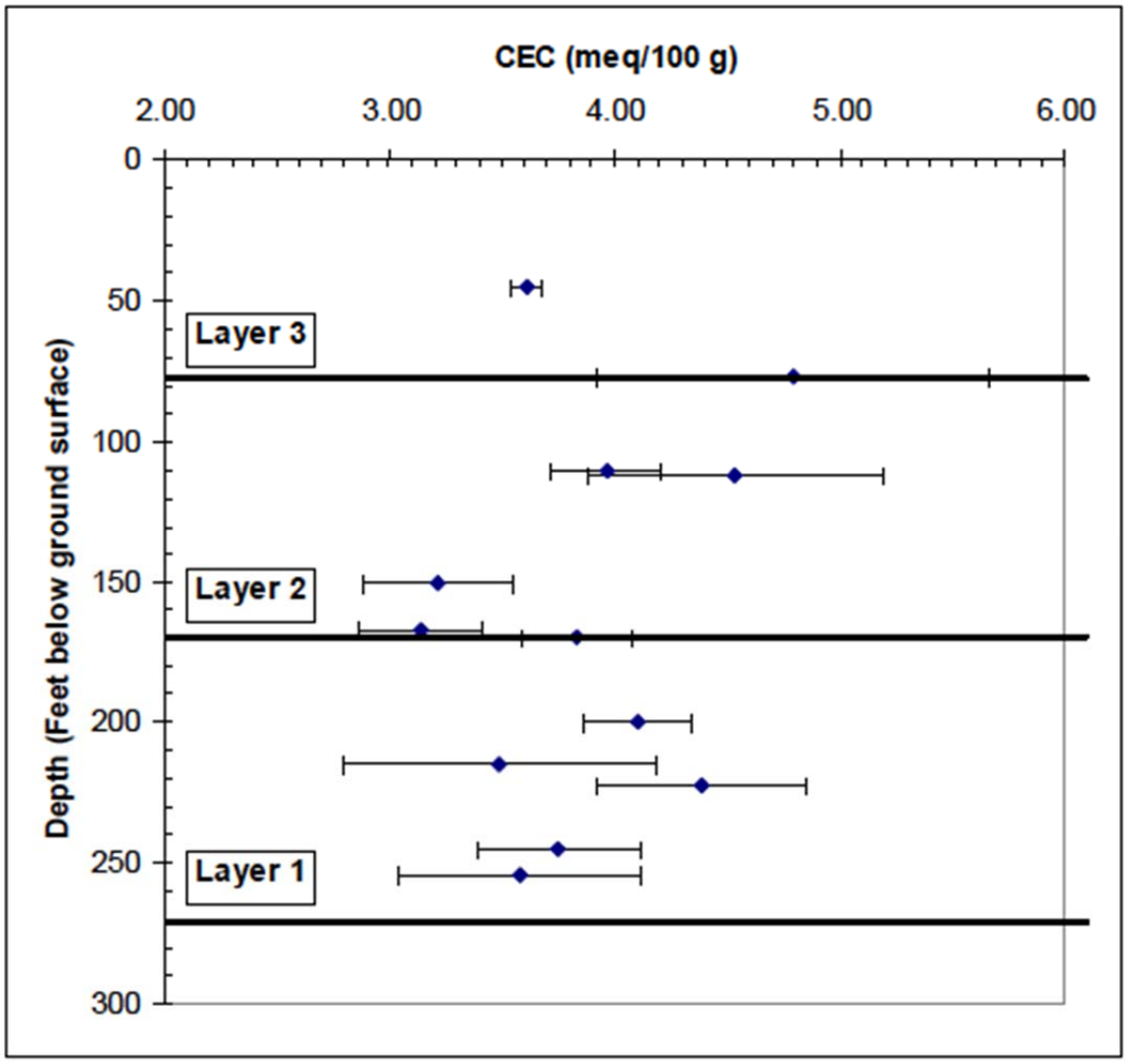

Figure 2.1. Calculated Cation Exchange Capacities of Samples from Borehole C3177 (from Horton et al. 2003). Note that the depth range relevant to composite sample C3177-215 is from 215 to 234 ft.

2.2.7 Linearity and Reversibility of Iodide Adsorption and pH Effects

Um et al. (2004) performed a series of adsorption and desorption experiments to determine the linearity and reversibility of iodide adsorption onto the <2-mm size fraction of sediment from borehole 299-E24-21 (near the IDF) and actual uncontaminated Hanford groundwater from well 699-S3-25. The sediments had first been equilibrated with unspiked groundwater several times until pH was stable at 7.5. The sediments were then oven dried and stored until tested. A suite of batch sorption-desorption tests were performed. Radiotracer (carrier-free) ^{125}I (as iodide) was spiked into groundwater at 3.7 x 10^{+5} Bq/L (5.75E-04 ppm I).

Other linear adsorption batch experiments were performed with stable iodide (0.001 to 500 mg/L) and ^{125}I radiotracer. Batch adsorption tests were run at 1g/10 mL solid-to-solution ratio. Some batch adsorption tests were performed with groundwater spiked with carrier-free ^{125}I that had pH adjusted from

pH = 3 to pH = 8.3. One set of batch adsorption tests was conducted with contact times from 1 to 29 days, but after it was established that steady-state sorption was attained after 7 days, most adsorption tests were run with 7-day contact times. Effluents were separated from the wet sediment by centrifugation followed by supernate filtration through 0.45-µm filters. ^{125}I was counted by liquid scintillation and stable iodide when present at >1 mg/L by ion chromatography (IC).

Results for the linearity tests containing both stable iodide and ^{125}I, all at pH = 7.5, yielded an iodide K_d that ranged from 0.1 to 0.3 mL/g with an average of 0.2 mL/g. Batch adsorption tests with carrier-free ^{125}I at pH values of 6.3, 7.2, and 8.3 yielded iodide K_d values of 1.04 ± 0.06, 0.28 ± 0.08, and 0.09 ± 0.03 mL/g, respectively. There was a definite trend for lower iodide K_d values as pH increased from 3 to 8.3, suggesting that the Hanford sediments contained some solid phases with variably charged pH-dependent surface charges that were protonated (and thus capable of attracting/sorbing anions) at low pH.

Desorption experiments were performed after removal of as much of the residual carrier-free ^{125}I spiked groundwater as possible, and fresh unspiked groundwater was added. The sediments were shaken for an additional 14 days before the final solution was separated by centrifugation and then filtered through 0.45-µm filters. After removing a small aliquot of supernate from the desorption test, an additional 14 days (for a total of 28 day) of desorption was performed. Results of the desorption experiments revealed that up to 60% of adsorbed iodide was readily desorbed after 14 days by iodide-free groundwater. No further desorption of the iodide was observed up to 28 days of contact with iodide-free groundwater. This result suggests that some of the adsorbed iodide is partially irreversibly sorbed or at least desorbs with much longer kinetics when contacted with iodide-free pore waters and uncontaminated groundwater. The resultant desorption iodide K_d was 1.4 mL/g.

It needs to be stressed that the empirical K_d values generated from short-term laboratory tests can be sensitive to the experimental procedures used. Iodide K_d studies may be especially sensitive to the contact time between the sediments and solutions and the type of iodide tracer (carrier-free ^{125}I vs. stable ^{127}I) used in the tests. Further, the short-term laboratory tests may not allow enough time for the sediment-solution slurries to reach true equilibrium adsorption-desorption conditions or perhaps even steady-state contaminant solution concentrations. If there are very slow sorption-desorption kinetics, measuring effluent contaminant concentrations in batch tests several times over a several days or a few weeks can appear to show near-constant (or steady-state) values when in fact the slurry is still slowly evolving. Thus, it is difficult to establish when true equilibrium or steady state is reached. Typically, adsorption reactions start with fast kinetics but can be followed by very slow final sorption kinetics. It is not uncommon to realize that true sorption-desorption equilibrium may never be achieved in laboratory tests and likely the same is true for field conditions. Therefore, statements that adsorption-desorption laboratory tests were performed for periods long enough to establish steady-state conditions are “relative” statements, which signify that a high percentage of the early fast kinetics adsorption-desorption has occurred.

Key conclusions from Um et al. (2004) were that iodide sorption onto Hanford sand-dominated sediments near the IDF facility requires at least 7 days to reach a steady state. The adsorption of iodide is sensitive to pH, with lower sorption being found as the pH rises from pH = 3 to 8.3. Above pH = 8.3, the authors speculated that iodide adsorption would be negligible. For groundwater contacting the IDF sediment at pH values between 7.5 and 8.3, iodide K_d ranged from 0.2 to 0.09 mL/g and there was some

degree of sorption irreversibility in groundwater at pH = 7.5, resulting in the desorption iodide K_d being 1.4 mL/g.

In a follow-up study, Um and Serne (2005) performed a series of batch sorption and column experiments to investigate sorption and transport behavior of ^{99}Tc, ^{129}I, ^{79}Se, and ^{90}Sr on and through IDF borehole (299-E24-21) sediments. Uncontaminated Hanford groundwater (from well 699-S3-25) and simulated glass leachate were spiked with individual radionuclides, carrier-free ^{125}I (as iodide), and ^{99}Tc (as pertechnetate) at 3.7 x 10^{+05} Bq/L (5.75E-04 ppm I and 0.59 ppm Tc). The batch adsorption tests were run at a solid-to-solution ratio of 1 g:10 mL. After 7 days, the slurries were centrifuged and then supernatant solution was passed through 0.45-µm pore size filters.

For the column tests, individual radiotracers were spiked into groundwater and then pumped through packed sediment columns (1.91 cm in diameter and 7.62 cm long) at a constant rate. The columns were first saturated with deionized water to establish the constant flow rate. Tritium (^3H) in deionized water was then injected as a step-function pulse to allow individual column dispersion coefficients to be calculated. As soon as the tritium pulse flushed from the columns, the spiked (3.7×10^5 Bq/L) groundwater was pumped at a flow rate equivalent to a 6.6-day residence time into the columns (again as a step-function pulse). Effluent samples were collected, filtered through 0.45-µm pore size filters, and then radiocounted using liquid scintillation. The computer code CXTFIT (a curve fitting code based on the advection-dispersion equation) was used to process the column breakthrough curves (BTCs) by first establishing the column dispersion and then calculating a K_d value from the BTC of each contaminant.

Of particular interest to this study are tests with simulated glass leachate. In 2005, the best estimate glass leachate had the composition shown in Table 2.7 (also shown is the "new" glass leachate chemical composition, used in the current study).

Table 2.7. Comparison of Glass Leachate Simulants

Constituent	New Simulant Used in Current Study	2005 Simulant, from Um and Serne (2005)
Al (M)	----	2.00E-04
B (M)	5.320E-03	7.23E-03
Na (M)	1.850E-01	3.85E-02
K (M)	3.270E-04	1.12E-02
Ca (M)	2.680E-04	1.00E-07
Mg (M)	6.520E-04	6.75E-04
OH (M)	1.270E-01	----
SO_4 (M)	1.460E-02	----
Si (M)	3.140E-03	1.95E-03
CO_3 (M)	3.880E-03	7.54E-03
HCO_3 (M)	---	2.68E-02
Cl (M)	8.670E-03	----
NO_3 (M)	5.567E-03	----
pH	8.6	8.5-9.5

---- Not added to this simulant

The Um and Serne (2005) results of the batch tests showed no sorption affinity for ^{99}Tc onto IDF sand-dominated sediment from both Hanford groundwater and the simulated glass leachate. The column

results for ^{99}Tc in groundwater also showed no adsorption (K_d = -0.01), and in fact showed some anion exclusion that manifests as the slightly negative calculated K_d.

For the carrier-free ^{125}I iodide, batch tests on three depth-discrete samples from borehole 299-E24-21 yielded K_d values for groundwater (pH = 7.8) ranging from 0.17 to 0.41 mL/g, with an overall average of 0.28 ± 0.12 mL/g. In the glass leachate simulant (pH = 9.0), the iodide batch K_d ranged from 0.04 to 0.16 mL/g with an overall average of 0.09 ± 0.06 mL/g. As found previously (Um et al. 2004; Kaplan et al. 1998a), the iodide K_d drops as the system pH increases. For the carrier-free iodide-spiked groundwater flow-through column test, the BTC was analyzed by both the classical equilibrium advection–dispersion equation and the nonequilibrium, two-region (mobile–immobile) conceptual modeling (van Genuchten and Wierenga 1976). The iodide BTC was slightly retarded compared with that of ^{3}H. Long tailing was found in the later stages of the iodide breakthrough. The best fit calculated non-equilibrium column K_d was 0.17 mL/g (on the low end of the batch iodide K_d values). The tailing of the desorbing iodide in the column test is caused either by slow kinetics or irreversibility, as described by Um et al. (2004), or from slow release of iodide from immobile pores.

The Um and Serne (2005) results of column experiments that measured transport behavior of iodide and pertechnetate through IDF Hanford formation sand sediment were similar to the mobility that can be calculated from the batch sorption results.

2.2.8 Geochemical Data Package for the 2001 Hanford ILAW PA

Kaplan and Serne (2000) documented the basis for selecting geochemical parameters and input values that would be used in the 2001 version of the ILAW PA. They presented the philosophy, key radionuclides, approach, and resulting tables of geochemical information. They identified five environmental/geochemical zones associated with the ILAW disposal system (now called the IDF) and the subsurface. They provided empirical K_d values (and solubility data) for each of these zones based on Hanford Site-specific experiments (where possible) or generic literature. Table 2.8 summarizes these relevant results for technetium and iodine. Note that their Zone 2 considered a concrete vault, which is not relevant to the current study.

Table 2.8. Technetium and Iodine K_d Values from Kaplan and Serne (2000) by Geochemical Zone

	Technetium			Iodine[(b)]		
Geochemical Zone	Conservative K_d (mL/g)	Best Estimate K_d (mL/g)	K_d Range (mL/g)	Conservative K_d (mL/g)	Best Estimate K_d (mL/g)	K_d Range (mL/g)
Zone 1 – Near Field	0.1	1	0.1 to 1.2	0	0	0 to 1.1
Zone 2 – Degraded Concrete Vault. Not relevant to the current study.						
Zone 3 – Chemically Impacted Far Field in Sand Sequence	0	0	0 to 0.1	0	0	0 to 2
Zone 4 – Chemically Impacted Far Field in Gravel Sequence[(a)]	0	0	0 to 0.01	0	0	0 to 0.2
Zone 5 – Far Field in Gravel Sequence[(a)]	0	0	0 to 0.06	0	0.01	0 to 1.5

(a) Corrected for gravel content.
(b) Assumed to be applicable to both I^- and IO_3^-

2.2.9 Geochemical Data Package for the 2005 Hanford IDF PA

Krupka et al. (2004) compiled the most recent geochemical data package that provides IDF-specific recommendations for the input data required to describe these interactions. The data package provides a detailed discussion and tabulation of recommended distribution coefficients and solubilities for use in the 2005 Hanford IDF PA (the 2005 IDF PA was never published). They provided best-estimate K_d values, a reasonable conservative value, and a range for different spatial zones in and surrounding the IDF system. They also supplied time-varying K_d values for cement-solidified waste. These were based on the data tabulated by Kaplan and Serne (2000) as well as applicable data from more recent investigations. However, the tabulated K_d and empirical solubility values for cement-solidified wastes did not include data for the current grout/Cast Stone formulations that include the reductant, blast furnace slag (BFS), as a major component of the grout dry blend. The inclusion of BFS in Cast Stone/grouts strongly influences sorption/desorption K_d and empirical solubility values for redox-sensitive contaminants such as Tc, Cr, and U. For example, see results in Langton (1988) that show significant differences in effective diffusion coefficients for Cr(VI) and ^{99}Tc in variants of the saltstone dry mix that includes BFS versus a mix without BFS for the same liquid waste simulant. When BFS is part of the dry mix at 25% of the final hardened saltstone, the effective diffusion coefficients for Cr(VI) and ^{99}Tc are 4 and almost 3 orders of magnitude lower, respectively, than when BFS is not present in the waste form. Effective diffusion coefficients can be related to K_d values using simple conceptual models that assume release of contaminants from grouts are controlled by a combination of physical and chemical processes, with the chemical processes quantified by the K_d. The key equations relating effective diffusion coefficients for contaminant release to the physical and chemical processes are found in Serne et al. (2015), Section 2.6, equations 3, 4, and 5.

The Krupka et al. (2004) recommended values are summarized in Table 2.9. Krupka et al. (2004) also discuss the evolution of the K_d values and the rationale for why some K_d values used in earlier ILAW PAs have changed with time.

We acknowledge that future IDF PA predictions may include the use of probabilistic calculations that require distribution functions for key variables such as the K_d. Table 2.9 through Table 2.11 provide recommended ranges of K_d values but do not discuss probability distributions. The reason that no probability distributions are given is that the amount of data for any given geochemical condition (sediment type/location, contacting solution composition, radionuclide concentration, and adsorption-desorption test details) is too sparse to objectively develop probability distribution functions for each geochemical condition. There are simply too many variables within each adsorption test to be confident that "replicate" tests using ostensibly the same sediment, contacting solution, contaminant, and test protocols are in fact yielding results for one population. At most, laboratory batch adsorption tests on Hanford Site materials have used three or four "replicates," which we consider too small a population to develop technically defensible probability distribution functions. Some geoscientists have speculated that K_d values would exhibit a log-normal probability distribution function, but we have no opinion.

Table 2.9. Technetium, Iodine, and Chromium K_d Values from Krupka et al. (2004) by Spatial Zone

Geochemical Zone	Technetium			Iodine[(b)]			Chromium(VI)		
	Conserv. K_d (mL/g)	Best Estimate K_d (mL/g)	K_d Range (mL/g)	Conserv. K_d (mL/g)	Best Estimate K_d (mL/g)	K_d Range (mL/g)	Conserv. K_d (mL/g)	Best Estimate K_d (mL/g)	K_d Range (mL/g)
Zone 1a – Near Field / Vitrified Waste	0	0	0 to 1	0.04	0.1	0.04 to 0.16	0	0	0 to 1
Zone 1b – Near Field / Cementitious Waste (Young)	0	0	0 to 2	10	20	10 to 150	0	0	0 to 2
Zone 1b – Near Field / Cementitious Waste (Mod. Aged)	0	0	0 to 2	5	8	5 to 15	0	0	0 to 2
Zone 1b – Near Field / Cementitious Waste (Aged)	0	0	0 to 1	1	2	1 to 5	0	0	0 to 1
Zone 2a – Chemically Impacted Far Field in Sand Sequence	0	0	0 to 0.1	0	0.1	0 to 0.2	0	0	0 to 0.1
Zone 2b – Far Field in Sand Sequence (no impact from wastes)	0	0	0 to 0.6	0	0.25	0.0 to 15	0	0	0 to 0.6
Zone 3a – Chemically Impacted Far Field in Gravel Sequence[(a)]	0	0	0 to 0.01	0	0	0 to 0.02	0	0	0 to 0.01
Zones 3b and 4 – Far Field in Gravel Sequence[(a)]	0	0	0 to 0.06	0	0.02	0 to 1.5	0	0	0 to 0.06
Zone 5 – Unconfined Far Field Aquifer	0	0	0 to 0.6	0	0.25	0.0 to 15	0	0	0 to 0.6

(a) Corrected for gravel content.
(b) Assumed to be applicable to both I^- and IO_3^-

2.2.10 Vadose Zone Hydrogeology Data Package for Hanford Assessments

Last et al. (2006) conducted an extensive review of the K_d measurements on Hanford sediments under various conditions available in Cantrell et al. (2003). Table 4.11 of Last et al. 2006 recommends K_d values for un-impacted groundwater or vadose zone pore water (Waste Chemistry/Source Category 4: Low Organic/Low Salt/Near Neutral – Groundwater), IDF vitrified waste (Waste Chemistry/Source Category 5: IDF Vitrified Waste), and cementitious waste (Waste Chemistry/Source Category 6: Cementitious Waste). For the IDF vitrified waste and cementitious waste, recommendations are provided for high impact, intermediate impact sand, and intermediate impact gravel. For the gravel cases, it was assumed that the sediment contained 90% gravel. The gravel corrections were made as indicated in Last et al. (2006) following the methods outlined in Kaplan and Serne (2000). Last et al. (2006) provide a range for the K_d values in terms of minimum and maximum values. The "best (Estimate)" K_d value recommendations provided in Last et al. (2006) are believed to be less conservative and more realistic than those provided in Krupka et al. (2004). The values recommended by Last et al. (2006) for the three key contaminants are found in Table 2.10.

Table 2.10. IDF K_d Value Estimates from Last et al. (2006)

	Technetium			Iodine[(b)]		
Geochemical Zone	Best Estimate K_d (mL/g)	Min. K_d (mL/g)	Max. K_d (mL/g)	Best Estimate K_d (mL/g)	Min. K_d (mL/g)	Max. K_d (mL/g)
IDF Vitrified Waste						
High Impact Zone	0	0	0.1	0.1	0.04	0.16
Intermediate Impact Zone – Sand	0	0	0.1	0.1	0	0.2
Intermediate Impact Zone - Gravel[(a)]	0	0	0.01	0	0	0.02
IDF Cementitious Waste						
High Impact Zone	0	0	0.1	2	1	5
Intermediate Impact Zone – Sand	0	0	0.6	0.25	0	15
Intermediate Impact Zone - Gravel[(a)]	0	0	0.01	0.02	0	1.5

(a) Corrected for gravel content.
(b) Assumed to be applicable to both I^- and IO_3^-

2.2.11 Geochemical Processes Data Package for the Vadose Zone in the Single-Shell Tank Waste Management Areas at the Hanford Site

Cantrell et al. (2007) summarized the most relevant information regarding geochemical processes that affect contaminant transport in vadose zone sediments beneath the single-shell tank (SST) waste management areas (WMAs) and the IDF. Their Appendix C includes summary tables of K_d values mostly taken from Krupka et al. (2004), with some minor updating for more-recent Hanford site-specific data. The vadose zone K_d values for the effluents and contaminants of concern to this study (^{99}Tc, ^{129}I, and Cr(VI)) are summarized in Table 2.11.

Table 2.11. K_d Values for IDF Vadose Zone Sediments (taken from Cantrell et al. [2007], Appendix C)

Constituent	Reasonable Conservative K_d (mL/g)	"Best" Estimate K_d (mL/g)	K_d Range (mL/g)
Near Field/Vitrified Waste			
Tc	0	0	0 to 1
Cr(VI)	0	0	0 to 1
I[(a)]	0.04	0.1	0.04 to 0.16
Near Field/Cementitious Secondary Wastes - Young Concrete (pH ~ 12.5)			
Tc	0	0	0 to 2
Cr(VI)	0	0	0 to 2
I[(a)]	10	20	10 to 20
Near Field/Cementitious Secondary Wastes – Moderately Aged Concrete (pH ~ 10.5)			
Tc	0	0	0 to 2
Cr(VI)	0	0	0 to 2
I[(a)]	5	8	5 to 15
Near Field/Cementitious Secondary Wastes – Aged Concrete (pH ~ 8.5)			
Tc	0	0	0 to 1
Cr(VI)	0	0	0 to 1
I[(a)]	1	2	1 to 5
Chemically Impacted Far Field in Sand Sequence			
Tc	0	0	0 to 0.1
Cr(VI)	0	0	0 to 0.1
I[(a)]	0	0.1	0 to 0.2
Far Field in Sand Sequence with Natural Recharge (No Impact from Wastes)			
Tc	0	0	0 to 0.6
Cr(VI)	0	0	0 to 0.6
I[(a)]	0	0.25	0 to 15
Chemically Impacted Far Field in Gravel Sequence (Gravel-Corrected)			
Tc	0	0	0 to 0.01
Cr(VI)	0	0	0 to 0.01
I[(a)]	0	0.25	0 to 0.02
Far Field in Gravel Sequence (no impact from waste, Gravel-Corrected)			
Tc	0	0	0 to 0.06
Cr(VI)	0	0	0 to 0.06
I[(a)]	0	0.02	0 to 15

(a) Assumed to be applicable to both I^- and IO_3^-

2.2.12 Geochemical Characterization Data Package for the Vadose Zone in the SST WMAs at the Hanford Site

Cantrell et al. (2008) summarized laboratory characterization data on contaminant mobility specific to the IDF and SST WMAs. Excerpts from this report (pages 3.42 through 3.46), with minor edits to improve clarity, succinctly describe the current conceptual understanding of adsorption properties and contaminant migration behavior specific to the IDF.

> *Two boreholes have been drilled in support of the IDF Performance Assessment (Reidel et al. 1998, Horton et al. 2003). Some hydrologic and geochemical characterization work was conducted on the first borehole (299-E17-21). In particular, batch K_d*

measurements were performed for key contaminants of concern (Kaplan et al. 199b). The K_d values, as well as other hydrologic data from measurements on sediments from this borehole, are found in the IDF data packages for the 2001 IDF performance assessment (see Khaleel [1999], Meyer and Serne [1999], and Krupka et al. [2004] for details). Samples from the second borehole (C3177/299-E24-21) were characterized for physical and geochemical properties and iodide sorption-desorption studies (Um et al. 2004). A summary of these results is discussed below. These results are included in this report because of their close proximity to the tank farms and the extensive characterization work that was done on the samples. Because of the location of the IDF boreholes relative to the 200 East Area, knowledge gained from the detailed characterization of the sediment geology at the IDF boreholes is important in understanding the geology at the 200 East Area tank farms.

As part of the IDF Performance Assessment, a geochemical data package (Krupka et al. 2004) was compiled to document the basis for selecting geochemical parameters and input values that were used in the 2005 version of the IDF Performance Assessment. Included in the Krupka et al. (2004) data package is a discussion of the philosophy and justification for selection and use of the empirical distribution coefficient (K_d) and empirical solubility concentration limits as inputs for contaminant migration analyses. Brief descriptions of the spatial zone approach and the resulting tables of information were provided in Krupka et al. 2004 and are also included in Appendix C of the Geochemical Processes Data Package (Cantrell et al. 2007).

Physical and geochemical properties were determined for six large composite sediment samples and six discrete-depth sediment samples from the second ILAW borehole C3177 (299-E24-21) (Horton et al. 2003). The composite samples were made to provide sufficiently large volumes of well-characterized material that would be available for future geochemical studies. The results of these characterization studies were used to determine the geochemical interactions between Hanford formation sediment and contaminants that may leach from the glass waste forms scheduled to be disposed in the IDF.

All the 299-E24-21 samples were analyzed for particle-size distribution, moisture content, whole sediment chemical composition, carbon content, surface area, and mineralogy. In addition, 1:1 sediment/ water extracts were analyzed for pH, electrical conductivity, alkalinity, and concentrations of major and trace metals and anions. This investigation determined that all composite samples are sand or gravelly sand. The moisture content ranges from 1.7 to 5.3 wt.%. The bulk chemistry and mineralogy of the samples are typical of the Hanford formation sand-dominated sequence. Likewise, the chemical characteristics of the 1:1 sediment/water extracts are similar to extracts from other samples of the Hanford formation sand-dominated sequence from other boreholes. The water extracts (and by inference the natural vadose zone pore water) from borehole C3177 are dominated by calcium, bicarbonate (as determined from the alkalinity values), magnesium, sodium, and sulfate.

Estimates of the geochemical properties of the materials comprising the IDF, the disturbed region around the facility, and the physically undisturbed sediments below the

facility (including the vadose zone sediments and the aquifer sediments in the upper unconfined aquifer) have been compiled in Krupka et al. (2004). The geochemical properties were expressed as parameters that quantify the adsorption of contaminants and the solubility constraints that might apply for those contaminants that may exceed solubility limits. The parameters used to quantify adsorption and solubility were the distribution coefficient (K_d) and the empirical constant concentration values, which are loosely related to true thermodynamic solubility product (K_{sp}), respectively.

In addition to the best-estimate K_d values, a reasonable conservative value and a range are provided in Krupka et al. (2004). The IDF data package provides both the K_d values and empirical solubility concentration limits for different spatial zones in and surrounding the IDF system and provides time-varying K_d values for cement solidified waste[1]. The IDF data package does not list estimates for the range in empirical solubility concentration limits or their uncertainties. The values for each impact zone and the rationale for their choice are found in tables in Krupka et al. (2004). However, the specific dimensions for each impact zone within the vadose zone are hypothetical because no wastes have been disposed and no field data are available to estimate the distance that waste leachates might travel and the distances over which waste leachate-sediment reactions would occur.

K_d values and empirical solubility concentration limits for each contaminant were presented in an earlier version of the IDF data package (Kaplan and Serne 2000) prepared for the 2001 ILAW Performance Assessment and were updated to include applicable data from investigations completed since 2000 when the first report was issued. These updated data are also presented in Appendix C of the Geochemical Processes Data Package (Cantrell et al. 2007). A discussion was also included in Krupka et al. (2004) on the evolution of the K_d values recommended from the original 1999 ILAW performance assessment (Mann et al. 1998) through the 2001 ILAW (Mann et al. 2001) and 2003 supplemental performance assessments (Mann et al. 2003) to the current values used for the 2005 IDF performance assessments for the key contaminants of concern: Cr(VI), nitrate, ^{129}I, ^{79}Se, ^{99}Tc, and U(VI). Krupka et al. (2004) provides rationale for why some K_d values have changed over time. Typically, these changes were based on more recent adsorption measurements for certain contaminants on IDF-specific sediment samples, or improved understanding of the adsorption properties and migration behavior of a contaminant.

[1] Time-varying K_d values for adsorption desorption on underlying sediments are implied by use of the "impact" zones, which are generally assumed to represent different spatial locations but may also represent time at one location as the waste form leachate chemistry changes from either buildup or dissipation of the moving leachate front. PA modelers should work closely with geochemists when developing the release conceptual models and selecting empirical K_d or solubility values to represent subsurface sediment-solution interactions.

3.0 Methods and Materials

Adsorption/desorption laboratory experiments were conducted for simulated vadose zone pore water and ILAW glass and Cast Stone leachates to reduce the uncertainty in vadose zone K_d values for ^{99}Tc as pertechnetate, ^{129}I as both iodide and iodate species, and Cr as chromate in far-field, sand-dominated Hanford formation sediments. These experiments were conducted using both standard batch and flow-through column tests. Because both adsorption and desorption reactions were expected to be time-dependent, all of the column tests were performed at the lowest practical flow rates. In addition, the stop-flow method was applied during both adsorption and desorption phases of the flow-through testing to increase the fluid residence time inside the columns and to assess how close the system was to equilibrium. A single-column test was performed using unsaturated water conditions to better simulate expected IDF subsurface conditions. Details of the methods and materials are described below.

3.1 Sediment Selection and Characterization

Khaleel (2004) assembled the far-field hydrology data package for the IDF PA. He defined the far-field environment as the distance from the disposal trench where geochemical conditions can be represented using simplifying assumptions (such as linear sorption, negligible precipitation/dissolution, no changes in hydraulic properties, and no density effects). He found that the dominant far-field facies underlying the IDF was a thick sequence of Hanford formation sandy sediments. Kaplan et al. (1998b) found that the K_d values for I (as I^-) in Layer 1 were statistically different, and slightly higher than, those in Layers 2 and 3 (see Table 2.2).

Thus, Layer 1 of the Hanford formation sandy sequence was selected for the adsorption/desorption experiments. Sediment used in these experiments was composite sample C3177-215, which originated from borehole C3177 (299-E24-21). These sediments have been well characterized (Reidel et al. 2001; Horton et al. 2003; Reidel 2005). This composite sample is a mixture of sediments from a depth of 215 to 234 ft near the IDF, representing a sand-dominated sequence (Layer 1) of the Hanford formation (Horton et al. 2003). Horton et al. (2003) measured the gravel (>2 mm) size fraction of this composite sample at 22.9 wt% and classified it as a gravelly sand. We used only the <2-mm size fraction for these experiments, excluding the gravel fraction, which has been shown to contribute little to sorption, as described by Kaplan and Serne (2000).

Horton et al. (2003) determined the physical and geochemical properties for this composite sample, including particle size distribution, moisture content, whole sediment chemical composition, carbon content, surface area, mineralogy, pH, electrical conductivity, alkalinity, and the major and trace metal and anion concentrations of 1:1 sediment-to-water extracts. These results are summarized in Section 2.2.6.

Supplemental sediment characterization was performed by using scanning electron microscopy (SEM) and scanning electron microscopy-energy dispersive spectroscopy (SEM-EDS) analyses. These analyses were performed on the Cr-contacted glass batch sample after 28 days of contact time with Cr-spiked glass leachate and following the desorption phase of the experiment. These analyses provide high-resolution images of surface morphology and particle size of individual sediment particles and elemental data for specific micron-size locations within the samples.

3.2 Solution Preparation

Three solutions were used in these experiments: 1) simulated vadose zone (IDF) pore water, 2) simulated ILAW glass leachate, and 3) simulated Cast Stone leachate. The specific recipes for each solution used in the experiments are described below.

Table 3.1. Simulated Vadose Zone (IDF) Pore Water Preparation (modified after Um et al. [2007] and Westsik and Serne [2012])

Order of Addition	Concentration (Molar)	Reagent	Molecular Weight (g/mol)	Quantity of Reagent Added (g/L)
1	6.905E-04	KCl	74.55	0.05148
2	3.387E-03	$NaNO_3$	84.99	0.2879
3	3.110E-03	$MgCl_2 \cdot 6H_2O$	203.3	0.6323
4	6.120E-04	$NaHCO_3$	84.01	0.05141
5	7.611E-04	Na_2SO_4	142.06	0.1081
6	2.033E-03	$MgSO_4$	120.37	0.2447
7	1.283E-02	$CaSO_4 \cdot 2H_2O$	172.17	2.209
pH adjusted to 7.0 to 7.2 with sulfuric acid.				

3.2.1 Simulated ILAW Glass Leachate

The simulated ILAW glass leachate composition was based on eSTOMP (stomp.pnnl.gov) simulations of LAWA44 glass waste packages in the IDF. The model was a revised version of the base case simulation used in the (unreleased) 2005 IDF PA (Bacon and McGrail 2005). Updates to the model included

- a coarser grid
- a new mineralogical composition for the backfill
- ion exchange for alkali and alkaline earth cations
- no assumption that gas phase CO_2 was fixed at atmospheric levels.

The two-dimensional grid had 12 grid cells in the horizontal x-direction and 91 grid cells in the vertical z-direction. Horizontal grid spacing varied from 10 to 18 cm, and vertical grid spacing varied from 17 to 23 cm.

The mineralogical composition for the backfill was based on samples from borehole C3177 (299-E24-21) (Horton et al. 2003). The mineral percentages were normalized to the porosities assumed for backfill and Hanford sand material (Table 3.2).

Table 3.2. Semi-quantitative X-ray Diffraction Results of Bulk Samples from Borehole C3177 (299-E24-21) (Horton et al. 2003)

	Mineral Phase (wt%)*								
Sample No.	Quartz	Amphibole	Plagioclase	K-Spar	Mica	Chlorite	Calcite	Goodness of Fit	
C3177-45	43	2	20	20	11	3		0.87	
C3177-80.3	41	2	15	28	16	2		0.94	
C3177-110	46	1	25	19	9	2		0.7	
C3177-113.3	40	4	15	31	8	2		1.22	
C3177-150	42	3	25	18	3	8		0.81	
C3177-168.5	40	4	23	22	10	2		1	
C3177-170.4	43	3	21	23	8	2		1.04	
C3177-200	37	4	31	16	10	3		0.77	
C3177-215	26	3	40	18	11	3		0.73	
C3177-223.5	33	4	34	18	8	3		0.56	
C3177-242	32	2	31	18	14	3		0.95	
C3177-251	32	4	35	18	9	3		0.67	
Average	37.92	3.00	26.25	20.75	9.75	3.00	0.10	100.77	Sum
Normalized	3.76E-01	2.98E-02	2.61E-01	2.06E-01	9.68E-02	2.98E-02	9.92E-04	1.00E+00	
									Porosity
Backfill	2.45E-01	1.94E-02	1.69E-01	1.34E-01	6.29E-02	1.94E-02	6.45E-04	6.50E-01	0.35
Hanford Sand	2.28E-01	1.80E-02	1.58E-01	1.25E-01	5.86E-02	1.80E-02	6.01E-04	6.06E-01	0.394

* SEM/EDS semi-quantitative measurements suggest the presence of minor/trace phases; it is, however, hard to determine their identity.

Ion exchange reactions were modeled assuming the Gaines-Thomas convention. The percentage of the total equivalents of cation exchange capacity per gram of soil in each of the 12 sediment samples from 299-E33-44 for Ca, Mg, Na, and K are shown in Table 3.3 and converted from meq/100 g to mol/L aqueous volumetric concentration for use as an eSTOMP initial condition. A porosity of 35% and a grain density of 2.68 g/cm^3 were assumed.

Table 3.3. Cation Exchange Capacity for Samples from 299-E33-44 (Jeff Serne, PNNL, personal communication)

Cation	Ca	Mg	Na	K	Total
Average	79.55%	13.95%	5.86%	0.64%	100.00%
meq/100 g	3.08	0.54	0.23	0.02	3.87
Charge	2	2	1	1	NA
mol/100 g	1.54E-03	2.70E-04	2.27E-04	2.48E-05	2.06E-03
mol/g	1.54E-05	2.70E-06	2.27E-06	2.48E-07	2.06E-05
mol/L aq	7.66E-02	1.34E-02	1.13E-02	1.23E-03	1.03E-01

NA = not applicable

The alkaline earth cations (Ca and Mg) dominate the exchange sites of native vadose zone sediments, and Na is a dominant cation that is leached from the glass. The leached Na will displace Ca and Mg from the ion-exchange sites in minerals of the backfill material and in Hanford formation vadose zone sediments.

The simulations were run for 2000 years with a recharge rate of 0.9 mm/y, the same as used in the 2005 IDF PA. Time steps were chosen automatically to ensure convergence of the numerical solution.

The water saturation surrounding the waste packages at 2000 years is shown in Figure 3.1. The average total aqueous species concentrations in the Hanford sand immediately below the trench are shown in Table 3.4. Without the pH buffering effect of the fixed CO_2 assumption used in the 2005 IDF PA, the glass corrosion rate is higher and Na concentrations below the glass waste packages average 0.227 mol/L.

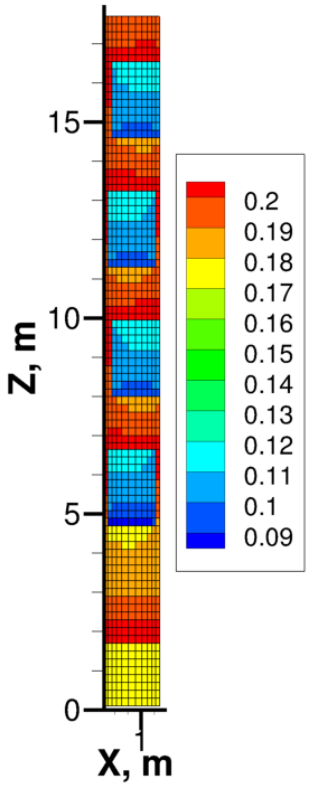

Figure 3.1. Water Saturation at 2000 Years Surrounding Four LAWA44 Waste Packages

Table 3.4. Simulated Aqueous Concentrations Below Waste Packages

Species	Concentration (mol/L)
h+	4.76E-10
total_alo2-	2.65E-03
total_b(oh)3(aq)	7.86E-02
total_ca++	2.54E-02
total_cl-	8.67E-03
total_cro4--	5.64E-05
total_fe(oh)3(aq)	1.72E-07
total_hco3-	9.36E-06
total_k+	2.27E-03
total_mg++	6.75E-07
total_na+	2.27E-01
total_no3-	3.40E-03
total_sio2(aq)	1.70E-01
total_so4--	1.46E-02
total_tco4-	1.27E-04
total_ti(oh)4(aq)	1.30E-06
total_zn++	2.02E-06
total_zr(oh)4(aq)	2.01E-08

The leachate concentrations used in the experiments were modified after Westsik and Serne (2012) based on the simulated concentrations (Table 3.5).

Table 3.5. Recipe for ILAW Glass Leachate Preparation (modified after Bacon and McGrail [2005] and Westsik and Serne [2012])

Order of Addition	Concentration (Molar)	Reagent	Molecular Weight (g/mol)	Quantity of Reagent Added (g/L)
1	7.33E-02	NaOH	40.00	2.930
2	1.46E-02	Na_2SO_4	142.04	2.070
3	3.14E-03	$Na_2SiO_3•9H_2O$	284.20	0.893
4	3.88E-03	Na_2CO_3	105.99	0.411
5	3.33E-04	$Na_2B_4O_7•10H_2O$	381.37	0.127
6	8.68E-03	NaCl	58.44	0.507
7	1.24E-03	$NaNO_3$	84.99	0.105
8	3.27E-04	KNO_3	101.10	0.0331
9	2.68E-04	$Ca(NO_3)_2•4H_2O$	236.15	0.0633
10	6.51E-04	$Mg(NO_3)_2•6H_2O$	256.41	0.167
HNO_3 added until pH = 8.6				

3.2.2 Simulated Cast Stone Leachate

The simulated Cast Stone leachate recipe (Table 3.6) was based on the average of two 92-day static leach tests of Hanford grout made from actual tank waste supernate from tank 241-AN-106 (Serne et al. 1989).

Table 3.6. Simulated Cast Stone Leachate Preparation (based on Hanford grout leach test from tank AN-106; modified after Serne et al. [1989])

Order of Addition	Concentration (Molar)	Reagent	Molecular Weight (g/mol)	Quantity of Reagent Added (g/L)
1	9.352E-03	NaOH	40.00	0.3741
2	4.707E-04	$NaAlO_2$	81.97	0.03858
3	1.258E-03	Na_2CO_3	105.99	0.1333
4	7.406E-04	$Na_2SiO_3 \cdot 9H_2O$	284.24	0.2105
5	2.320E-02	$NaNO_3$	84.99	1.972
6	7.017E-05	$Na_2B_4O_7 \cdot 10H_2O$	381.42	0.02676
7	3.224E-03	Na_2SO_4	142.04	0.4579
8	3.435E-04	NaCl	58.44	0.02008
9	1.174E-02	$NaNO_2$	69.00	0.8100
10	9.476E-04	KCl	74.55	0.07064
11	6.842E-05	NaF	41.99	0.002873
12	6.895E-04	$Na_3PO_4 \cdot 12H_2O$	380.18	0.2621
13	1.654E-04	$CaCl_2$	110.99	0.01835
NaOH added until pH = 12.1				

3.2.3 Contaminant Spike Concentrations

Contaminants of concern (^{99}Tc, ^{129}I, and Cr) were spiked into the solutions in concentrations expected to be representative of the predicted leachates (Table 3.4). Specific forms of the contaminants were as follows: for Tc, $^{99}TcO_4^-$ was used; for iodine, both I^- and IO_3^- were used; and for Cr, CrO_4^{2-} was used. Stable ^{127}I was used as a surrogate for ^{129}I.

Table 3.7. Measured Contaminant Spike Concentrations

Contaminant	IDF Pore Water	Glass Leachate	Cast Stone Leachate
Cr	0.35 mg/L	0.52 mg/L	0.5 mg/L
Tc	0.045 mg/L	0.044 mg/L	0.382 mg/L
Iodide	41 µg/L	105 µg/L	45µg/L
Iodate	50 µg/L	80 µg/L	50 µg/L

3.3 Batch Adsorption/Desorption Experiments

Batch adsorption experiments were conducted to quantify adsorption kinetics by allowing adsorption to occur over the following time intervals: 1 day, 3 days, 7 days, 14 days, and 28 days. Because the contaminants of concern are known to adsorb weakly, a high solid-to-solution ratio of 1 g:1 mL was used.

Each batch adsorption/desorption experiment was conducted in a 50-mL polytetrafluoroethylene (PTFE) centrifuge tube at room temperature (~22 °C). The experiments were performed at a solid-to-solution ratio of 25 g sediment to 25 mL solution (IDF pore water, ILAW glass leachate, or Cast Stone leachate). Batch experiments were conducted in duplicate for each sampling time, individually for each contaminant ($^{99}TcO_4^-$, I^-, IO_3^-, and CrO_4^{2-}) and each of the three solutions, for a total of 120 individual experiments: 5 sampling times × 2 (duplicate tests) × 4 contaminants × 3 leaching solutions = 120 tests. Twenty-five grams of the composite ILAW sediment C3177-215 (<2-mm size

fraction, unwashed) were weighed out in each centrifuge tube. Twenty-five milliliters of solution spiked with contaminant were added and then placed on an orbital shaking table to equilibrate.

Control samples (designated as "blanks") consisted of 25 mL of the spiked solution in a centrifuge tube, without sediment, and were run through the same protocol. The final concentration of contaminant in each blank tube at the time of sampling the other tubes containing the sediment-leachant slurry was used as the initial concentrations needed to calculate K_d values. The control samples (blanks) allow one to check for contaminant adsorption onto the centrifuge tube walls and/or contaminant instability (e.g., precipitation or volatilization).

Sampling was performed nominally at 1, 3, 7, 14, and 28 days. Effluent was sampled by first centrifuging the tube to consolidate the solids. The solution was then decanted from the tube, filtered through a 0.45-µm filter membrane, and then divided into aliquots for the following analyses: pH, alkalinity, IC, inductively coupled plasma-optical emission spectroscopy (ICP-OES), and inductively coupled plasma-mass spectrometry (ICP-MS). The ICP-OES and ICP-MS aliquots were acidified with Optima grade 70% HNO_3 (except those aliquots for iodine analysis). The pH was measured as soon as was reasonably practical. Alkalinity and IC aliquots were not preserved.

Batch desorption data were collected using the adsorption sediment after long periods (generally between 44 and 97 days for the Cr; 34 and 80 days for the Tc; and 142 and 206 days for the iodide and iodate tubes) wherein the adsorption sediments sat in their respective residual spiked leachants (between 6 and 8 mL) before unspiked leachant was added to return to the 1:1 solid-to-solution ratio.

Prior to addition of the unspiked solution, the remaining volume of the contacting solution in each batch reactor was measured. This was done to 1) accurately calculate the amount of unspiked solution to be added to maintain the same solid-to-solution ratio (1 g:1 mL) as that used in the adsorption experiments, and 2) calculate residual contaminant concentrations that would contribute to the contaminant fraction desorbed. After the unspiked leachants were added, the tubes were shaken for an additional 28 days. After the 28-day desorption contact time, the tubes were centrifuged and the supernate solution was removed and filtered before being analyzed for the contaminant of concern.

The adsorption K_d values were calculated using the following equation:

$$K_d = \frac{\left(C_{blank} - C_{eff}\right) * V}{C_{eff} * M_{sed}}$$

where

C_{blank} = concentration of contaminant in blank tube supernate for contact time X (µg/mL)
C_{eff} = concentration of contaminant in sediment tube supernate for contact time X (µg/mL)
V = volume of spiked solution contacting sediment (mL)
M_{sed} = mass of oven dry sediment used in test (g).

In all the adsorption tests, the volume of spiked solution was 25 mL and the mass of sediment was 25 g of <2-mm size fraction.

The equation used to calculate the desorption K_d values is

$$K_{d\ (desorption)} = \frac{\left[\left(C_{eff} * V_{res}\right) + \left(C_{blank} - C_{eff}\right) * V_{ads}\right] - \left[C_{desorb} * V_{desorb}\right]}{C_{desorb} * M_{sed}}$$

where

C_{blank} = concentration of contaminant in blank adsorption tube supernate for contact time X (µg/mL)
C_{eff} = concentration of contaminant in sediment adsorption tube supernate for contact time X (µg/mL)
C_{desorb} = concentration of contaminant in sediment desorption tube supernate for contact time X (µg/mL)
V_{ads} and V_{desorb} = volume of solution in tube during contact with sediment (= 25 mL in both cases)
V_{res} = volume of residual spiked adsorption solution (C_{eff}) left in tube at end of adsorption step
M_{sed} = mass of sediment in the tube (=25 g in all cases).

The numerator in the desorption K_d equation is the mass of contaminant remaining on the sediment at the end of the desorption testing. The first term in brackets, [ ], is the mass of contaminant in the tube at the end of the adsorption phase of the test, and the numerator term in the second set of brackets is the mass in the desorption solution. Thus, the mass left on the sediment at the end of the desorption portion of the test can be calculated. The batch data results show that the second term in the desorption K_d numerator, $\left(C_{blank} - C_{eff}\right) * V_{ads}$, is often negative, which is physically impossible as long as the sediment does not release (leach) additional contaminant naturally present. This negative value is caused by there being so little adsorption of these mobile contaminants that analytical variability or anion exclusion (anions concentrate into the bulk solution) creates the negative values. When measuring the two concentrations, C_{blank} and C_{eff}, which will be nearly the same value for both quantities as long as there is no significant container wall adsorption in the blank tubes and the contaminant in solution is stable (i.e., not precipitating or volatilizing), the difference between two concentrations is dominated by analytical variability. This can then lead to negative values that are not physically meaningful. The second cause of negative values is anion exclusion (see Kaplan et al. [1998a] for explanation and details).

3.4 Saturated Column Adsorption/Desorption Experiments

Saturated column adsorption-desorption experiments for $^{99}TcO_4^-$, CrO_4^{2-}, I^-, and IO_3^- transport were conducted following the method described in previously published papers (Qafoku et al. 2004, 2009). Three solutions of synthetic IDF pore water, ILAW glass leachate, and Cast Stone leachate were used for the saturated column experiments. Duplicate columns were prepared only for TcO_4^- in each solution.

IDF sediments (<2-mm size fraction only) were used to pack uniformly in 15-cm-long and 2.5-cm inner-diameter acid-washed glass columns (Figure 3.2). The columns were packed with sediment to a bulk density of 1.85 to 1.93 g/cm^3. A 0.25-cm-thick membrane support at both ends of the column (10-µm pore size) allowed passage of the fluids while retaining the particles. Column-specific parameters such as porosity, bulk density, average linear velocity, Darcy velocity, and fluid residence time were calculated for each column based on measurements taken during packing (Table 3.8).

Darcy's velocity was determined by using the equation:

$$q = \mathrm{Q/A}$$

where

q = Darcy velocity (cm/hr)
Q = volumetric flow rate (cm^3/hr)
A = flow area perpendicular to flow path (cm^2).

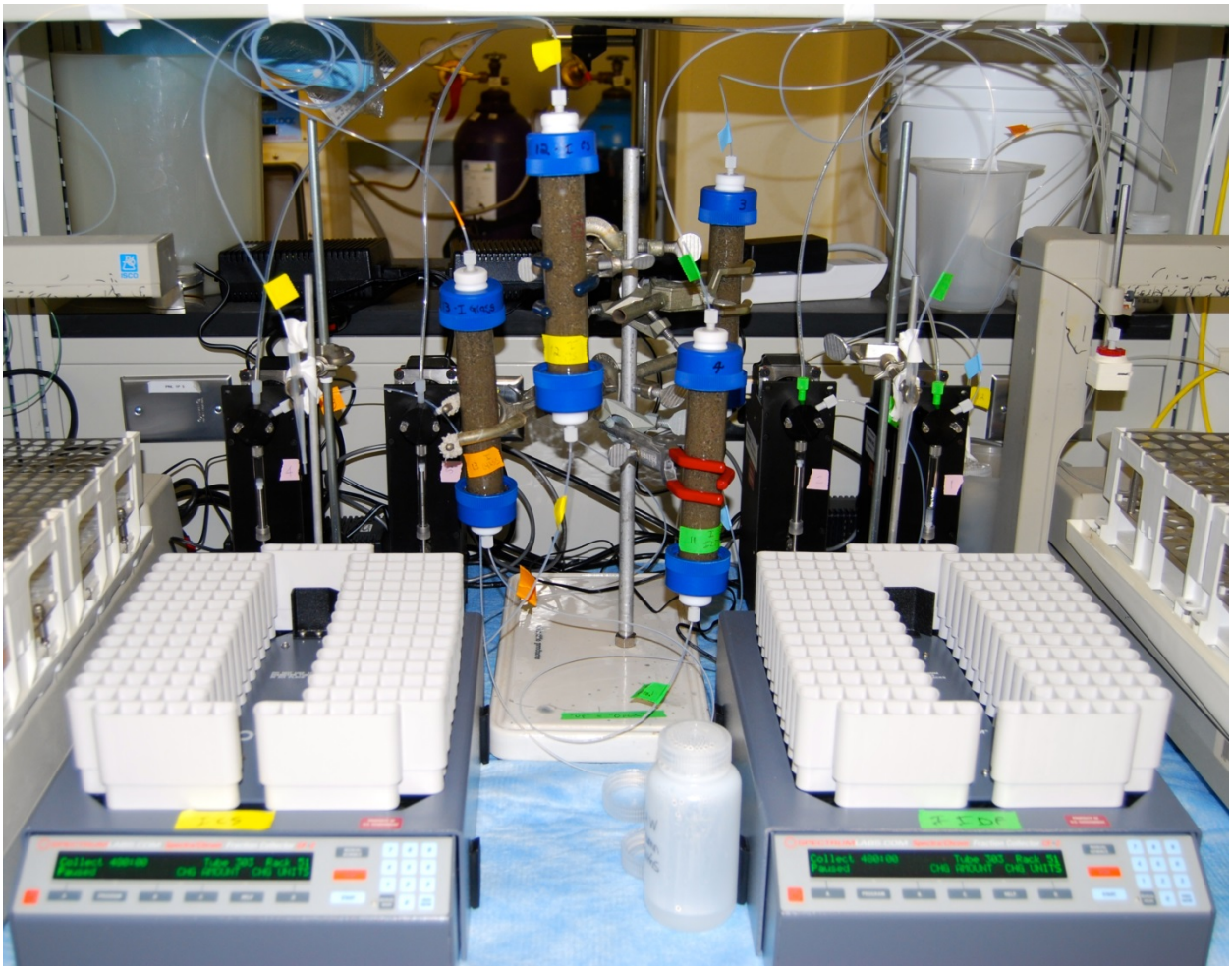

Figure 3.2. Hydraulically Saturated Column Experiments for Iodide in IDF Pore Water (right two columns) and Cast Stone Leachate (left columns)

Table 3.8. Column Conditions and Transport Parameters

Columns	Solutions	Porosity [-]	Bulk Density (g/cm^3)	Darcy Velocity (cm/hr)	Average Linear Velocity (cm/hr)
^{99}Tc-1	IDF pore water	0.27	1.87	0.11	0.42
^{99}Tc-2 (dup)	IDF pore water	0.29	1.88	0.12	0.41
^{99}Tc-1	ILAW glass leachate	0.22	1.85	0.10	0.47
^{99}Tc-2 (dup)	ILAW glass leachate	0.22	1.86	0.12	0.53
^{99}Tc-1	Cast Stone leachate	0.17	1.87	0.10	0.62
^{99}Tc-2 (dup)	Cast Stone leachate	0.17	1.88	0.12	0.69
CrO_4^{2-}	IDF pore water	0.20	1.89	0.11	0.56
CrO_4^{2-}	ILAW glass leachate	0.27	1.91	0.12	0.44
CrO_4^{2-}	Cast Stone leachate	0.19	1.89	0.12	0.62
I^-	IDF pore water	0.25	1.90	0.12	0.47
I^-	ILAW glass leachate	0.27	1.93	0.12	0.44
I^-	Cast Stone leachate	0.26	1.93	0.12	0.45
IO_3^-	IDF pore water	0.18	1.88	0.12	0.63
IO_3^-	ILAW glass leachate	0.18	1.89	0.12	0.65
IO_3^-	Cast Stone leachate	0.18	1.93	0.12	0.64

Kloehn syringe pumps were used to continuously inject leachant solution (contaminant-spiked leachants during the adsorption phase and unspiked leachant during the desorption phase) through the columns at a constant flow rate to provide sufficient adsorption equilibrium time inside the column. Nominally, the flow rate was ~0.018 mL/min, yielding a fluid residence time (time required for one pore volume to pass through the column) of ~21 to 36 hours. Each column was pre-saturated from the bottom with the appropriate unspiked leachate solution until full saturation was reached (as indicated by effluent coming out of the column and column mass reaching a maximum constant value), and the unspiked leachate solution was continuously introduced for 24 to 48 hours to remove any dispersible particles and obtain a constant flow condition. Then, spiked leachant was continuously pumped through the column for 5 pore volumes, after which flow in the column was stopped for 48 hours, and then restarted for another 3 to 4 pore volumes before being switched with unspiked leachate solution for the desorption part of the column experiment. After 5 pore volumes of leachate were collected in the desorption part of the column experiment, a second 48-hour stop-flow event was performed, followed by collecting an additional 5 pore volumes of effluent.

Effluent subsamples of about 5 mL were collected at predetermined time intervals (depending on the actual flow rate). Each effluent sample was filtered through a 0.45-µm filter membrane and analyzed for the contaminant of concern. Complete analyses were performed on selected samples (every tenth sample), including pH, alkalinity, IC (major anions), ICP-OES (major cations), and ICP-MS (selected trace elements). Each of these selected effluent samples was divided into two aliquots, with the first aliquot (~3 mL) for IC analysis. Alkalinity and pH were measured on adjacent samples due to the small volume of each sample. The second aliquot (2 mL) was acidified with Optima grade 70% HNO_3 (for Tc and Cr samples only) and analyzed by ICP-OES and ICP-MS for major cations and Tc, respectively.

At the conclusion of the flow-through testing, a bromide (100 ppm in NaBr) tracer test was conducted. The bromide (Br^-) was used as a non-reactive tracer to compare Br^- mobility to the transport results for the contaminant of concern. Three pore volumes of the bromide-containing leachant were pumped through the columns at the previously used flow rate. After 3 pore volumes, the leachant was

switched to the bromide-free leachant and pumping continued at the same rate for 3 more pore volumes. Effluent subsamples were collected every 5 mL and analyzed for bromide only.

Transport parameters were determined by curve fitting (based on the advection-dispersion equation) to the measured BTCs using the CXTFIT code (Parker and van Genuchten 1984; Toride et al. 1999). BTCs were graphically represented by plotting the relative concentration, C/C_o, versus pore volumes eluted. The equilibrium model (Toride et al. 1999) was applied to analyze the experimental column breakthrough data. The equilibrium model, described in dimensionless terms, is

$$R\frac{\partial C}{\partial T} = \frac{1}{P}\frac{\partial^2 C}{\partial Z^2} - \frac{\partial C}{\partial Z}$$

where

$$T = \frac{vt}{L}, \quad Z = \frac{x}{L}, \quad C = \frac{c}{c_o}, \quad P = \frac{vL}{D}, \quad R = 1 + \frac{\rho_B K_d}{\theta}$$

and T = dimensionless time equal to pore volume; t = time (T); L = column length (L); v = linear pore water velocity (LT^{-1}); Z = dimensionless distance; x = distance from the input (L); C = relative concentration between initial (c_o) and effluent (c) concentrations (ML^{-3}); P = Peclet number [-]; D = hydrodynamic dispersion coefficient (L^2T^{-1}); R[-] = retardation factor determined by the equation containing bulk density (ρ_b) (ML^{-3}), porosity (Θ) (L^3L^{-3}), and distribution coefficient (K_d) ($M^{-1}L^3$).

3.5 Unsaturated Column Adsorption/Desorption Experiments

A hydraulically unsaturated column experiment, at approximately 35% saturation, was conducted to evaluate the impact of unsaturated conditions on contaminant transport through IDF sediments relative to saturated conditions. The unsaturated column experiment was only conducted using Tc-spiked IDF pore water.

An acrylic column with a 3.175-cm internal diameter and a 20-cm length was packed with IDF sediment (Figure 3.3). Porous ceramic tensiometers made of 1-cm outside diameter acrylic tubing with a 0.67-cm outside diameter ceramic porous cup (2.54 cm long) were placed at the upper and lower end of the column. The two tensiometers were positioned 4 cm from each end, yielding a 12-cm length between the two tensiometers. Each tensiometer was connected to a pressure transducer (PX26-015GV, Omega Engineering, Inc.) with a pressure range up to ±1 bar and compensated temperature range of -30 to 70 °C, and data were recorded with a datalogger (CR3000, Campbell Scientific Inc., Logan, UT) to monitor water potential. Prior to the start of the test, the tensiometer and data acquisition system were calibrated (Figure 3.4) using a pressure controller (PCD series, 1 bar range, Alicat Scientific, Tucson, AZ). A low-flow mass flow controller (LC series, 5 cm^3 range, Alicat Scientific, Tucson, AZ) was used to inject solution into the packed column inlet at the top of the column. The inlet was covered with a nylon membrane. Constant water potential (suction) was maintained by using a hanging water column attached to the outlet at the bottom of the column. The solution was introduced from the top of the column and the weight of the column was periodically measured using a balance to monitor the water content change before, during, and after the experiment. The level of saturation was adjusted by varying both the input flow rate and the water potential at the bottom of the column.

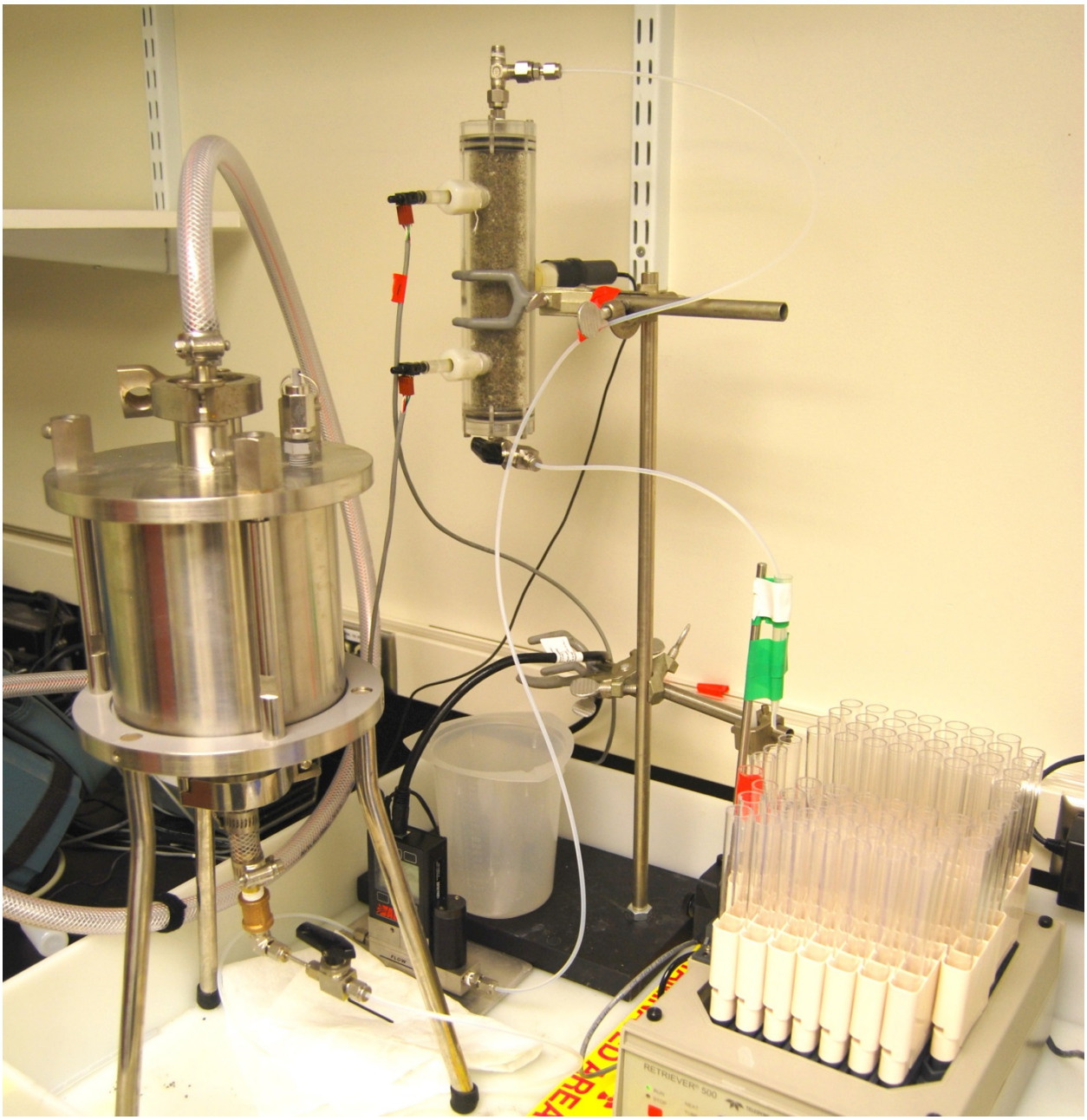

Figure 3.3. Hydraulically Unsaturated Column Experiment for ^{99}Tc in IDF Pore Water

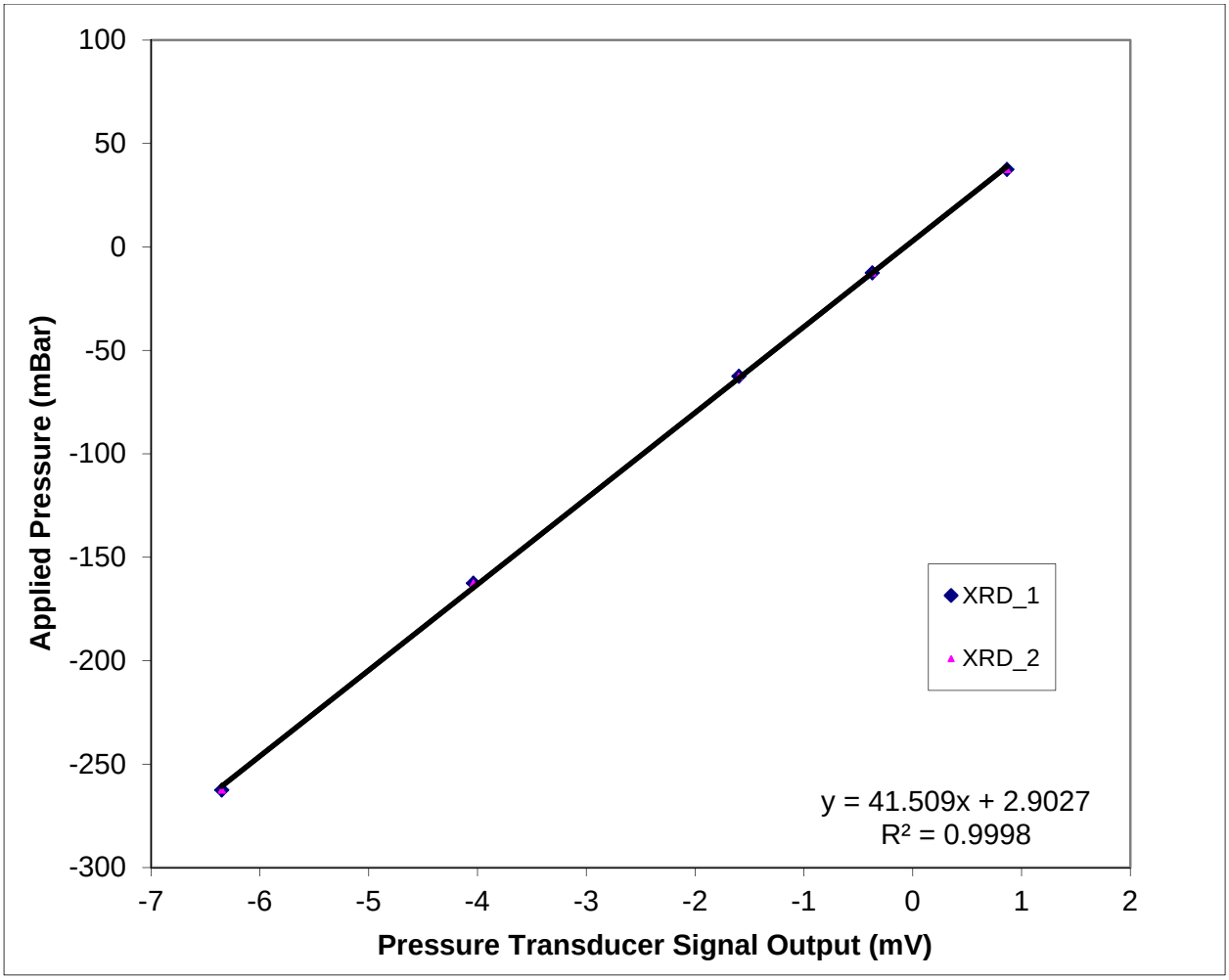

Figure 3.4. Tensiometer Calibration Results

Similar to the saturated column experiments, a Tc-spiked solution equivalent to 3 saturated pore volumes was flowed through the column and effluent samples of approximately 5 mL were collected hourly using an autosampler. Each effluent sample was filtered through a 0.45-µm filter membrane and analyzed for the contaminant of concern. Complete analyses were performed on selected samples (every tenth sample), including pH, alkalinity, IC (major anions), ICP-OES (major cations), and ICP-MS (selected trace elements). Each of these selected effluent samples was divided into two aliquots, with the first aliquot (3 mL) analyzed for pH, IC, and alkalinity. The second aliquot (2 mL) was acidified with Optima grade 70% HNO_3 and analyzed by ICP-OES and ICP-MS.

After the above-described contaminant breakthrough test was completed, the influent solution was switched to the unspiked/contaminant-free leachant, and the flow-through experiment continued. A complete suite of analyses was conducted on selected samples (every tenth sample) as described above.

At the conclusion of the flow-through testing, a bromide (100 ppm NaBr) tracer test was conducted. A solution with bromide-containing leachant equivalent to 3 saturated pore volumes was pumped through the columns at the previously used flow rate. After 3 saturated pore volumes, the leachant was switched

to the bromide-free leachant and pumping continued at the same rate for 3 more saturated pore volumes. Effluent subsamples were collected every 5 mL and analyzed for bromide only.

3.6 Effluent Analysis

Effluent solution analyses were conducted to quantify the concentrations of major cations, key contaminants, major anions, pH, and alkalinity. Inductively coupled plasma analyses (ICP-OES and ICP-MS) were used to quantify the major cations and key contaminants.

Major cation analyses (including Al, Si, Ca, Mg, Na, K, Fe, Ti, P, and Mn, as well as B, Zn, and S) of extract/test solutions were performed on either a Perkin Elmer OPTIMA 3300 DV or OPTIMA 8300 (Waltham, MA) ICP-OES using procedure PNNL-ESL-ICP-OES, *Inductively Coupled Plasma-Optical Emission Spectrometry (ICP-OES) Analysis*[1], which is similar to EPA Test Method SW-846 6010C, *Inductively Coupled Plasma-Atomic Emission Spectrometry* (EPA 2007). A serial dilution was made of select samples to investigate and correct for matrix interferences.

Trace element analyses (e.g., ^{99}Tc, I [stable ^{127}I], and Cr) were performed by Perkin Elmer ELAN DRC II (Waltham, MA) ICP-MS following procedure PNNL-ESL-ICPMS, *Inductively Coupled Plasma Mass Spectrometry (ICP-MS) Analysis)*[2]. A serial dilution was made of select samples to investigate and correct for matrix interferences. Instrument detection limits in high-saline matrices such as glass and grout leachates for ICP-MS are expected to be in the part-per-billion range or better.

Major anions (F^-, Cl^-, NO_2^-, NO_3^-, Br^-, PO_4^{3-}, and SO_4^{2-}) were determined using IC. Analytical instrumentation consisted of a Dionex ion chromatograph with a Dionex AS17 column using a gradient elution of 1 to 35 mM potassium hydroxide and measured with a conductivity detector.

The alkalinity was determined by standard titration with acid, and pH was measured with a solid-state pH electrode and a user-calibrated pH meter calibrated with NIST-traceable standards.

Iodide (I^-) and iodate (IO_3^-) speciation analyses were conducted using a Thermo X-Series II Quadrapole ICP-MS using an ESI FAST Autosampler system and Iodine Speciation Kit. The ESI Autosampler and Iodine Speciation Kit consisted of a sampling loop designed to inject a known volume of sample into a proprietary in-line 4 x 50-mm anion exchange column that separates iodide and iodate species from each other. The sample loop also has valves and pumps that are programmed to quickly flush the anion exchange column between sample injections. Each sample was first loaded onto the front end of the anion exchange column that separated the iodate from the iodide using the ESI FAST autosampler. Once the iodine-containing sample was injected into the anion exchange column, it was eluted using 2% nitric acid. Within the iodine specific anion exchange column, the iodate was separated

[1] PNNL. 2014a. *Inductively Coupled Plasma-Optical Emission Spectrometry (ICP-OES) Analysis.* Technical Procedure PNNL-ESL-ICP-OES, Rev. 3, Pacific Northwest National Laboratory, Richland, Washington.
[2] PNNL. 2014b. *Inductively Coupled Plasma Mass Spectrometry (ICP-MS) Analysis*. Technical Procedure PNNL-ESL-ICPMS, Rev. 3, Pacific Northwest National Laboratory, Richland, Washington.

from the iodide[1]. Given the specific system flow rates, iodate begins to elute off of the column after approximately 70 seconds while the peak representing iodide begins after approximately 340 seconds. The anion exchange column effluent was introduced directly into the Thermo X-Series II Quadrapole ICP-MS and the separated iodine peaks were quantified by collecting data at the 127 mass channel (iodine). Mass data were collected for 80 continuous short periods totaling ~8 minutes of real time, and the two peak areas (representing first iodate and later iodide) were calculated using periSPEC 6.0 software (ESI). Calibration curves were generated using known concentrations of iodate and iodide (both separately and mixed) solutions in deionized water. The outputs from the ICP-MS and periSPEC 6.0 software were processed using Microsoft Excel. The iodide and iodate standards were SPEX CertiPrep single element (single-species) standards (1000 ppm).

3.7 Geochemical Modeling

Geochemical modeling of selected effluent solutions (e.g., Cr-spiked Cast Stone leachate) was conducted to determine if mineral phases are dissolving or precipitating and to assess if this had any influence on the adsorption/desorption reactions, and to determine dominant species of the contaminant(s).

[1] It should be noted that there is likely no correlation between transport of iodate and iodide in this proprietary ion exchange column and their transport through Hanford sediments. In the former the process separating the iodine species is a physical process while in sediments iodine species transport is controlled by chemical interactions.

4.0 Results

This section presents the results of adsorption/desorption batch K_d and flow-through column experiments for Tc as $^{99}TcO_4^-$, iodine as both I^- and IO_3^-, and Cr as CrO_4^{2-} under conditions relevant to the far-field, sand-dominated Hanford formation sediments beneath the IDF, using simulated ILAW glass and Cast Stone leachates, and uncontaminated vadose zone pore water. Section 4.1 presents characterization data for the sediment used in the experiments. Section 4.2 presents the results of the batch adsorption and desorption experiments. Section 4.3 presents the results of saturated flow-through column experiments, and Section 4.4 presents the results of an unsaturated flow-through column experiment. Section 4.5 describes the macro solution analyses and iodine speciation, and Section 4.6 presents some geochemical modeling results.

4.1 Supplemental Sediment Characterization

SEM and SEM-EDS analyses were performed on a batch sediment sample that had been contacted with Cr-spiked simulated glass leachate (28-day contact time, post desorption) and on a sediment sample that had not been contacted with any of the solutions described in this report. These analyses provided high-resolution images of surface morphology and particle size of individual sediment particles and semi-quantitative elemental concentration data for specific micron-size locations within the samples (the EDS detection limit for different elements is approximately 1%) (Figure 4.1). The modeling results presented in Section 4.6 of this report suggested that carbonate minerals have formed during these experiments. In addition, Fe oxides might have also formed. (The presence of Fe-bearing coatings was suggested in a few SEM-EDS measurements taken in the post-treatment sample – data not shown.) Both carbonate minerals and Fe oxides have been shown to incorporate contaminants, such as Cr, into their crystal structure. However, Cr-bearing precipitates were not observed on the surfaces of the particles using this technique, although many particles in the sample were carefully inspected. This is to be expected based on the EDS detection limit.

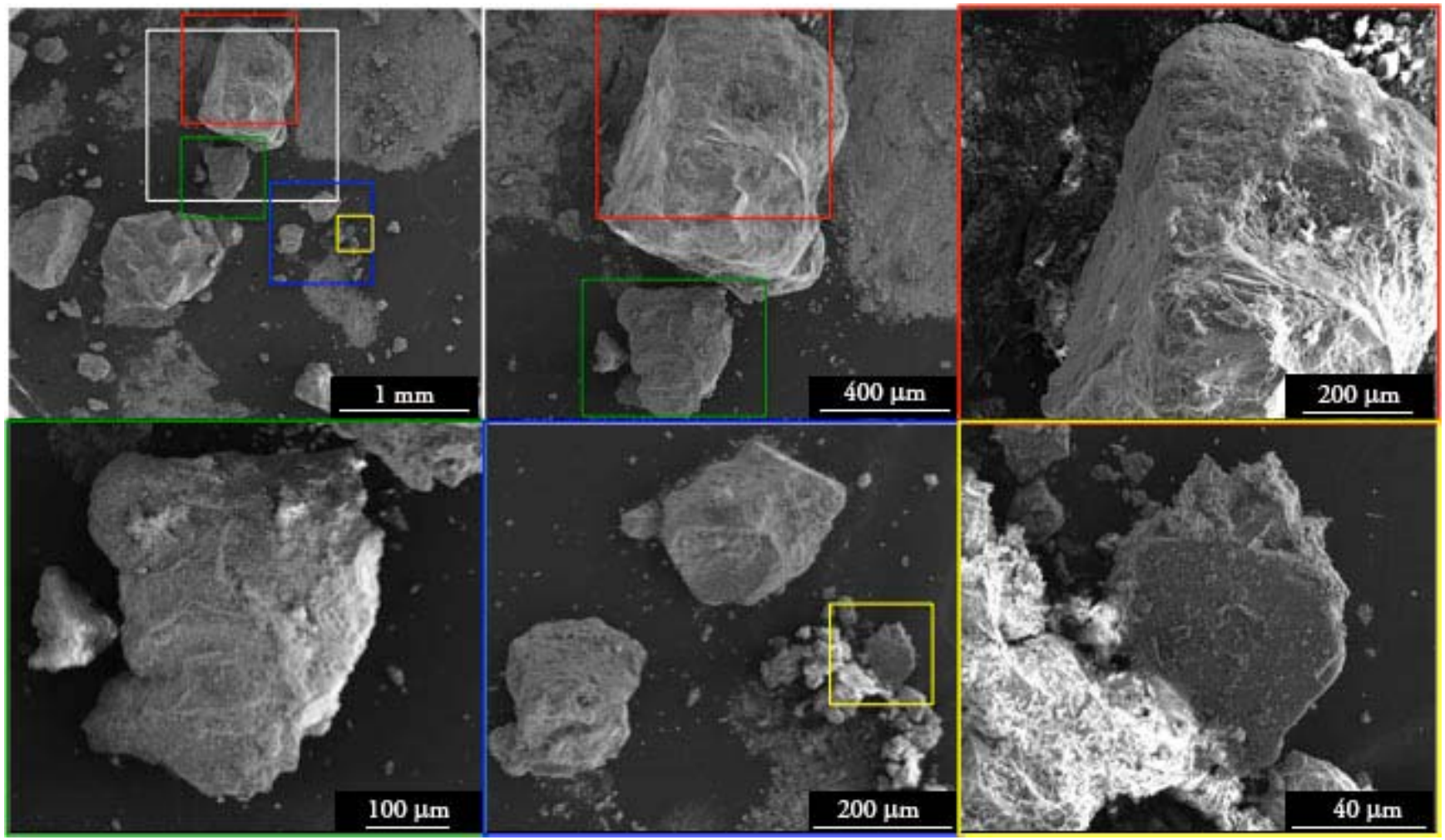

Figure 4.1. SEM Images of the Cr-contacted Glass Batch Sample (post desorption)

4.2 Batch Adsorption/Desorption Experiments

The results of the batch adsorption-desorption K_d experiments are provided in this section. The data are described for each of the four mobile contaminants in separate subsections starting with technetium, followed by chromium, iodide, and ending with iodate.

Both the calculated adsorption and desorption K_d values are often negative, which are shown in bold type in Table 4.1 and Table 4.2. These negative K_d values should be considered as representing no significant adsorption, or K_d equal to zero. As noted in EPA 1999, the batch K_d methodology is not well suited for measuring K_d values for non-sorbing species. Rather, the flow-through column methods described in Sections 3.4 and 3.5 are recommended.

4.2.1 Technetium ($^{99}TcO_4^-$)

The batch adsorption K_d values for the pertechnetate anion in the three different leachants are shown in Table 4.1. The pertechnetate desorption K_d values are shown in Table 4.2.

4.2.1.1 IDF Pore Water

The pertechnetate batch adsorption K_d values for IDF vadose zone pore water contacting the Hanford formation sand as a function of contact time for three of the contact times (1, 14, and 28 days) are negative and for the other two contact times (3 and 7 days) are very low positive numbers (ranging from 0.04 to 0.10 mL/g). There is no trend versus contact time, and we interpret the data as showing no adsorption. The starting pH of the IDF pore water blanks averaged 7.51 ± 0.16 and the IDF effluents that contained Tc averaged 7.76 ± 0.05,[1] which suggests little change occurs during the test, and the concentration of ^{99}Tc in the blank tubes at all five contact times remained stable and close to the value spiked into the pore water (see Table 3.7). Therefore, the pertechnetate added to the IDF vadose zone pore water appears to be stable over time and does not appreciably adsorb to the centrifuge tube walls. There was no ^{99}Tc observed in the batch adsorption test results where the IDF sand sediment was contacted with unspiked IDF vadose zone pore water, as one would expect.

Thus, we conclude that the batch adsorption results for ^{99}Tc spiked into the IDF vadose zone pore water suggest that there is no appreciable adsorption occurring over the 28-day contact period, and the slightly negative to slightly positive calculated K_d values represent inherent analytical imprecision in measurements of the C_{blank} and C_{eff} values or perhaps anion exclusion that forces anions away from the inherent negatively charged sediment surfaces. For batch K_d testing with a solid-to-solution ratio of 1, after centrifugation to separate solution from solids, anions concentrate in the bulk solution above the wet sediment, and this may contribute to the C_{eff} values being larger than the C_{blank} values. Kaplan et al. (1998a) and EPA (1999, Section 2.8) discuss the anion exchange phenomenon in greater detail.

[1] Note that the pH values for each blank and batch adsorption effluent for the four contaminants (TcO_4^-, CrO_4^{2-}, I^-, and IO_3^- are presented in Table 4.4 in the discussion of the changes in chemical composition of the batch K_d solutions.

4.2.1.2 Cast Stone Leachate

The pertechnetate batch adsorption K_d values are negative for simulated Cast Stone leachate contacting the Hanford formation sand for four of the contact times (1, 3, 14, and 28 days) as well as at least one or both of the replicates, and for the other contact time (7 days) the replicates are very low positive numbers (ranging from 0.03 to 0.04 mL/g). There is no trend versus contact time and we interpret the data as showing no adsorption. The starting pH in all the Cast Stone blanks was 11.94 ± 0.06 and final pH of the Cast Stone leachates that contained Tc dropped to 10.3 within 1 day and down to 9.3 after 28 days of contact, suggesting that contact with the sediments buffers the caustic Cast Stone leachate pH, perhaps by dissolution of some sediment solid phases. The concentration of ^{99}Tc in the Cast Stone blank tubes at all five contact times remained stable and close to the value spiked into the simulated Cast Stone leachate (see Table 3.7). Therefore, the pertechnetate added to the Cast Stone leachate appears to be stable over time and does not appreciably adsorb to the centrifuge tube walls. There was no ^{99}Tc observed in the batch adsorption test where the IDF sand sediment was contacted with unspiked Cast Stone leachate, as one would expect. Thus, we conclude that the batch adsorption results for ^{99}Tc spiked into the Cast Stone leachate suggest that there is no appreciable adsorption occurring over the 28-day contact period and the slightly negative to slightly positive calculated K_d values represent inherent analytical imprecision in measurements of the C_{blank} and C_{eff} values or alternatively the impacts of anion exclusion.

4.2.1.3 ILAW Glass Leachate

The pertechnetate batch adsorption K_d values are slightly positive numbers (ranging from 0.00 to 0.02 mL/g) for simulated ILAW glass leachate contacting the Hanford formation sand as a function of contact time for all but two of the replicates of the contact times (1 and 28 days). There is no trend versus contact time and we interpret the data as showing no significant adsorption. The starting pH of the simulated ILAW glass leachate blanks was 8.63 ± 0.05 and the glass leachate effluents containing Tc had an average pH of 7.93 ± 0.10, suggesting minor buffering by the sediment. The sediment buffering of the glass leachates occurs rapidly and there is no continual decrease in effluent pH with time as was observed for the Cast Stone effluents. The concentration of ^{99}Tc in the glass leachate blank tubes at all five contact times remained stable and close to the values spiked into the ILAW glass leachate (see Table 3.7). Therefore, the pertechnetate added to the simulated ILAW glass leachate appears to be stable over time and does not appreciably adsorb to the centrifuge tube walls. There was no ^{99}Tc observed in the batch adsorption test where the IDF sand sediment was contacted with unspiked ILAW glass leachate, as one would expect. Thus, we conclude that the batch adsorption results for ^{99}Tc spiked into the ILAW glass leachate suggest that there is at most very minor adsorption (K_d = 0.01 mL/g), but just as likely one could conclude that there is no appreciable adsorption over the 28-day contact period. The few slightly negative to several slightly positive calculated K_d values likely represent inherent analytical imprecision in measurements of the C_{blank} and C_{eff} values.

4.2.1.4 Desorption/Discussion

The ^{99}Tc desorption batch K_d results, shown in Table 4.2, for all three solutions contacting the IDF Hanford formation sand show more variation (desorption K_d values range from -0.38 to 0.98 mL/g) than the adsorption results. However, the calculated desorption K_d results show no trend versus adsorption contact time or solution type. Further, because there was a significant hiatus (during which time the moist

sediment remained in contact with residual spiked C_{eff}) between the end of the adsorption portion of the batch testing and the start of the desorption tests, all the desorption data should be considered contact time-independent. After 28 days of desorption into unspiked leachants, the average desorption K_d for the IDF sediment contacting the IDF vadose zone pore water was 0.04 ± 0.23 mL/g; for the Cast Stone leachate 0.00 ± 0.19 mL/g; and for the ILAW glass leachate 0.18 ± 0.27 mL/g (0.09 ± 0.04 mL/g, excluding one anomalously high value). These batch ^{99}Tc adsorption and desorption K_d values are not statistically different from zero. Thus, we recommend assuming that there is no adsorption or desorption of ^{99}Tc as pertechnetate in these three solutions contacting the IDF sand-dominated sediment. This conclusion is consistent with the most recent IDF and Hanford Site geochemical data packages that also assign a ^{99}Tc K_d value of zero (e.g., Krupka et al. 2004, Last et al. 2006; see Table 2.9 and Table 2.10).

4.2.2 Chromium (CrO_4^{2-})

The batch adsorption K_d values for the chromate anion in the three different leachants are shown in Table 4.1. The chromate desorption K_d values are shown in Table 4.2.

4.2.2.1 IDF Pore Water

The chromate batch adsorption K_d values for at least one of the replicates for IDF vadose zone pore water contacting the Hanford formation sand as a function of contact time show negative K_d values for the first two contact times (1 and 3 days). For the longer contact times, the chromate K_d values are positive (ranging from 0.14 to 0.67 mL/g). There appears to be a trend of increasing K_d versus contact time for the IDF vadose zone pore water contacting the Hanford sand-dominated sediment. The pH of all the IDF pore water blanks averaged 7.51 ± 0.16 while the pH of the IDF pore water effluents that contained Cr was 7.71 ± 0.06, suggesting little buffering is occurring. The concentration of Cr in the IDF pore water blank tubes at all five contact times remained stable and close to the value spiked into the pore water (see Table 3.7). Therefore, the chromate added to the IDF vadose zone pore water appears to be stable over time and does not appreciably adsorb to the centrifuge tube walls. There was no Cr observed in the batch adsorption test where the IDF sand sediment was contacted with unspiked IDF vadose zone pore water, so it does not appear that the sediment leaches measurable natural Cr, as expected.

Thus, we conclude that the batch adsorption results for chromate spiked into the IDF vadose zone pore water may show some adsorption, K_d values ranging from 0.14 to 0.67 mL/g, after 7 days of contact. However, there were measureable changes in the concentrations of some of the macro constituents in the effluents compared to the blank solutions such that dissolution/precipitation reactions might be physically incorporating chromate within newly formed solids. A much better method of measuring chromate sorption potential to the IDF sand sediment is using the flow-through column tests described in Section 3.4.

4.2.2.2 Cast Stone Leachate

The chromate batch adsorption K_d values for simulated Cast Stone leachate contacting the Hanford formation sand as a function of contact time suggest some adsorption after 7 days of contact. K_d values between 7 and 28 days of Cast Stone leachate contact with the IDF sand-dominated sediment range from 0.03 to 0.64 mL/g. The starting pH of all the Cast Stone blanks was 11.94 ± 0.06 and final pH of the Cast Stone leachate effluents that contained chromate dropped to 9.8 within 1 day and down to 9.1 after

28 days of contact, suggesting that contact with the sediments buffers the caustic Cast Stone leachate pH by dissolution of some sediment solid phases. The concentration of Cr in the Cast Stone leachate blank tubes at all five contact times remained stable and close to the value spiked into the simulated Cast Stone leachate (see Table 3.7). Therefore, the chromate added to the Cast Stone leachate appears to be stable over time and does not appreciably adsorb to the centrifuge tube walls.

There was no Cr observed in the batch adsorption test where the IDF sand sediment was contacted with unspiked Cast Stone leachate, suggesting that no naturally occurring Cr in the sediment was leached during reaction with Cast Stone leachate. It is likely that some of the observed adsorption of chromate after 7 days or more of contact is caused by dissolution/precipitation reactions as the caustic Cast Stone leachate is buffered to pH values of about 9. At least 150 to 275 µg of silicon precipitates from the Cast Stone leachate during contact with the sediment, and it is possible that some chromate is captured in the newly formed precipitate. The batch samples that show an adsorption K_d of 0.637 mL/g only removed ~4 µg of chromate from the starting Cast Stone leachate.

The significant change in pH and precipitation/sorption of constituents such as Si, Na, and K, and the release of Ca (data discussed in Section 4.5) from the Cast Stone leachate, confound the batch adsorption test interpretation. The proper methodology for running adsorption tests is to pre-equilibrate unspiked solution with the sediment until almost all chemical changes have occurred and the slurry is at "equilibrium." At this point, the spiked solution is added and only adsorption reactions should occur. In the batch tests presented herein there was no pre-equilibration of the three starting solutions with the IDF Hanford formation sand. The macro chemistry of the C_{eff} for all three solutions shows appreciable changes in several constituents in comparison to the C_{blank} compositions, especially for the Cast Stone leachate.

Thus, we conclude that the batch adsorption results for chromate spiked into the Cast Stone leachate suggest that there may be some adsorption, K_d ranging 0.03 to 0.64 mL/g, over the 28-day contact period. However, co-precipitation or physical entrainment in newly formed solid phases may also be the cause for all or some of the observed loss of chromate from the Cast Stone leachate. We suggest that the flow-through column tests, described in Section 4.3, might better address chromate adsorption onto the IDF sediment.

4.2.2.3 ILAW Glass Leachate

The chromate batch adsorption K_d values for simulated ILAW glass leachate contacting the Hanford formation sand as a function of contact time suggest adsorption occurs at all contact times (1 through 28 days) and the sorption steadily increases with contact time. Calculated K_d values range from 0.02 to 2.1 mL/g after 1-day and 28-day contact times, respectively. The pH of the simulated ILAW glass leachate blanks was 8.63 ± 0.05, while the pH of glass leachate effluents that contained chromate averaged 7.98 ± 0.04, suggesting that the sediments buffered the glass leachate somewhat through dissolution reactions. The concentration of chromate in the glass leachate blank tubes at all five contact times remained stable and close to the values spiked into the ILAW glass leachate (see Table 3.7). Therefore, the chromate added to the simulated ILAW glass leachate appears to be stable over time and does not appreciably adsorb to the centrifuge tube walls. There was no chromate observed in the batch adsorption test where the IDF sand sediment was contacted with unspiked ILAW glass leachate, suggesting that no naturally occurring Cr in the sediment was leached during reaction with glass leachate.

There were some macro chemistry changes in the ILAW glass leachate during the 28-day contact with the sediment. Silicon precipitated (up to 1.2 mg) and K, Mg, and Ca were released, most likely from cation exchange sites as the high sodium concentration in the glass leachates replaced these other cations on sediment exchange sites. The relatively large amount of silicon that is lost from solution (precipitated) might have captured some of the chromate that was lost from solution (from 0.4 to 8.7 mg); however, more chromate than silicon is removed from solution, so it would appear that chromate adsorption onto the Hanford sand sediment is occurring when contacted by glass leachate. One other possibility is that leachate interactions with the sediment could be caused by the reduction of dissolved Cr(VI) to Cr(III) by the slow release of Fe(II) from basaltic minerals in the Hanford sediment (Cantrell et al. 2003; Qafoku et al. 2003; Zachara et al. 2003). This reduction results in the precipitation of solid $Cr(OH)_3$ and results in apparent high K_d values. However, the leaching of Fe(II) from basaltic minerals occurs only at acidic or very caustic conditions and the glass leachate pH varied only from 8.7 down to 8. It would appear that Fe(II) release from interactions with the sediment and subsequent reduction of Cr(VI) to Cr(III) might be more plausible for the Cast Stone leachate than for the glass leachate. Thus, we conclude that the batch adsorption results for chromate spiked into the ILAW glass leachate suggest that there could be some adsorption (K_d ranging from 0.02 to 2.1 mL/g) when glass leachate contacts IDF sand sediments. However, we recommend that the flow-through column results discussed in Section 4.3 may be a more definitive set of data on chromate adsorption onto the IDF sand sediment in contact with simulated glass leachate.

4.2.2.4 Desorption/Discussion

The chromate desorption batch K_d results, shown in Table 4.2, for all three solutions contacting the IDF Hanford formation sand exhibit more variation than the adsorption results and show a pronounced increase with adsorption contact time. However, because there was a significant hiatus (during which time the moist "adsorption" sediment remained in contact with residual spiked C_{eff}) between the end of the adsorption portion of the batch testing and the start of the desorption tests, all the desorption data could be considered contact time-independent. That is, the sediments sat in the residual adsorption solution for between 44 and 97 days before the 28-day desorption test started. Thus, the observed trend showing significantly increasing desorption K_d values based on the 1- to 28-day adsorption contact times is not consistent with expected behavior in a system wherein only adsorption-desorption mechanisms are occurring.

After 28 days of desorption, the average Cr desorption K_d for the IDF sediment contacting the IDF vadose zone pore water was 4.6 ± 3.1 mL/g, for the Cast Stone leachate the Cr desorption K_d was 0.42 ± 1.05 mL/g, and for the ILAW glass leachate Cr desorption K_d was 79 ± 60 mL/g. These batch Cr desorption K_d values are significantly higher than the Cr adsorption K_d values, and we have no explanation aside from the fact that the Cr-containing sediment remained in the residual spiked effluents for up to 97 days, wherein continued dissolution/precipitation reactions may have physically sequestered Cr or perhaps reduced chromate to insoluble Cr(III) hydroxides. Both K_d data sets suggest chromate does adsorb to the Hanford sand-dominated sediment from all three solutions, which differs from past IDF and Hanford Site geochemical data packages that assign a chromate K_d value of zero (e.g., Krupka et al. 2004; Last et al. 2006; see Table 2.9 and Table 2.10). Again, we recommend that the flow-through column tests be given more weight than these batch adsorption-desorption tests given their questionable results.

4.2.3 Iodide (I^-)

The batch adsorption K_d values for the iodide anion in the three different leachants are shown in Table 4.1. The iodide desorption K_d values are shown in Table 4.2.

4.2.3.1 IDF Pore Water

All of the iodide batch adsorption K_d values for IDF vadose zone pore water contacting the Hanford formation sand as a function of contact time show negative K_d values. The iodide K_d values range from -0.02 to -0.12 mL/g with no trend versus contact time. The pH of all the IDF pore water blanks averaged 7.51 ± 0.16 while the pH of effluents with iodide spike averaged 7.68 ± 0.11, suggesting little buffering is occurring. The concentration of iodide in the blank tubes at all five contact times remained stable and close to the value spiked into the pore water (see Table 3.7). Therefore, the iodide added to the IDF vadose zone pore water appears to be stable over time and does not appreciably adsorb to the centrifuge tube walls. There was no iodide observed in the batch adsorption test where the IDF sand sediment was contacted with unspiked IDF vadose zone pore water, so it does not appear that the sediment leaches measurable natural iodide. Thus, we conclude that the batch adsorption results for iodide spiked into the IDF vadose zone pore water may show some impact from anion exclusion, which results in slightly negative calculated K_d values, or the slightly negative calculated K_d values represent inherent analytical imprecision in measurements of the C_{blank} and C_{eff} parameters.

As noted in EPA (1999), the batch K_d methodology is not well suited for measuring K_d values for non-sorbing species. Rather, the flow-through column methods described in Section 3.4 are recommended to measure iodide K_d values. Selecting a K_d equal to zero for vadose zone pore water and groundwater based on these results differs from the most recent IDF geochemical data package (Krupka et al. 2004), which chose an iodide adsorption K_d value of 0.25 mL/g based on batch K_d tests run by Um and Serne (2005) and Um et al. (2004).

4.2.3.2 Cast Stone Leachate

The iodide batch adsorption K_d values for simulated Cast Stone leachate contacting the Hanford formation sand as a function of contact time suggest some minor adsorption only after 28 days of contact. K_d values between 1 and 14 days of Cast Stone leachate contact with the IDF sand-dominated sediment are slightly negative (ranging from 0.00 to -0.05 mL/g). The pH of all the Cast Stone leachate blanks was 11.94 ± 0.06, while the pH of the effluents that contained iodide spike varied from 10 after 1 day of contact and 9.26 after 28 days of contact, suggesting that contact with the sediments buffers the caustic Cast Stone leachate pH by dissolution of some sediment solid phases. The concentration of iodide in the blank tubes containing Cast Stone leachate at all five contact times remained stable and close to the value spiked into the simulated Cast Stone leachate (see Table 3.7). Therefore, the iodide added to the Cast Stone leachate appears to be stable over time and does not appreciably adsorb to the centrifuge tube walls. There was no iodide observed in the batch adsorption test where the IDF sand sediment was contacted with unspiked Cast Stone leachate, suggesting that no naturally occurring iodide in the sediment was leached during reaction with Cast Stone leachate. We conclude that the batch adsorption results for iodide spiked into the Cast Stone leachate exhibit no appreciable adsorption for contact times less than 28 days.

It is not clear whether some slight iodide sorption is occurring at 28 days contact. A similar increase in iodide sorption with long contact times (up to almost a year) was observed by Kaplan et al. (1998a) for iodide-spiked groundwater contacting a Hanford Site sediment similar to the IDF sediments. However, there was some concern that microbiological activity may have been occurring in the long-term batch adsorption tests and was causing the increased iodide sorption. We suggest that the flow-through column tests might better address iodide adsorption onto the IDF sediment from the various solutions used in this study. The choice of an iodide K_d equal to zero for the caustic Cast Stone leachate agrees with results found in Kaplan et al. (2003), wherein sediments and pure minerals subjected to 0.3 M NaOH solutions spiked with various contaminants showed no adsorption of iodide. However, 0.3 M NaOH is significantly more caustic than the Cast Stone leachate used herein.

4.2.3.3 ILAW Glass Leachate

The iodide batch adsorption K_d values for simulated ILAW glass leachate contacting the Hanford formation sand as a function of contact time suggest little to no adsorption occurs at all contact times (1 through 28 days). Calculated iodide adsorption K_d values range from -0.05 to 0.17 mL/g, with 8 of the 10 data yielding negative K_d values regardless of contact time. The pH of the simulated ILAW glass leachate blanks was 8.63 ± 0.05, while the pH of effluents that contained the iodide spike averaged 7.92 ± 0.09, suggesting some minor buffering by the sediments. The concentration of iodide in the glass leachate blank tubes started at 110 µg/L, near the value spiked (105 µg/L; see Table 3.4) but then decreased monotonically to a value of 68 µg/L in the 28-day blank glass leachate simulant. Thus, either the iodide is not stable in the ILAW glass leachate or it starts to adsorb onto the container walls. This decreasing iodide concentration (from 110 µg/L down to 87 and then down 68 µg/L between 7 and 28 days) confounds the calculation of an accurate K_d.

Past work (Um and Serne 2005) using a different simulated glass leachate and carrier-free ^{125}I as iodide found some slight iodide adsorption onto sand-dominated sediment from the same borehole as used herein. Um and Serne (2005) found iodide K_d values that ranged from 0.04 to 0.16 mL/g in batch tests performed at a solid-to-solution ratio of 1 g:10 mL for the carrier-free (no mass of stable iodide) ^{125}I simulated glass leachate. Our current batch results were for a slightly different glass leachate spiked with ~110 µg/L iodide and performed at a solid-to-solution ratio of 1 g:1 mL solution. Use of carrier-free ^{125}I may have allowed some adsorption onto select iodide-low abundant sediment adsorption sites that would be swamped out by the larger starting concentration of stable iodide in the current testing. The net effect of using the higher starting concentration of stable iodide would result in lower sorption and thus lower K_d values. On the other hand, using the higher solid-to-solution ratio in the current tests compared to the Um and Serne (2005) tests should result in more relative sorption in the current tests. Given the apparent instability of iodide in the current blanks, we would recommend that the flow-through column data be used to replace the past iodide K_d values found in Um and Serne 2005, which were selected by Krupka et al. (2004) for IDF PA usage because the glass leachate used by Um and Serne (2005) is no longer an accurate glass leachate simulant.

4.2.3.4 Desorption/Discussion

The iodide desorption batch K_d results, shown in Table 4.2, for the IDF pore water and Cast Stone leachate solutions contacting the IDF Hanford formation sand exhibit more variation than the adsorption results and yield negative K_d values. The desorption K_d values for the glass leachate are slightly more

positive for the early contact data, but are negative values for the later adsorption contact times. However, given the apparent instability of iodide in the glass leachate blank containers, the equation used to calculate desorption K_d values may not be valid. Further, because there was a significant hiatus (during which time the moist "adsorption" sediment remained in contact with residual spiked C_{eff}) between the end of the adsorption portion of the batch testing and the start of the desorption tests, all the desorption data should be considered contact time-independent. That is, the sediments sat in the residual adsorption solution for between 142 and 168 days before the 28-day desorption test started. Thus, we are reluctant to use the iodide desorption data to make any recommendations for future IDF PA use[1].

4.2.4 Iodate (IO_3^-)

The batch adsorption K_d values for the iodate anion in the three different leachants are shown in Table 4.1. The iodate desorption K_d values are shown in Table 4.2.

4.2.4.1 IDF Pore Water

All of the iodate batch adsorption K_d values for IDF vadose zone pore water contacting the Hanford formation sand as a function of contact time show positive K_d values (0.19 to 0.38 mL/g) with no trend versus contact time. The pH of the IDF pore water blank averaged 7.51 ± 0.16 and the IDF pore water effluents that contained iodate spike averaged 7.62 ± 0.08, suggesting little buffering is occurring during the tests. The concentration of iodate in the blank tubes at all five contact times remained stable near the value spiked into the pore water (see Table 3.7). There was no total iodine observed in the batch adsorption test where the IDF sand sediment was contacted with unspiked IDF vadose zone pore water, so it does not appear that the sediment leaches measurable natural iodate. Thus, we conclude that the batch adsorption results for iodate spiked into the IDF vadose zone pore water may show some slight adsorption, which results in slightly positive calculated K_d values. In general sorption literature for iodine species it is often reported that iodate adsorbs to sediments more readily than iodide (e.g., Krupka et al. 2004). However, as noted in EPA (1999), the batch K_d methodology is not well suited for measuring K_d values for non-sorbing and weakly sorbing species. Rather, the flow-through column methods described in Sections 3.4 and 3.5 are recommended to measure K_d for mobile contaminants. None of the most recent geochemical data packages (e.g., Krupka et al. 2004 and Cantrell et al. 2003) discusses iodate separately from total iodine. The current recommendation for an iodine (generally assumed to iodide) adsorption K_d value is 0.25 mL/g when vadose zone pore water or groundwater is the solution of interest. The value is based on batch K_d tests run by Um and Serne (2005) and Um et al. (2004). For now, we recommend use of an iodate K_d value between zero and 0.4 mL/g in sensitivity cases for far-field, relatively natural geochemical conditions.

4.2.4.2 Cast Stone Leachate

The iodate batch adsorption K_d values for simulated Cast Stone leachate contacting the Hanford formation sand as a function of contact time suggest some adsorption occurs from contact times between

[1] Data from blank tubes (containing only spiked simulants) show significant loss of total iodine with time. That is, it appears that total iodine mass deceased, either by container wall sorption or volatilization (escape from the blank tubes and perhaps also tubes containing wet sediment). Additionally, the long hiatus between the end of the adsorption test and beginning of the desorption test takes the desorption data outside the reasonable assurance of absorption/desorption equilibrium conditions. Thus, we do not recommend using them to effect K_d parameters.

1 and 28 days. Iodate K_d values range between 0.11 and 0.27 mL/g regardless of contact time for Cast Stone leachate contacting the IDF sand-dominated sediment. The starting pH was 11.9 and final pH of the Cast Stone leachate dropped to 9.8 within 1 day and down to 9.1 after 28 days of contact, suggesting that contact with the sediments buffers the caustic Cast Stone leachate pH, perhaps by dissolution of some sediment solid phases. The concentration of iodate in the blank tubes containing Cast Stone leachate at all five contact times remained stable and close to the value spiked into the simulated Cast Stone leachate (see Table 3.7). Therefore, the iodate added to the Cast Stone leachate appears to be stable over time and does not appreciably adsorb to the centrifuge tube walls.

There was no total iodine observed in the batch adsorption test where the IDF sand sediment was contacted with unspiked Cast Stone leachate, suggesting that no naturally occurring iodine (and thus no iodate) is in the sediment. There were some macro chemistry changes in the Cast Stone leachate during the 28-day contact with the sediment. Silicon precipitated (up to 0.3 mg) and Ca was released, most likely from cation exchange sites on the sediment. The high sodium concentration in the Cast Stone leachate replaced Ca on sediment exchange sites. The silicon that was lost from solution (precipitated) might have captured some of the iodate that was lost from solution (from 0.15 to 0.28 mg). Thus, we conclude that the batch adsorption results for iodate spiked into the Cast Stone leachate may suggest that there is some adsorption (K_d ranging from 0.11 and 0.27 mL/g), but other reactions besides adsorption might have removed some of the iodate from solution. Better test methods are needed, where sediments are pre-equilibrated with the Cast Stone leachate such that other macro chemistry reactions are completed before performing the iodate adsorption tests. We recommend that the slightly positive observed iodate K_d values be used only in IDF PA sensitivity analyses should the use of a zero K_d result in unacceptable groundwater ^{129}I concentrations.

4.2.4.3 ILAW Glass Leachate

The iodate batch adsorption K_d values for simulated ILAW glass leachate contacting the Hanford formation sand as a function of contact time show large variability but in general suggest some adsorption occurs at all contact times (1 through 28 days). Calculated iodate adsorption K_d values range from -0.13 to 1.5 mL/g, with 8 of the 10 data yielding positive K_d values regardless of contact time. The pH level of the simulated ILAW glass leachate blanks was 8.63 ± 0.05 and the pH of the glass leachate effluents that contained iodate averaged 7.91 ±0.07, suggesting small amounts of buffering by the sediment. One disconcerting issue is that the concentration of iodate in the glass leachate blank tubes decreased significantly and monotonically from the starting iodate concentration (80 µg/L) spiked into the glass leachate to 49 µg/L in the 3-day contact blank to about 40 µg/L in the 14- and 28-day contact blanks. When this same iodate glass leachate solution was used in the flow-through column tests, the iodate concentration was only 33.9 µg/L. Thus, either the iodate is not stable in the ILAW glass leachate or it starts to adsorb onto the container walls. This decreasing iodate concentration (from ~82 to 38 µg/L between 3 and 28 days) confounds the calculation of an accurate K_d. Therefore, the iodate added to the glass leachate appears to exhibit significant container adsorption or perhaps some volatility (loss from the blank tubes).

Interestingly, the iodate in the effluent solutions separated from the sediment also shows dramatic decreases in concentration. These observed decreased iodate concentrations may create the positive adsorption K_d values. Based on the decreased iodate concentrations in the effluent supernate solution, we suspect that there is a loss of iodate from the tubes containing sediment similar to that observed in the

blank tubes. Total iodine instability when trace concentrations are present in solutions with near-neutral to acidic pH is commonly observed (see for example Brown et al. 2005, 2007). This apparent loss of iodate in the blank tubes results in the consistent positive calculated K_d values. Thus, we are reluctant to recommend the measured batch iodate adsorption K_d values for glass leachate reported herein for use in future IDF PAs. If these iodate adsorption K_d values (range -0.13 to 1.5 mL/g with average 0.40 ± 0.48 mL/g) are used for the glass leachate solution in future IDF PA activities, we recommend also performing a sensitivity analysis using a K_d equal to zero to compare predicted groundwater concentrations. There has been no past work spiking iodate into IDF-relevant leachates that were then contacted with Hanford Site sediments. All the past work used iodide-spiked solutions (e.g., Um and Serne 2005; Um et al. 2004).

4.2.4.4 Desorption/Discussion

The iodate desorption batch K_d results, shown in Table 4.2, for the IDF pore water contacting the IDF Hanford formation sand exhibit more variation than the adsorption results and yield positive K_d values ranging from 0.37 to 0.82 mL/g. The desorption K_d for the Cast Stone leachate also exhibits all positive K_d values ranging from 0.20 to 0.44 mL/g. The desorption K_d for the glass leachate are quite variable (range -0.57 to 1.41 and average 0.41 ± 0.67 mL/g). Given the apparent instability of iodate in the glass leachate blank containers (and likely the effluents from the sediment slurries), the equation used to calculate desorption K_d values may not be valid. Further, because there was a significant hiatus (during which time the moist "adsorption" sediment remained in contact with residual spiked C_{eff}) between the end of the adsorption portion of the batch testing and the start of the desorption tests, all the desorption data could be considered contact time-independent. That is, the sediments sat in the residual adsorption solution for between 180 and 206 days before the 28-day desorption test started. It is quite possible that more iodate was removed from the solution in the centrifuge tubes either by volatilization or container wall adsorption during the 180 to 206 days that the tubes were stored. Thus, we are reluctant to use the iodate desorption data for the glass leachate to make any recommendations for future IDF PA use[1].

Although desorption K_d values for contaminants often are greater than adsorption K_d values, referred to as some element of irreversible or kinetically slow sorption (see EPA [1999] and Um et al. [2004] for more discussion), the desorption data for all four contaminants studied in each of the simulants herein are suspect because of the long hiatus before starting the desorption portion of the batch tests. We do not recommend using the desorption data generated from this work in future IDF PA modeling that accommodates two-tiered (adsorption-desorption) or irreversibility constructs. The flow-through column breakthrough tests described elsewhere in this report, especially those column tests that used stop-flow periods, are much better tests to address sorption kinetics/irreversibility issues.

[1] The potential loss of iodate by container wall sorption or volatilization, along with the long hiatus between the end of the adsorption test and beginning of the desorption test takes the desorption data outside the reasonable assurance of absorption/desorption equilibrium conditions. Thus, we do not recommend using them to effect K_d parameters.

Table 4.1. Batch Adsorption K_d Values (mL/g) for Three Solutions Contacting Hanford Formation Sand

	^{99}Tc as Pertechnetate			Cr as Chromate			Iodide (I^-)			Iodate (IO_3^-)		
Sample ID	K_d (mL/g)	AVG K_d (mL/g)	std dev.	K_d (mL/g)	AVG K_d (mL/g)	std dev.	K_d (mL/g)	AVG K_d (mL/g)	std dev.	K_d (mL/g)	AVG K_d (mL/g)	std dev.
IDF PW 1 day	**-0.10**	**-0.07**	0.04	**-0.08**	**-0.09**	0.01	**-0.12**	**-0.11**	0.01	0.24	0.21	0.03
IDF PW 1 day DUP	**-0.04**			**-0.09**			**-0.10**			0.19		
IDF PW 3 day	0.06	0.05	0.01	0.08	0.04	0.07	**-0.04**	**-0.06**	0.04	0.19	0.24	0.07
IDF PW 3 day DUP	0.04			**-0.01**			**-0.09**			0.28		
IDF PW 7 day	0.10	0.09	0.02	0.14	0.17	0.04	**-0.04**	**-0.04**	0.01	0.22	0.26	0.05
IDF PW 7 day DUP	0.08			0.20			**-0.03**			0.30		
IDF PW 14 day	**-0.01**	**-0.01**	0.01	0.41	0.35	0.09	**-0.02**	**-0.03**	0.02	0.33	0.29	0.05
IDF PW 14 day DUP	**-0.01**			0.28			**-0.04**			0.25		
IDF PW 28 day	**-0.07**	**-0.03**	0.05	0.61	0.64	0.04	**-0.05**	**-0.06**	0.01	0.39	0.36	0.03
IDF PW 28 day DUP	0.01			0.67			**-0.06**			0.34		
Cast Stone 1 day	**-0.04**	**-0.01**	0.04	**-0.11**	**-0.15**	0.05	**-0.01**	**-0.03**	0.03	0.13	0.14	0.01
Cast Stone 1 day DUP	0.02			**-0.18**			**-0.05**			0.15		
Cast Stone 3 day	0.00	**-0.03**	0.03	**-0.15**	**-0.13**	0.02	0.00	0.00	0.00	0.16	0.14	0.04
Cast Stone 3 day DUP	**-0.05**			**-0.11**			**-0.01**			0.11		
Cast Stone 7 day	0.03	0.04	0.01	0.10	0.06	0.05	**-0.01**	**-0.03**	0.02	0.18	0.18	0.01
Cast Stone 7 day DUP	0.04			0.03			**-0.04**			0.17		
Cast Stone 14 day	**-0.08**	**-0.02**	0.08	0.07	0.08	0.01	**-0.03**	0.00	0.03	0.27	0.23	0.05
Cast Stone 14 day DUP	0.03			0.09			0.02			0.20		
Cast Stone 28 day	0.03	0.00	0.03	0.64	0.62	0.03	0.00	0.02	0.03	0.26	0.24	0.02
Cast Stone 28 day DUP	**-0.02**			0.60			0.04			0.23		
Glass 1 day	0.00	0.00	0.01	0.00	0.02	0.02	**-0.12**	0.02	0.19	0.22	0.28	0.09
Glass 1 day DUP	0.01			0.03			0.16			0.35		
Glass 3 day	0.01	0.01	0.00	0.04	0.04	0.00	0.17	0.05	0.17	0.58	1.06	0.70
Glass 3 day DUP	0.01			0.04			**-0.08**			1.53		
Glass 7 day	0.01	0.01	0.01	0.19	0.15	0.07	**-0.22**	**-0.20**	0.03	**-0.09**	**-0.11**	0.03
Glass 7 day DUP	0.01			0.10			**-0.18**			**-0.13**		
Glass 14 day	0.00	0.01	0.01	0.60	0.79	0.27	**-0.14**	**-0.14**	0.00	0.12	0.14	0.03
Glass 14 day DUP	0.02			0.98			**-0.14**			0.17		
Glass 28 day	0.01	0.00	0.01	2.18	2.11	0.09	**-0.19**	**-0.12**	0.10	0.61	0.65	0.05
Glass 28 day DUP	0.00			2.05			**-0.05**			0.69		

Bold type signifies negative adsorption—physically not meaningful unless anion exclusion is operative.

Note: The possible precipitation of calcium carbonate minerals during the test could overstate the derived K_d values, at a minimum for Cr and iodate. See Section 4.6.

Table 4.2. Batch Desorption K_d Values (mL/g) for Three Solutions Contacting Hanford Formation Sand

	^{99}Tc as Pertechnetate			Cr as Chromate			Iodide (I^-)			Iodate (IO_3^-)		
Sample ID	K_d (mL/g)	AVG K_d (mL/g)	std dev.	K_d (mL/g)	AVG K_d (mL/g)	std dev.	K_d (mL/g)	AVG K_d (mL/g)	std dev.	K_d (mL/g)	AVG K_d (mL/g)	std dev.
IDF PW 1 day	**-0.38**	**-0.25**	0.19	**1.14**	**0.90**	0.33	**-0.48**	**-0.43**	0.07	**0.75**	0.72	0.04
IDF PW 1 day DUP	**-0.11**			**0.67**			**-0.38**			**0.70**		
IDF PW 3 day	0.19	0.18	0.02	4.26	3.56	0.99	-0.33	-0.34	0.02	0.53	0.56	0.05
IDF PW 3 day DUP	**0.16**			**2.86**			**-0.36**			**0.60**		
IDF PW 7 day	0.38	0.35	0.04	2.89	4.05	1.64	-0.20	0.40	0.85	0.37	0.44	0.10
IDF PW 7 day DUP	**0.32**			**5.21**			**0.99**			**0.51**		
IDF PW 14 day	-0.04	-0.03	0.01	5.38	4.82	0.79	-0.10	-0.16	0.08	0.54	0.55	0.03
IDF PW 14 day DUP	**-0.02**			**4.26**			**-0.21**			**0.57**		
IDF PW 28 day	-0.13	-0.04	0.12	NA	9.72	0.15	-0.14	-0.21	0.10	0.82	0.79	0.04
IDF PW 28 day DUP	**0.04**			**NA**			**-0.28**			**0.77**	0.72	0.04
Cast Stone 1 day	**-0.16**	**-0.02**	0.20	**-0.36**	**-0.51**	0.21	**-0.15**	**-0.19**	0.05	**0.33**	0.34	0.02
Cast Stone 1 day DUP	**0.12**			**-0.66**			**-0.22**			**0.35**		
Cast Stone 3 day	**-0.01**	**-0.10**	0.13	**-0.50**	**-0.42**	0.12	**-0.12**	**-0.12**	0.01	**0.20**	0.21	0.01
Cast Stone 3 day DUP	**-0.19**			**-0.34**			**-0.13**			**0.22**		
Cast Stone 7 day	**0.14**	0.13	0.01	**0.33**	0.28	0.08	**-0.07**	**-0.14**	0.10	**0.31**	0.27	0.06
Cast Stone 7 day DUP	**0.13**			**0.23**			**-0.21**			**0.23**		
Cast Stone 14 day	**-0.20**	**-0.07**	0.20	**0.48**	0.54	0.08	**-0.15**	**-0.06**	0.13	**0.44**	0.40	0.06
Cast Stone 14 day DUP	**0.07**			**0.59**			**0.03**			**0.36**		
Cast Stone 28 day	**0.35**	0.05	0.42	**2.06**	2.22	0.22	**-0.05**	-0.01	0.06	**0.20**	0.24	0.06
Cast Stone 28 day DUP	**-0.24**			**2.38**			**0.03**			**0.28**		
Glass 1 day	**0.07**	0.08	0.01	**28.66**	28.91	0.35	**-0.48**	0.09	0.81	**0.50**	0.66	0.23
Glass 1 day DUP	**0.08**			**29.15**			**0.66**			**0.83**		
Glass 3 day	**0.10**	0.09	0.02	**91.80**	82.37	13.33	**0.36**	0.09	0.39	**0.75**	0.96	0.30
Glass 3 day DUP	**0.08**			**72.95**			**-0.19**			**1.18**		
Glass 7 day	**0.13**	0.13	0.01	**29.53**	44.49	21.15	**-0.67**	-0.65	0.03	**-0.55**	-0.56	0.01
Glass 7 day DUP	**0.14**			**59.44**			**-0.63**			**-0.57**		
Glass 14 day	**0.95**	0.54	0.58	**54.95**	64.00	12.80	**-0.42**	-0.42	0.01	**0.12**	0.23	0.16
Glass 14 day DUP	**0.14**			**73.05**			**-0.41**			**0.35**		
Glass 28 day	**0.04**	0.04	0.00	**227.54**	176.18	72.63	**-0.64**	-0.26	0.54	**1.41**	0.74	0.95
Glass 28 day DUP	**0.03**			**124.82**			**0.12**			**0.07**		

Red type signifies that one or more terms in the desorption equation are not physically meaningful (negative mass sorbed on sediment).
NA = effluents not submitted for analysis
Note: The possible precipitation of calcium carbonate minerals during the test could overstate the derived K_d values, at a minimum for Cr and iodate. See Section 4.6.

4.3 Saturated Column Adsorption/Desorption Experiments

The results of the saturated flow-through adsorption/desorption experiments are provided in this section. The data are described for each of the four mobile contaminants in separate subsections starting with technetium, followed by chromium and iodide, and ending with iodate. Note that the relative concentrations (C/C_0) from these column experiments, including those of the bromide tracer, often exceed 1, reflecting analytical uncertainty within the experiments.

4.3.1 Technetium ($^{99}TcO_4^-$)

The migration of TcO_4^- spiked into IDF pore water, ILAW glass leachate, and Cast Stone leachate through IDF composite sediment (C3177-215) was evaluated using flow-through saturated column experiments. BTCs of TcO_4^- in three different solutions were developed with relative concentration (C/C_0) of TcO_4^- versus pore volume. The BTC of a non-reactive tracer, Br^-, was also plotted for qualitative comparison with TcO_4^- transport data.

4.3.1.1 IDF Pore Water

Duplicate columns were prepared for TcO_4^- in IDF pore water. The BTCs for TcO_4^- and Br^- spiked in IDF pore water solutions are presented with different colors and symbols in Figure 4.2. The transport behavior of TcO_4^- in IDF pore water was identical to that of the non-reactive tracer (Br^-). Relative concentration (C/C_0) of 0.5 was found close to 1.0 pore volume for both the TcO_4^- and Br^- BTCs in IDF pore water. This indicates that there is no retardation of TcO_4^- relative to that of Br^-, yielding a retardation factor of 1.0 and a K_d for TcO_4^- of zero from the following equation:

$$R = 1 + \frac{\rho_b}{\theta} K_d$$

where R = retardation factor [dimensionless], ρ_b = bulk density [g/cm^3], K_d = sorption distribution coefficient [mL/g], and θ = porosity [dimensionless]. Calculations using CXTFIT yielded K_d values of 0 and -0.01.

The pH values in the effluents ranged from 7.5 to 7.9, which is slightly higher than the initial IDF pore water pH (~7.2) due to additional carbonate mineral dissolution during the column experiment. Although a 48-hour stop-flow event was performed in both adsorption and desorption phases, there was no significant decrease or increase in TcO_4^- concentration in the effluents, suggesting no TcO_4^- sorption reaction on the IDF sediment in contact with IDF pore water. No sorption of TcO_4^- (i.e., $K_d = 0$) determined from the column experiment agrees well with the batch results (see Section 4.2.1) and previous Hanford site-specific reports discussed in Section 2.2.

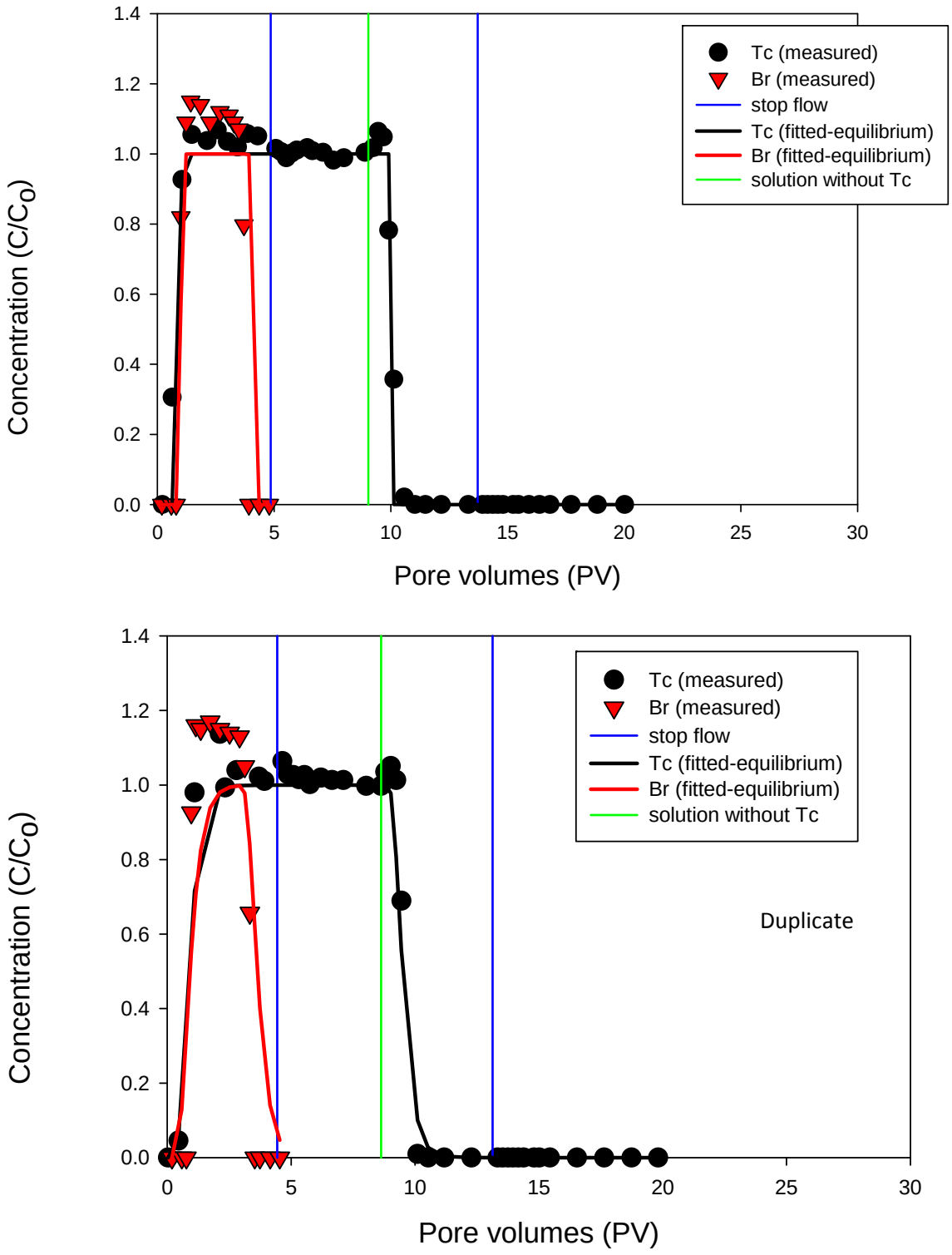

Figure 4.2. Breakthrough Curves for TcO_4^- and Br^- in IDF Pore Water (top) and Its Duplicate (bottom). The blue lines on the graph show the 48-hour stop-flow events. The green line represents where the solution was switched from IDF pore water containing TcO_4^- to IDF pore water without TcO_4^-.

4.3.1.2 Glass Leachate

The BTCs for TcO_4^- and Br^- in glass leachate columns also showed identical transport behavior between TcO_4^- and Br^- (Figure 4.3). The measured retardation transport parameter at $C/C_0 = 0.5$ indicated no chemical sorption (i.e., $K_d = 0$) of TcO_4^- on the IDF sediment in contact with simulated glass leachate. Similar calculations using CXTFIT yielded K_d values of 0 and -0.1. These results are consistent with the batch K_d results.

The pH of the initial effluents (<0.4 pore volume) was close to 8.1, which is lower than the starting pH of the simulated ILAW glass leachate (pH ~8.6). However, the pH in the effluent gradually increased and reached 8.6 to 8.7 after 18 pore volumes. The early effluent pH decrease in the column experiment was likely due to precipitation and ion exchange reactions between the glass leachate solution and the sediment. Similar small decreases in pH were observed in the batch effluents with simulated glass leachate. Despite the pH changes, there was no indication that TcO_4^- was sorbing on the sediment. In addition, there was no change of TcO_4^- concentration in the effluents with extended reaction of 48 hours after stop-flow.

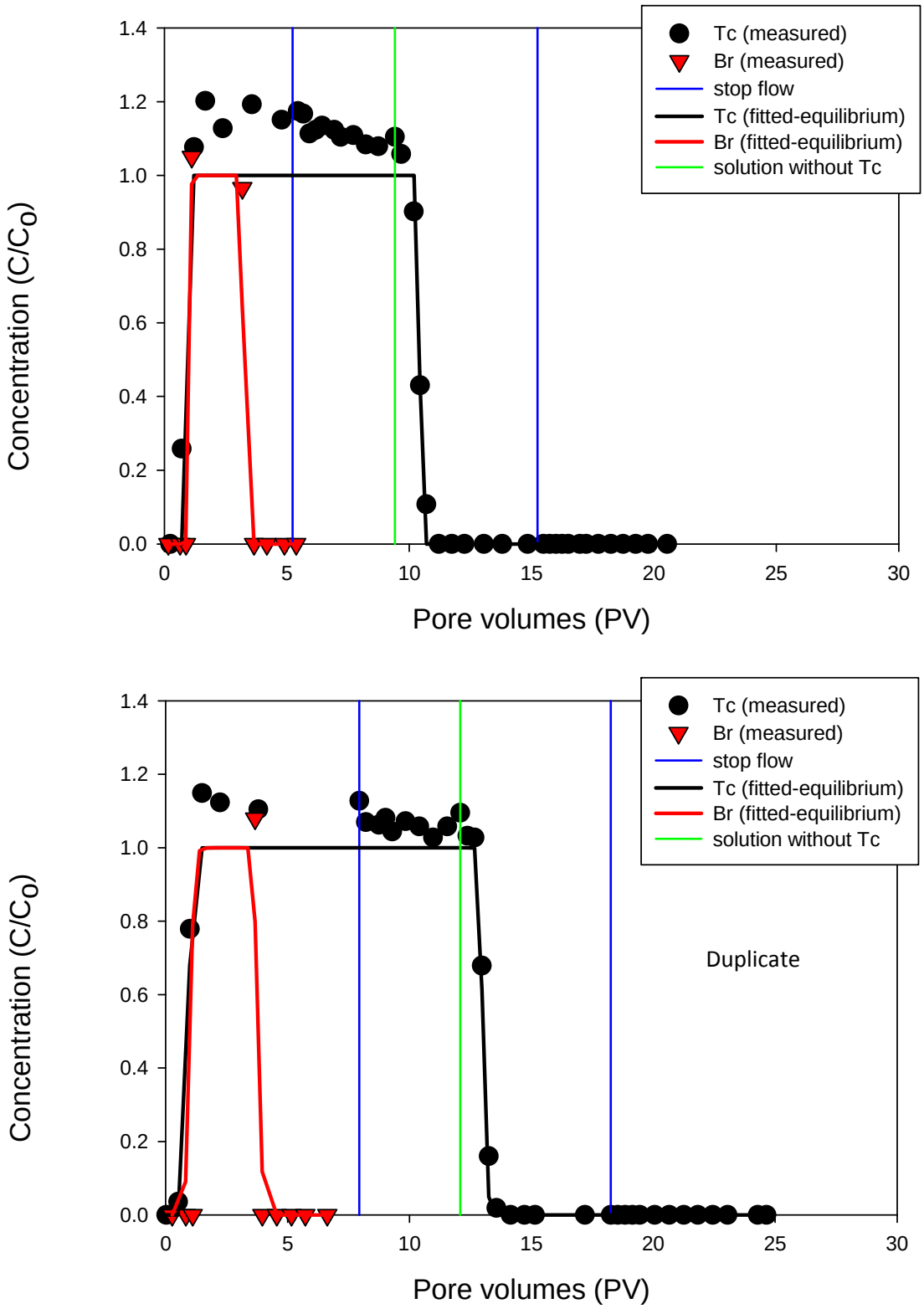

Figure 4.3. Breakthrough Curves for TcO_4^- and Br^- in Glass Leachate (top) and Its Duplicate (bottom). The blue lines on the graph show the 48-hour stop-flow events. The green line represents where the solution was switched from glass leachate containing TcO_4^- to glass leachate without TcO_4^-.

4.3.1.3 Cast Stone Leachate

The BTCs for TcO_4^- and Br^- in Cast Stone leachate are shown in Figure 4.4. They show very similar transport behavior, indicating no interaction with the sediment, resulting in a near-zero K_d for TcO_4^- in Cast Stone leachate. Calculations using CXTFIT yielded K_d values of 0.01 and 0.03 from the two columns.

The pH values of initial effluents were 7.7 to 8.0, but the pH levels increased up to 9.6 to 9.8 at the later stage after 20 pore volumes. However, these values are still lower than the starting pH (~11.9) of Cast Stone leachate. Despite having a low-pH condition like 7.7 in an early stage of adsorption phase, TcO_4^- transport was similar to non-reactive Br^-, indicating no chemical sorption of TcO_4^- on the IDF sediment in contact with Cast Stone leachate. In addition, no TcO_4^- concentration changes were found in the effluents after 48 hours of stop-flow.

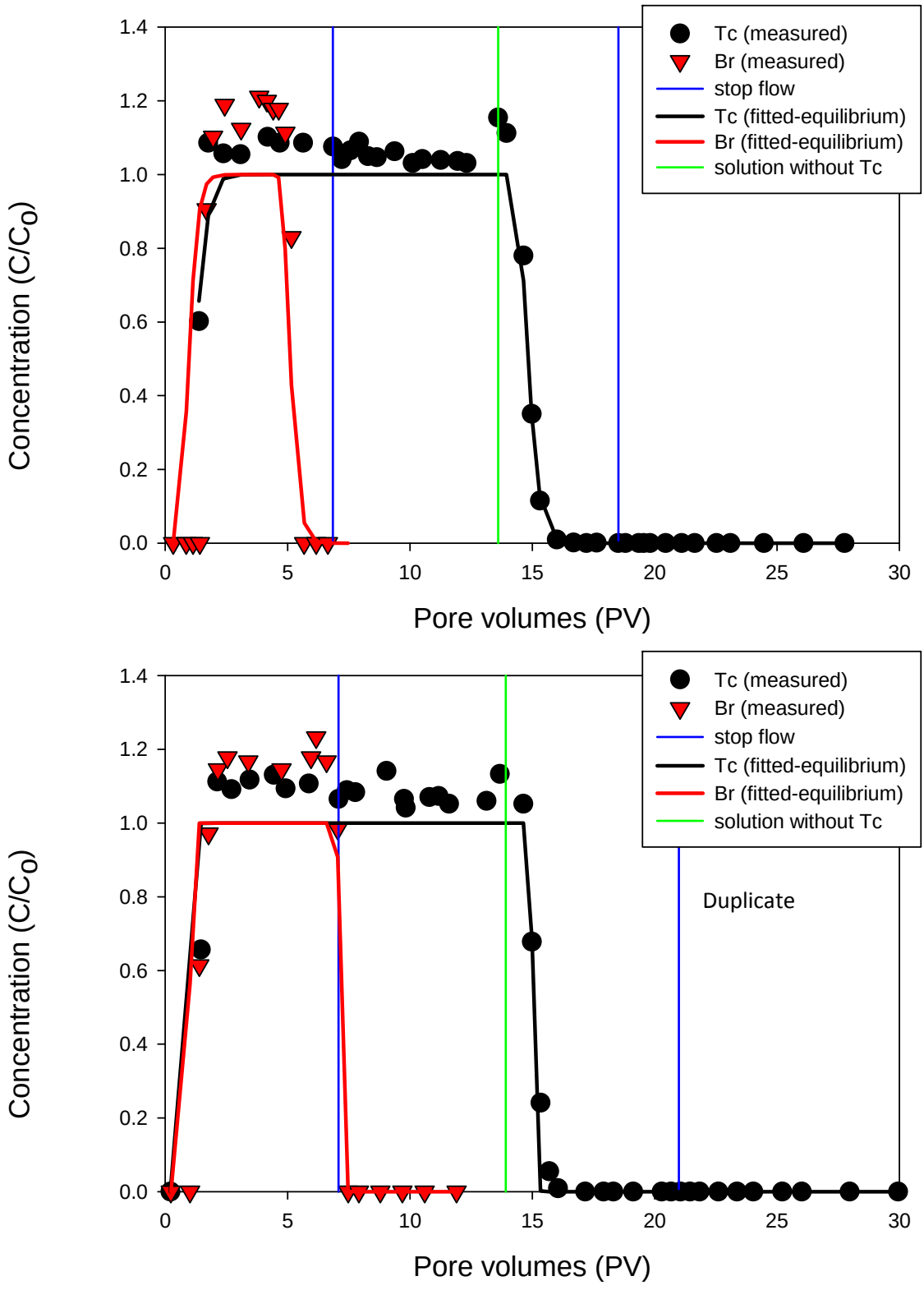

Figure 4.4. Breakthrough Curves for TcO_4^- and Br^- in Cast Stone Leachate (top) and Its Duplicate (bottom). The blue lines on the graph show the 48-hour stop-flow events. The green line represents where the solution was switched from cast stone leachate containing TcO_4^- to cast stone leachate without TcO_4^-.

4.3.2 Chromium (CrO_4^{2-})

Flow-through saturated column experiments were conducted for transport of chromium (CrO_4^{2-}) in IDF pore water, ILAW glass leachate, and Cast Stone leachate. BTCs of CrO_4^{2-} in three different solutions were developed with relative concentration (C/C_0) of CrO_4^{2-} versus the eluted pore volumes. The BTC of a non-reactive tracer, Br^-, was also developed and compared with the CrO_4^{2-} BTC qualitatively.

4.3.2.1 IDF Pore Water

The BTCs for CrO_4^{2-} and Br^- in IDF pore water are presented with different colors and symbols in Figure 4.5. Adsorption portions of the BTCs for CrO_4^{2-} and Br^- were very similar, showing no adsorption of CrO_4^{2-} on the sediment in IDF pore water solution condition. Because there is only one data point for CrO_4^{2-} relative concentration (C/C_0) for the pore volume region between 0 and 1.0, it is not easy to determine precise retardation and K_d values for CrO_4^{2-} directly from the column data. However, calculations using CXTFIT yielded a K_d value of 0.03. The lower K_d value (~zero) of CrO_4^{2-} from the column experiment compared with the batch K_d values as well as potentially early breakthrough of CrO_4^{2-} may be the result of a relatively short residence time (~1 day) or fast flow conditions in the column experiment.

Thus, because of the test conditions run for the column tests, it was not possible to evaluate whether there might be some slow adsorption processes for CrO_4^{2-} in IDF pore water with the IDF sediment as was hinted at for contact times of 28 days in the batch tests described in Section 4.2.2. Even though stop-flow was conducted for 48 hours (see the lines in Figure 4.5), no measurable and credible concentration changes were found. The pH values of initial effluents were between 7.7 and 7.9, but the pH levels in the later effluents decreased to 7.5, which was close to the initial IDF pore water solution pH (~7.2).

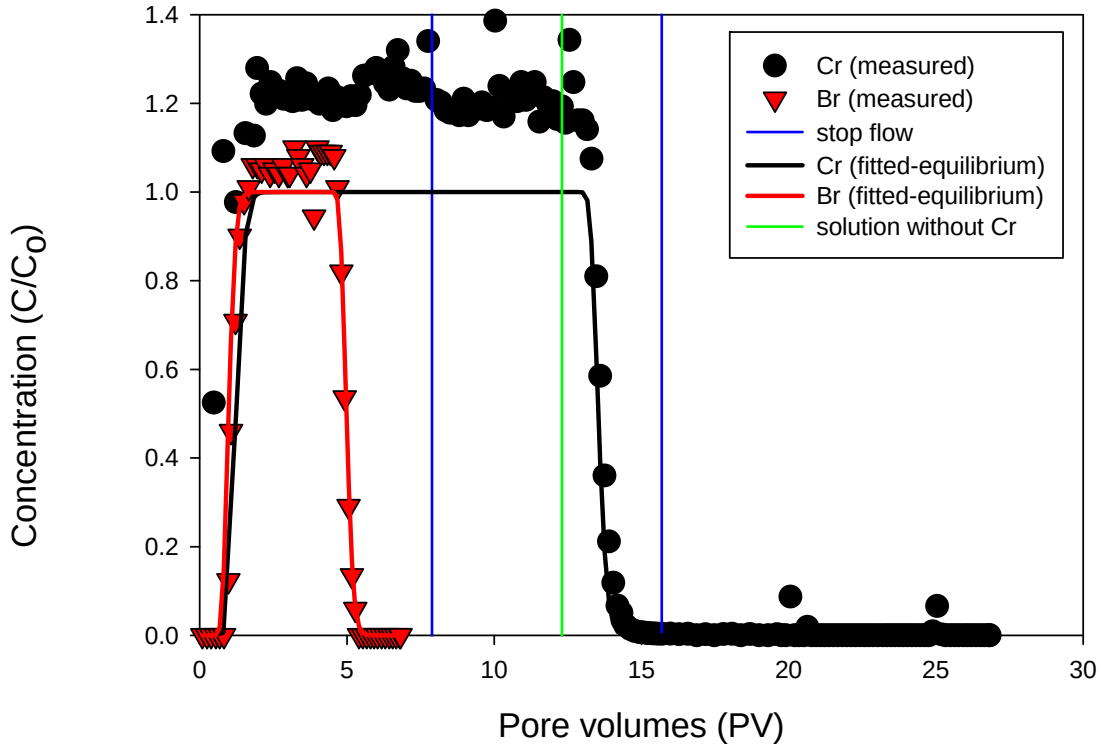

Figure 4.5. Breakthrough Curves for CrO_4^{2-} and Br^- in IDF Pore Water. The blue lines on the graph show the 48-hour stop-flow events. The green line represents where the solution was switched from IDF pore water containing CrO_4^{2-} to IDF pore water without CrO_4^{2-}.

4.3.2.2 Glass Leachate

The BTCs for CrO_4^{2-} and Br^- in glass leachate are shown in Figure 4.6. Insufficient data points of CrO_4^{2-} concentrations in the adsorption phase of the CrO_4^{2-} BTC made it difficult to interpret the data. However, based on the projection of the two initial CrO_4^{2-} data points in the pore volume region between 0 and 1.0, the CrO_4^{2-} BTC was also similar to the Br^- BTC, showing no adsorption of CrO_4^{2-} on sediment in glass leachate. Calculations using CXTFIT yielded a K_d value of -0.02. The potentially early breakthrough of CrO_4^{2-} may be the result of a relatively short residence time (~1 day) or fast flow conditions in the column experiment.

Initial pH of the effluent was close to 8.0, but the pH levels reached to 8.7 after 15 pore volumes. Due to the high-pH condition, CrO_4^{2-} had little chance to adsorb on the negatively charged mineral surfaces. The column results showing CrO_4^{2-} transporting through the IDF sediment with no sorption seem to contradict the results of the batch testing, which show very slight adsorption at all contact times. Aside from the short residence time of CrO_4^{2-} in the column test, we have no explanation for the differences in results between the two types of adsorption tests.

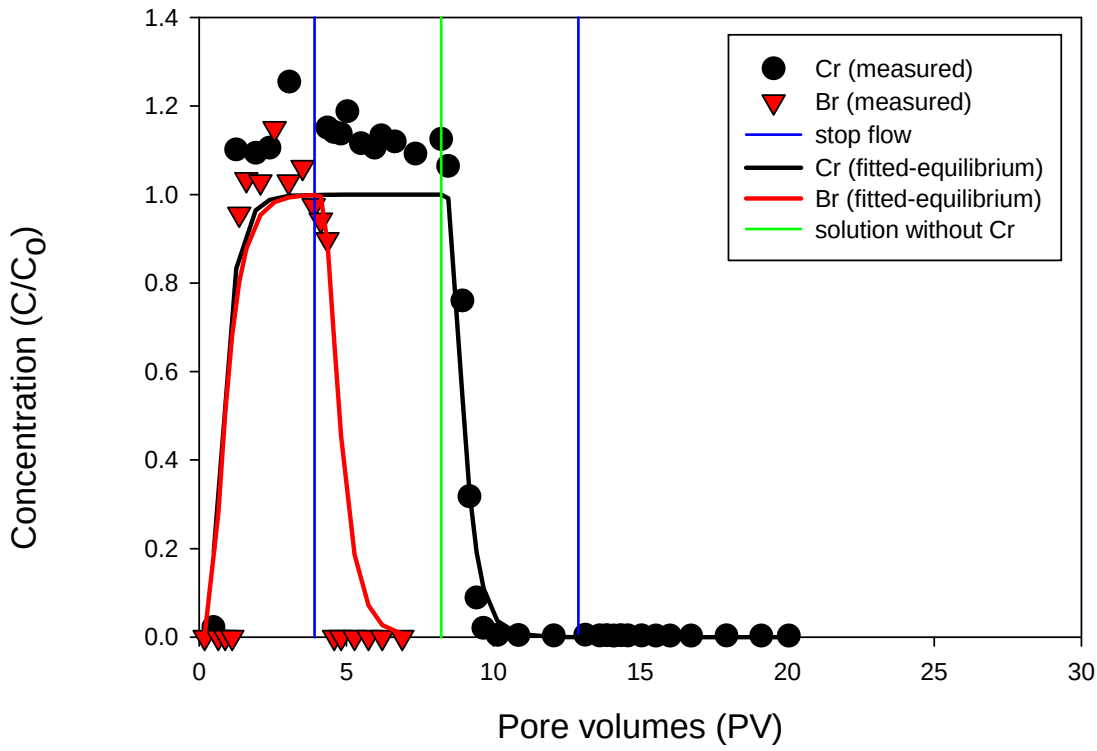

Figure 4.6. Breakthrough Curves for CrO_4^{2-} and Br^- in Glass Leachate. The blue lines on the graph show the 48-hour stop-flow events. The green line represents where the solution was switched from glass leachate containing CrO_4^{2-} to glass leachate without CrO_4^{2-}.

4.3.2.3 Cast Stone Leachate

The BTCs for CrO_4^{2-} and Br^- in Cast Stone leachate are shown in Figure 4.7. The adsorption phase of the CrO_4^{2-} BTC showed earlier breakthrough compared to that of the Br^- BTC. Anion exclusion is the most likely cause of this early breakthrough for CrO_4^{2-} transport. In addition, relatively short residence time (~1 day) of solution flow can increase the early breakthrough in alkaline pH solutions. The K_d value of CrO_4^{2-} is considered to be negative or zero because of the early breakthrough result, consistent with batch K_d values for CrO_4^{2-} measured after a 1-day reaction (see Table 4.1). Calculations using CXTFIT yielded a K_d value of 0.04.

The pH of initial effluents was 7.7 to 7.9, but the pH levels increased up to 10.6 after 20.5 pore volumes were flushed through the column. This large change in pH indicates that many chemical reactions (dissolution of sediment solids and re-precipitation of new phases) are occurring when Cast Stone leachate advects through the IDF sediment. However, there is no indication that the CrO_4^{2-} is being sequestered in the solids based on $C/C_{(0)}$ remaining at or above 1 as long as spiked Cast Stone leachate is being flushed through the sediment.

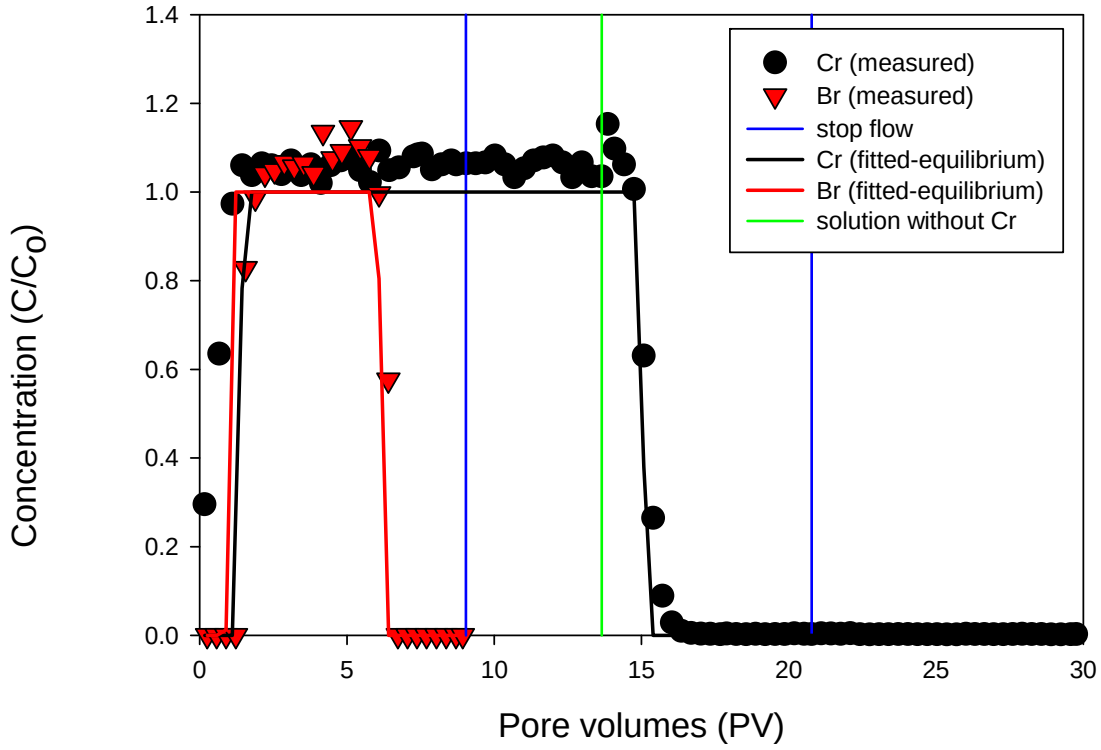

Figure 4.7. Breakthrough Curves for CrO_4^{2-} and Br^- in Cast Stone Leachate. The blue lines on the graph show the 48-hour stop-flow events. The green line represents where the solution was switched from Cast Stone leachate containing CrO_4^{2-} to Cast Stone leachate without CrO_4^{2-}.

4.3.3 Iodide (I^-)

Flow-through saturated column tests of iodide (I^-) spiked in IDF pore water, ILAW glass leachate, and Cast Stone leachate were conducted using IDF composite sediment C3177-215. BTCs of the iodide in all three solutions were compared using the relative concentration (C/C_o) of I^- versus the pore volume. A BTC using Br^- (a non-reactive tracer) was also developed and compared to the I^- BTC.

4.3.3.1 IDF Pore Water

The BTCs for I^- and Br^- in IDF pore water are shown in Figure 4.8. The BTCs for I^- and Br^- were both very similar, indicating no sorption of I^- on the IDF sediment. Additionally, there was no discernable change in the concentration of I after the 48-hour stop flow events. Calculations using CXTFIT yielded a K_d value of -0.02.

The pH in the effluent ranged from 7.7 to 8, which is slightly higher than the initial IDF pore water pH of approximately 7.2. This increase in pH is likely due to carbonate mineral dissolution occurring during the column experiment.

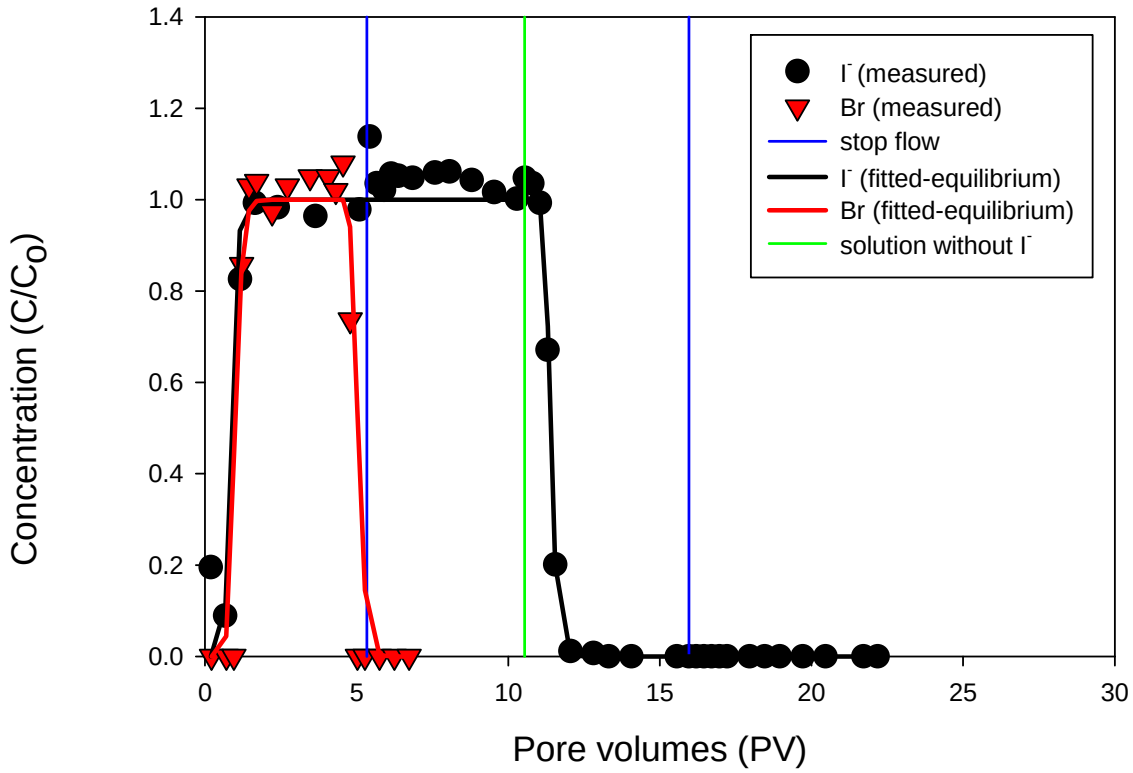

Figure 4.8. Breakthrough Curves for I^- and Br^- in IDF Pore Water. The blue lines on the graph show the 48-hour stop-flow events. The green line represents where the solution was switched from IDF pore water containing I^- to IDF pore water without I^-.

4.3.3.2 Glass Leachate

The BTCs for I^- and Br^- in ILAW glass leachate are shown in Figure 4.9. Similar to the IDF pore water, BTCs for I^- and Br^- were both very similar, indicating little to no sorption of I^- on the IDF sediment in the glass leachate. Calculations using CXTFIT yielded a K_d value of -0.03.

The pH of the effluent started at 8.0 at <0.5 pore volume and gradually increased to a pH of 8.6 after 20 pore volumes. The initial pH of 8 is slightly lower than the starting pH of the ILAW glass leachate (~8.6). However, there was little to no change in the I^- concentration after the 48-hour stop-flow.

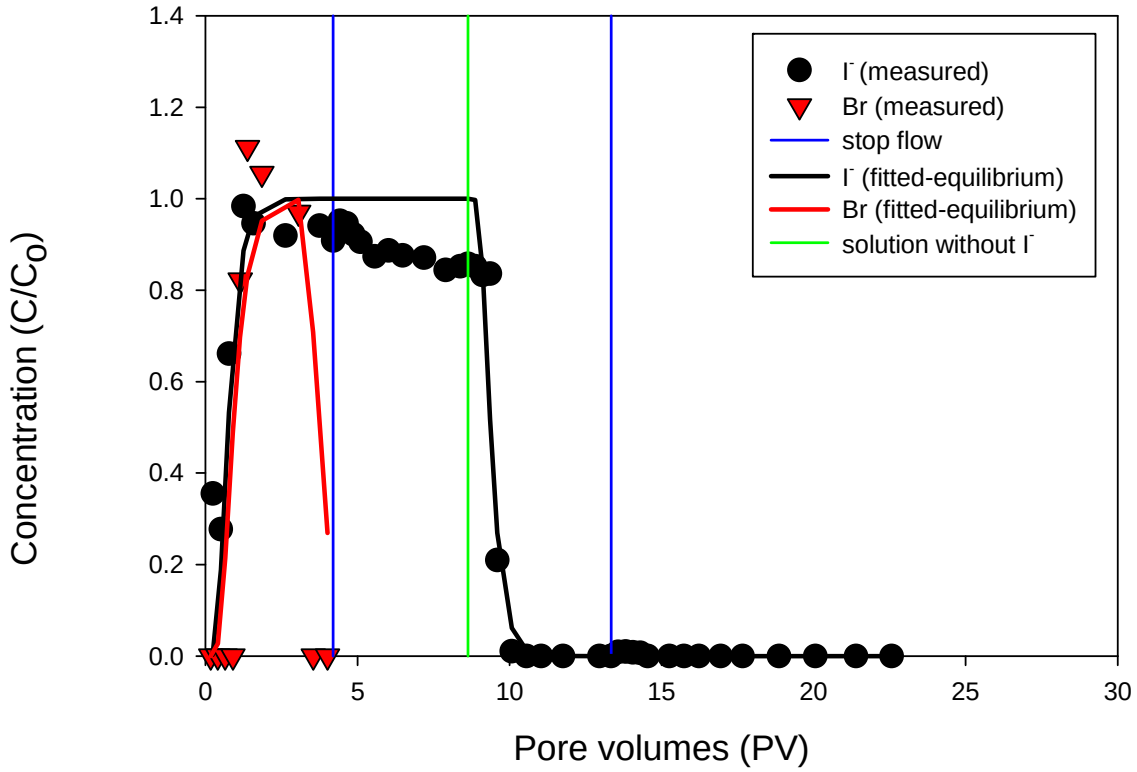

Figure 4.9. Breakthrough Curves for I^- and Br^- in ILAW Glass Leachate. The blue lines on the graph show the 48-hour stop-flow events. The green line represents where the solution was switched from glass leachate containing I^- to glass leachate without I^-.

4.3.3.3 Cast Stone Leachate

The BTCs for I^- and Br^- in Cast Stone leachate are shown in Figure 4.10. As with the I^- in the IDF pore water and ILAW glass leachate, the I^- and Br^- BTCs were very similar and showed little to no sorption of I^- in the Cast Stone leachate. Calculations using CXTFIT yielded a K_d value of -0.02.

The pH of the effluent started out at 8 after <0.5 pore volumes and increased throughout the experiment up to a pH of 11.4 after 20 pore volumes. Even at the highest pH of 11.4, the effluent pH was still lower than the starting pH of the Cast Stone leachate (~12.1). The high-pH conditions result in a negatively charged mineral surface in the IDF sediment, and do not create an environment for sorption of anions, such as I^-. Additionally, there was no change in the I^- concentration after the 48-hour stop-flow, confirming there was no sorption of I^- on the IDF sediment in IDF glass leachate.

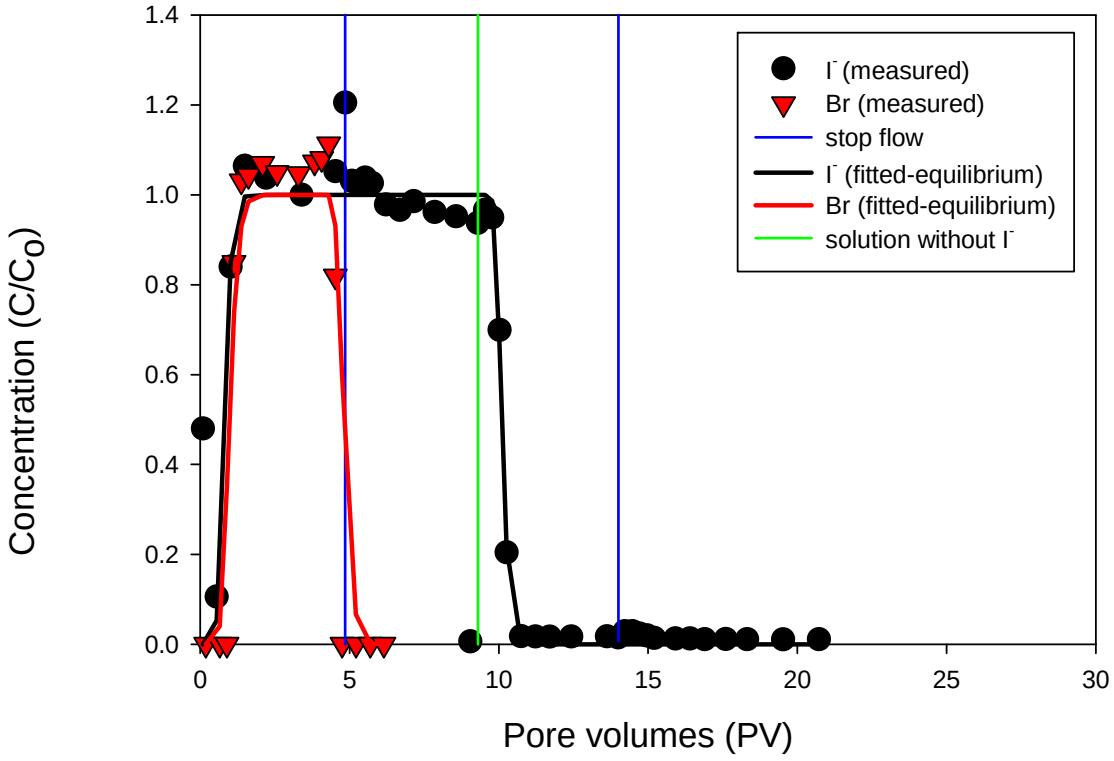

Figure 4.10. Breakthrough Curves for I^- and Br^- in Cast Stone Leachate. The blue lines on the graph show the 48-hour stop-flow events. The green line represents where the solution was switched from Cast Stone leachate containing I^- to Cast Stone leachate without I^-.

4.3.4 Iodate (IO_3^-)

Flow-through saturated column tests of iodate (IO_3^-) spiked in IDF pore water, ILAW glass leachate, and Cast Stone leachate were conducted using IDF composite sediment C3177-215. BTCs of the IO_3^- in all three solutions were compared using the relative concentration (C/C_o) of IO_3^- versus the pore volume. A BTC using Br^- (a non-reactive tracer) was also developed and compared to the IO_3^- BTC to help determine whether sorption of the IO_3^- occurred.

4.3.4.1 IDF Pore Water

The BTCs for IO_3^- and Br^- in IDF pore water are shown in Figure 4.11. The BTC for IO^{3-} compared to Br- shows a little delay in the breakthrough of IO_3^-. Unlike the Br-, which reaches full breakthrough around 2 pore volumes, the IO_3^- does not reach a relative concentration of 1.0 until after 4 pore volumes. Calculations using CXTFIT yielded a K_d value of 0.05.

At 7.9, the pH of the effluent solution started out higher than the starting pH of the IDF pore water (~7.2) and decreased to a pH of 7.6 toward the end of the column study at around 27 pore volumes. This increase in pH may indicate precipitation in the IDF pore water solution.

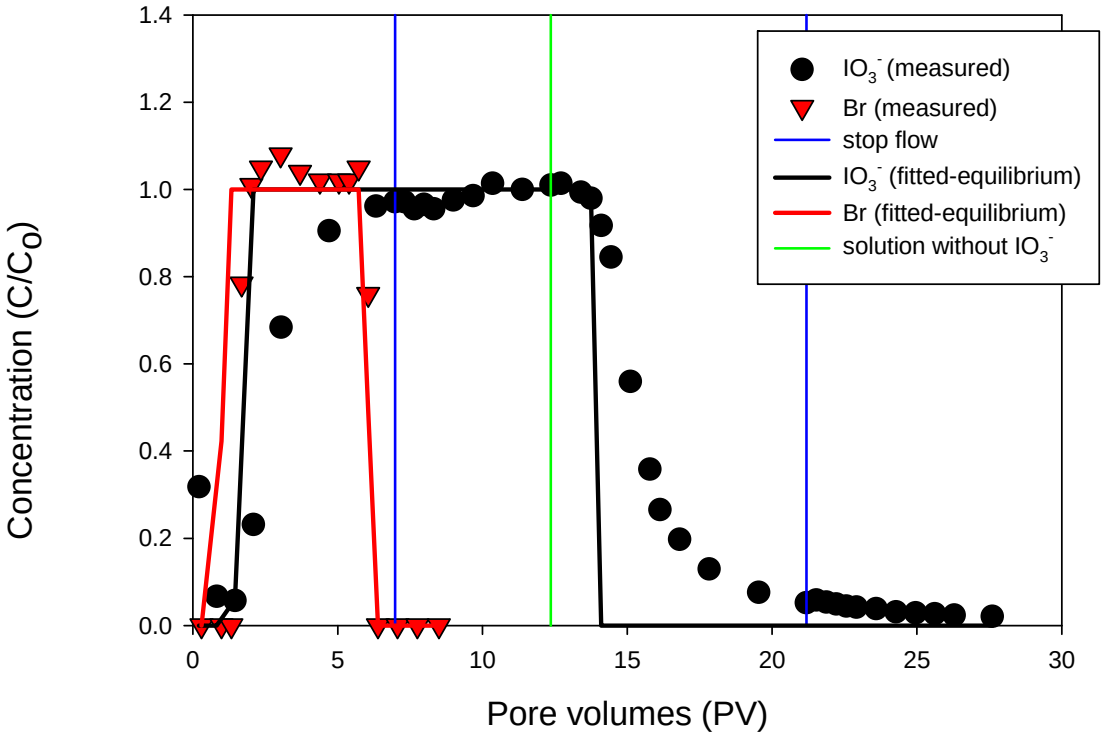

Figure 4.11. Breakthrough Curves for Iodate and Br^- in IDF Pore Water. The blue lines on the graph show the 48-hour stop-flow events. The green line represents where the solution was switched from IDF pore water containing IO_3^- to IDF pore water without IO_3^-.

4.3.4.2 Glass Leachate

The BTCs for IO_3^- and Br^- in ILAW glass leachate are shown in Figure 4.12. Similar to IO_3^- in IDF pore water, the BTC for the IO_3^- was slightly retarded when compared to the BTC for Br^-. The IO_3^- does not reach breakthrough until after 4 pore volumes compared to the Br^-, which reaches breakthrough after 2 pore volumes. The relative iodate concentrations (C/C_0) from the glass leachate column were much reduced from those of the non-reactive Br tracer and iodate in either IDF pore water or Cast Stone columns. Lower C/C_0 value (~0.8) of iodate for the glass leachate may be the result of iodate precipitation. Calculations using CXTFIT yielded a K_d value of 0.14.

The pH in the effluent increased from 7.9 to 8.5 after 27 pore volumes. The increase in pH may indicate precipitation in the glass leachate solution. There was no change in the iodine concentration after the 48-hour stop-flow events.

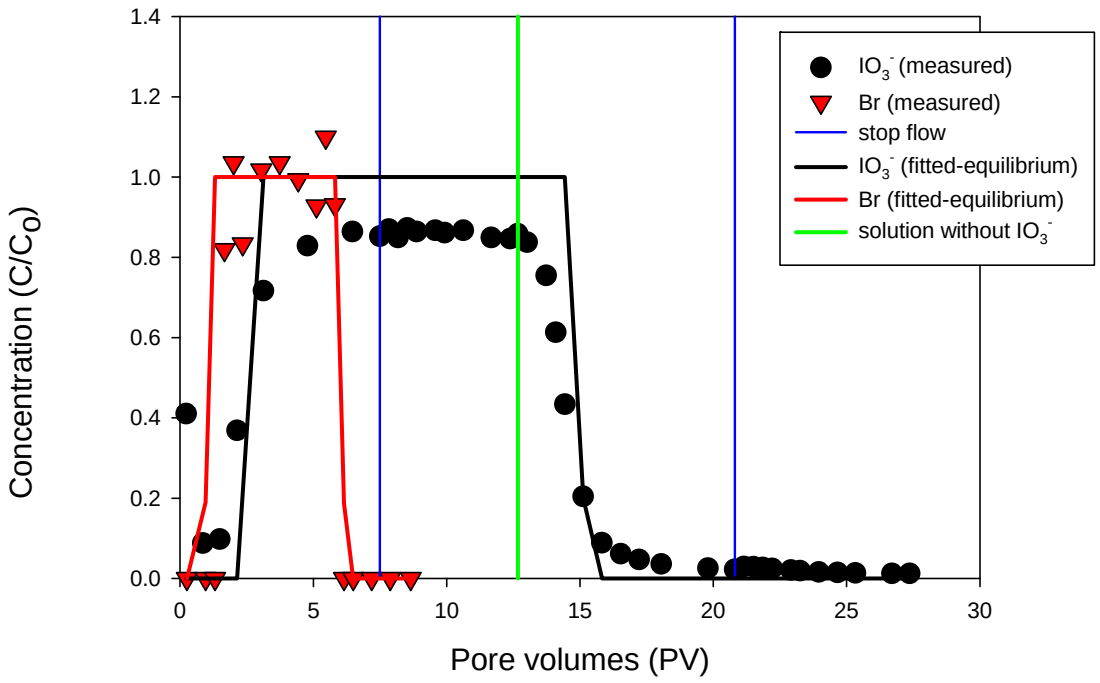

Figure 4.12. Breakthrough Curves for Iodate and Br^- in Glass Leachate. The blue lines on the graph show the 48-hour stop-flow events. The green line represents where the solution was switched from glass leachate containing IO_3^- to glass leachate without IO_3^-.

4.3.4.3 Cast Stone Leachate

The BTCs for IO_3^- and Br^- in Cast Stone leachate are shown in Figure 4.13. Similar to IO_3^- in IDF pore water and glass leachate, the BTC for the IO_3^- in Cast Stone leachate was slightly retarded when compared to the BTC for Br^-. The IO_3^- did not reach breakthrough until approximately 4 pore volumes compared to the Br^-, which reached breakthrough after 2 pore volumes. Calculations using CXTFIT yielded a K_d value of 0.01.

The pH in the effluent started at 7.8 and increased to 10.8 after more than 20 pore volumes.

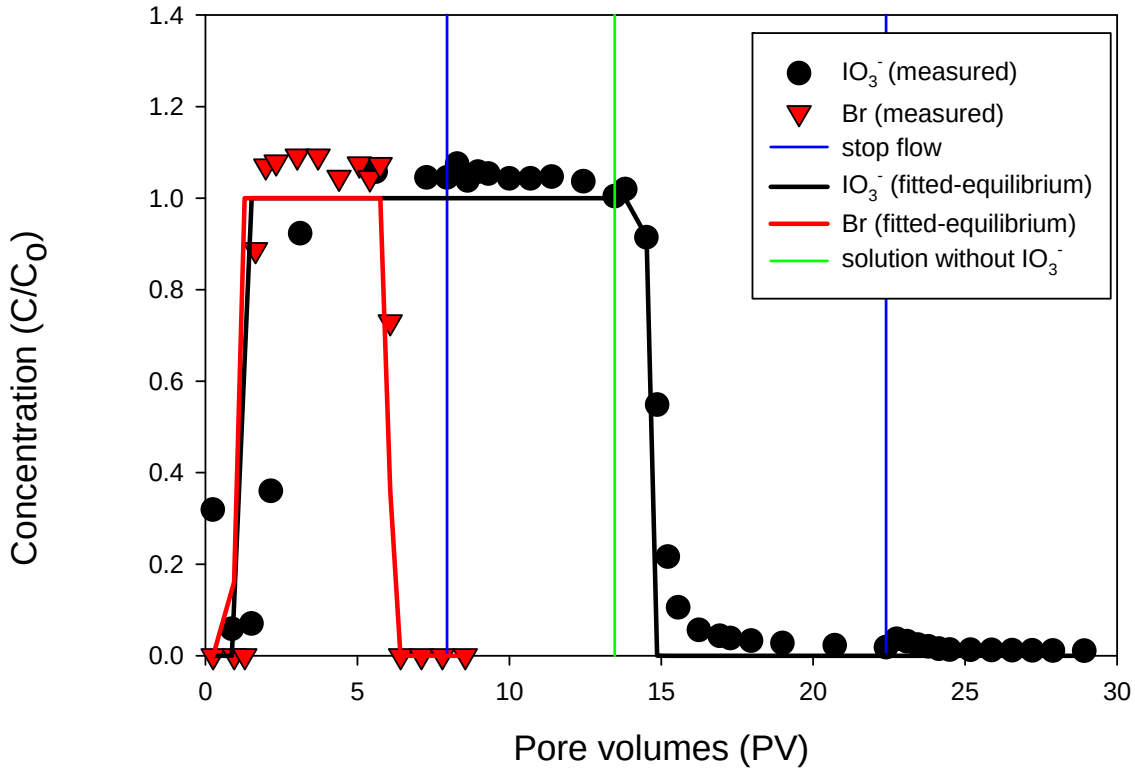

Figure 4.13. Breakthrough Curves for Iodate and Br^- in Cast Stone Leachate. The blue lines on the graph show the 48-hour stop-flow events. The green line represents where the solution was switched from Cast Stone leachate containing IO_3^- to Cast Stone leachate without IO_3^-.

Table 4.3. K_d Values (mL/g) Calculated from Column Tests Containing Hanford Formation Sand

	^{99}Tc as Pertechnetate		Cr as Chromate		Iodide (I^-)		Iodate (IO_3^-)	
Column Test	R_f	K_d (mL/g)	R_f	K_d (mL/g)	R_f	K_d (mL/g)	R_f	K_d (mL/g)
IDF PW	1.02	0.00	1.26	0.03	0.87	-0.02	1.48	0.05
IDF PW Dup	0.95	-0.01	-	-	-	-	-	-
IDF PW (unsaturated)	0.86	-0.02	-	-	-	-	-	-
Cast Stone	1.28	0.03	1.42	0.04	0.82	-0.02	1.13	0.01
Cast Stone Dup	1.12	0.01	-	-	-	-	-	-
Glass	1.03	0.00	0.87	-0.02	0.82	-0.03	2.43	0.14
Glass Dup	0.94	-0.01	-	-	-	-	-	-

R_f = retardation factor from CXTFIT software.
K_d calculated using: $R_f = 1 + ((K_d * \text{bulk density})/\text{porosity})$. Refer to Table 3.8 for porosity and bulk density values.
- = not performed.

4.4 Unsaturated Column Adsorption/Desorption Experiment

The migration of TcO_4^- spiked into IDF pore water through IDF composite sediment (C3177-215) was also evaluated using one flow-through unsaturated column experiment. BTCs were determined for both TcO_4^- and Br^-.

The flow rate through the column was maintained at approximately 5.5 mL/hr (Figure 4.14) using a liquid mass flow controller as described in Section 3.5. Water potentials in the column were -10 to -20 mbar and remained reasonably constant throughout the flow-through test (Figure 4.15).

As described in Section 3.5, both Tc- and Br-spiked solutions equivalent to 3 saturated pore volumes were pumped through the column. Unsaturated column experiments were conducted at approximately 35% saturation and resulted in approximately 6 and 10 unsaturated pore volumes of Br^- and Tc spiked solutions, respectively, that were run through the column. The BTCs for both Br^- and Tc (Figure 4.16) show that the relative concentration is very close to 0.5 at 1 pore volume, indicating that the retardation factor is close to 1. This is equivalent to having a K_d equal to zero. Calculations using CXTFIT yielded a K_d value of -0.02.

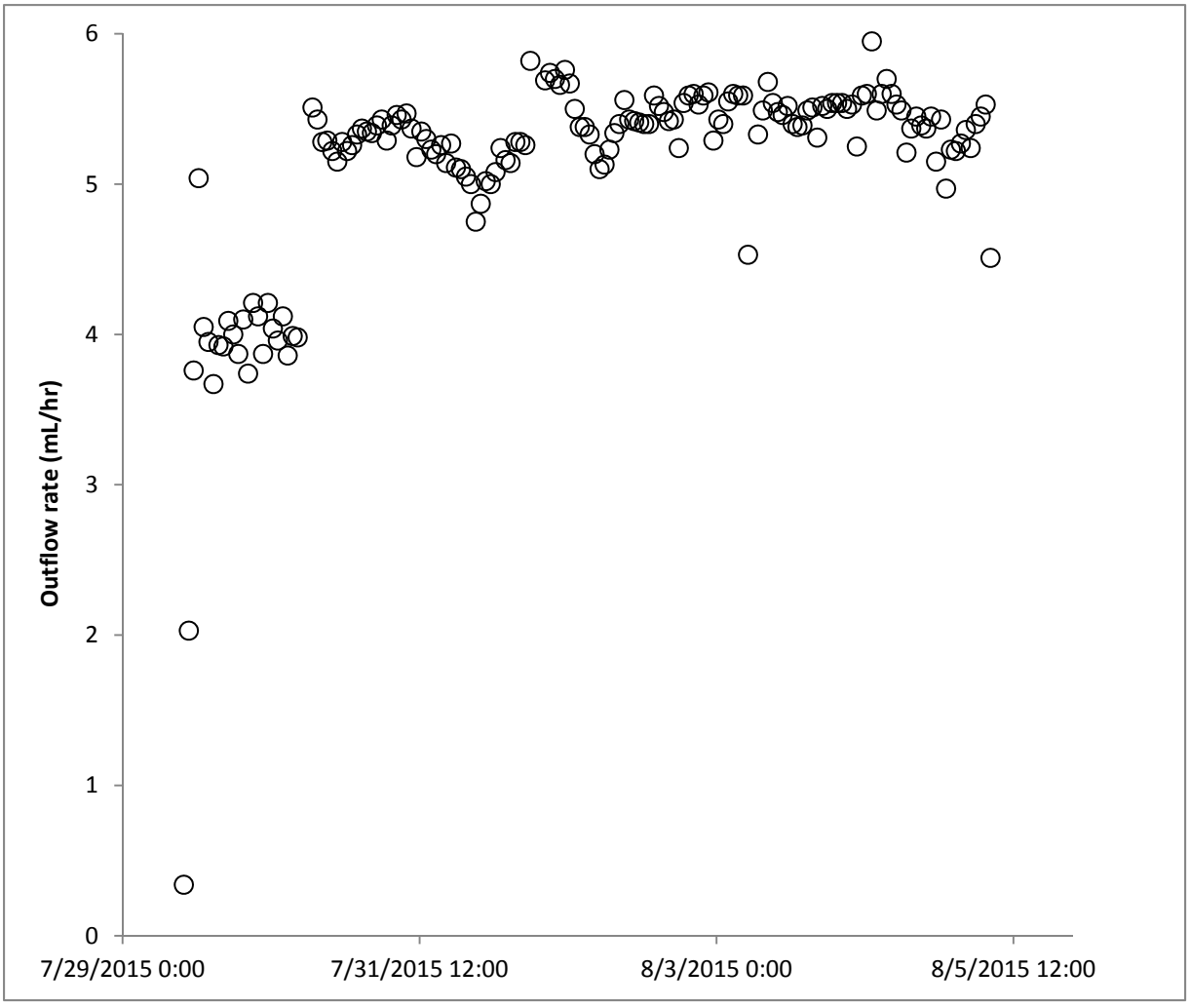

Figure 4.14. Flow Rate Through the Unsaturated Flow Column

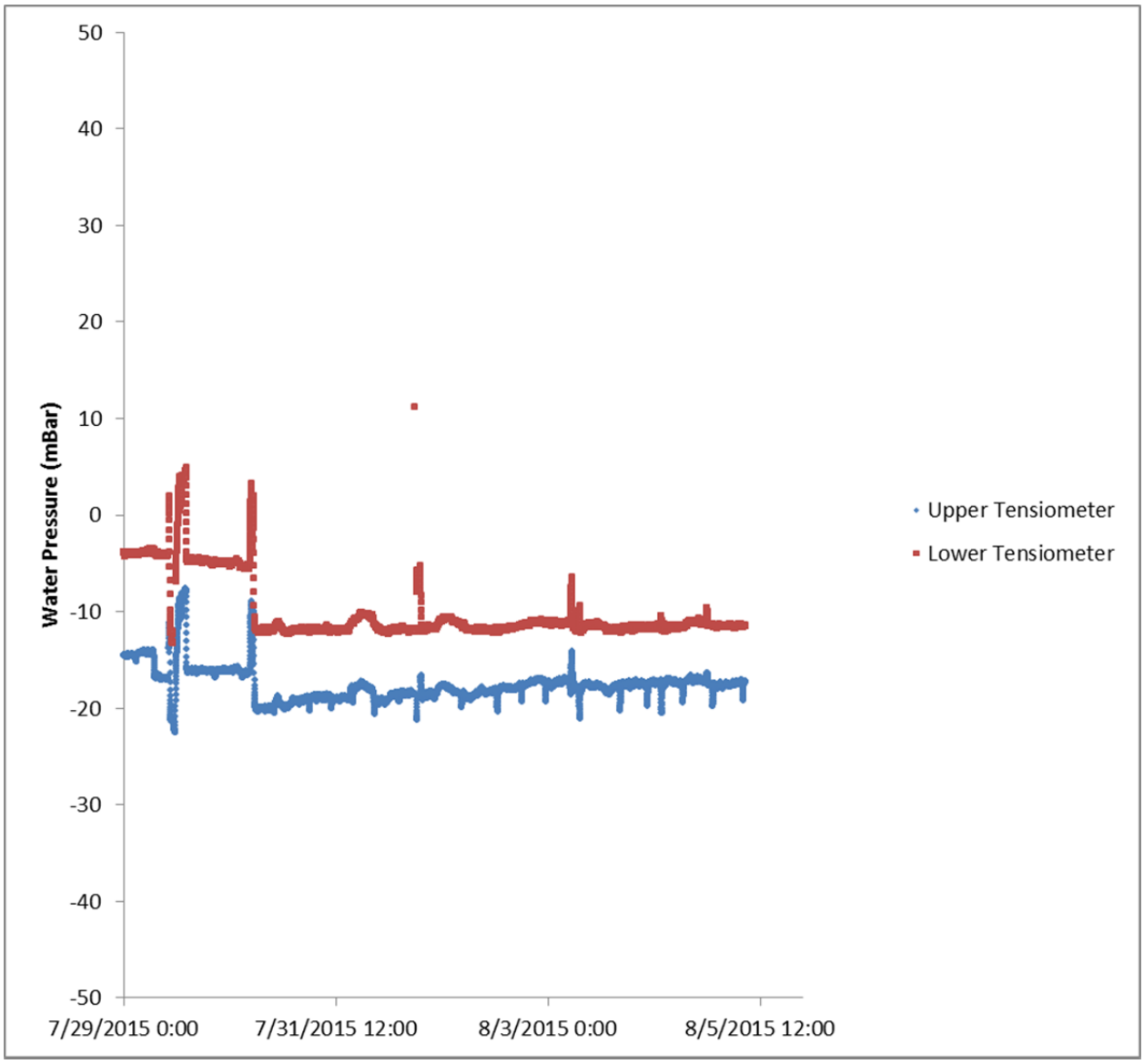

Figure 4.15. Water Potentials Throughout the Duration of the Unsaturated Column Experiment

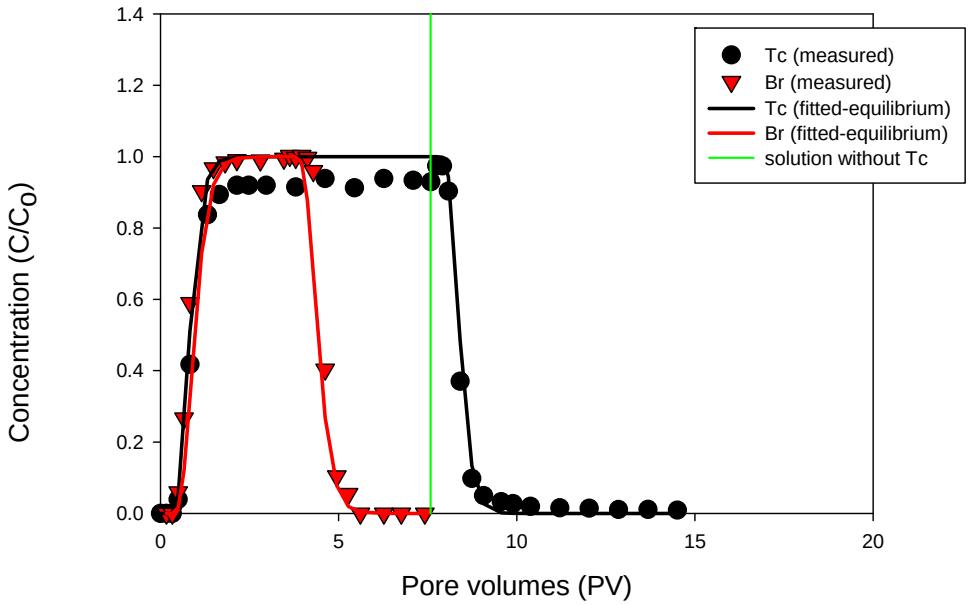

Figure 4.16. Breakthrough Curves for TcO_4^- and Br^- for the Unsaturated Flow Column Using TcO_4^- Spiked into IDF Pore Water. The blue low-density dotted line represents where the solution was switched from IDF pore water containing TO_4^- to IDF pore water without TO_4^-.

4.5 Macro Solution Analysis and Iodine Speciation

The following discussion on the macro chemistry of the batch and column experiments is qualitative. Geochemical modeling may be needed to more fully understand the processes controlling these macro concentrations.

4.5.1 Macro Chemistry of Batch Solutions

Changes in the macro solution composition in the batch K_d and flow-through column test leachants contacting the IDF sand sediment were monitored in hopes of gaining insight into the processes that control the adsorption-desorption attributes of the contaminants of concern. Albeit, the anions of interest to this work are known to be quite mobile in the subsurface and thus may not be interacting with the IDF sediments much regardless of which leachant (vadose zone pore water, Cast Stone leachate, or glass leachate) is considered. The major cations and anions in the starting leachants and effluents from both the batch K_d and flow-through columns were analyzed by the methods outlined in Section 3.6. The resultant data in most cases was directly uploaded from the measuring instrument to an electronic database and then sorted by analyte and solution ID to construct Excel files. We then assimilated the data in the Excel files for each analyte to identify changes that occurred in chemical composition when the starting influent solution contacted the IDF sediment.

For the batch K_d tests, we focused on assessing changes in pH and changes in the concentration of Al, Si, Ca, Mg, and common anions (Cl, NO_3, NO_2, SO_4). Al, Si, and pH are important because they represent constituents or factors that are involved in sediment dissolution and precipitation reactions. Na

is generally a major component of Hanford liquid waste and waste form leachates, and Ca is the major cation-exchangeable constituent present in Hanford Site sediments. The high Na content of most waste form leachates interacts with native sediments and replaces Ca on the sediment exchange sites, thus releasing Ca to solution. Ca can also be involved in dissolution-precipitation reactions (e.g., dissolution/precipitation of calcium carbonate as acidic or caustic liquids contact the sediment). Table 4.4 shows the evolution of pH in the batch K_d tests as a function of solution type and contact time with the sediment. Detailed descriptions of the pH data are found in Section 4.15 in the batch K_d results. Table 4.5 through Table 4.8 list the batch K_d data for Al, Si, Na, and Ca, respectively, in the blank solutions and effluents after contact with the IDF sediment versus time for each of the three leachants and the four different contaminants.

As shown in Table 4.5, there appear to be unresolved differences in Al concentrations in both the blank (starting solution) and the effluents in the Tc-spiked IDF pore water compared to the other two IDF pore waters spiked with iodide and iodate. There does not appear to be any time dependency in the concentration of Al found in the blanks or sediment effluents. Using the average and standard deviation of the Al data for all sampling times (1 through 28 days), we compared the difference between the blanks (starting solution IDF pore water and the effluents after contact with the sediments). Using the student's T-test for the differences, we found that the sediments release small amounts of Al (likely via dissolution reactions) to the IDF pore water effluents, but the amount of Al released is not statistically significant at the 95% probability level.

On the other hand, the sediments remove Al from the Cast Stone starting solutions, and the difference between the effluent Al concentrations and the starting Cast Stone solution is significant. As mentioned in the batch K_d results section, any slightly positive sorption for the four mobile anions may be caused by co-precipitation or physical trapping in Al and silicon solids formed when the sediments interact with the Cast Stone leachant. There were no usual Al data in the electronic database on the starting glass leachate and effluents for the glass leachate contacting the IDF sediment, so we cannot comment on the fate of Al in the glass leachate-sediment slurry.

The blank solutions and effluents for the IDF pore water show little difference in Si among the four contaminant spikes as a function of time (see Table 4.6). Thus, we averaged the Si data for each of the four spiked leachants and compared the averages to those for the Si concentrations in each sediment IDF pore water effluent. There was no detectable Si in the IDF pore water blanks, but there was readily measureable Si in all the IDF pore water effluents after contacting the sediment. Thus, the IDF sand sediment releases Si into the pore water.

The Cast Stone starting solution contained about 19 ppm of Si. After contact with the sediment, the Si concentrations significantly decreased for all but the Tc-spiked leachate tests, suggesting precipitation of Si-bearing solid phases. The amount of Si that precipitates increases with contact time, suggesting that along with the pH decline with time, Si precipitates continue with time as the effluent pH drops. This Si precipitation process may be responsible for the slightly positive K_d values for Cr and iodate described in Section 4.3.

For the glass leachate there is about 65 to 70 ppm of Si present before contacting the IDF sediment (see Table 4.6). The effluents from the batch K_d tests have lower Si concentrations ranging from 18 to 29 ppm. Thus, the sediments contacting glass leachate cause precipitation of Si (as well as Al), and it is quite possible that the observed slightly positive K_d values for Tc, Cr, and iodate in the glass leachate

batch sorption tests might be partially caused by co-precipitation or physical trapping in Al and Si solids formed during the interaction of the sediments with the glass leachate.

The Na and Ca data from the batch leachate tests (see Table 4.7 and Table 4.8, respectively) suggest that for the IDF pore water there is very little change in Na or Ca concentration as a result of contact with the IDF sediments. However, for both the Cast Stone and glass leachates, the starting solutions, both relatively high in Na, generate effluent solutions after contact with the IDF sediment that have lower Na concentrations. Conversely, the Ca concentration in the effluents from these two waste form leachates increases. This dynamic of loss of Na and gain of Ca in effluent solutions is caused by the cation exchange of native sediment Ca by Na in the waste leachants.

Similar comparisons for the common anions in the three starting solutions with their effluents after contacting the IDF sediment show very minor changes that are not statistically significant. Thus, anions such as Cl, NO_3, NO_2, and SO_4 in the starting solutions are not interacting with the sediment in any significant solubility-precipitation or adsorption-desorption reactions.

At the present time there are no studies that address (and separate) true surface adsorption processes from solubility and co-precipitation processes for dynamic near-field environments where changes in geochemical conditions (e.g., pH, macro pore water composition, and Eh) are occurring over short time frames and over small spatial scales. Thus, the use of the empirical K_d construct to parameterize contaminant interactions between fluids contacting near-field backfill and sediments remains the practical approach. It is acknowledged that empirical K_d values are a lumped parameter that melds all contaminant sequestering processes into one lumped value. In the future, two approaches could be used to improve this situation. First, future laboratory sorption tests could be performed wherein the contacting solution and sediment/backfill slurry is rigorously pre-equilibrated, via numerous washing steps, until key macro constituents such as pH, Eh, and macro solute concentrations reach a steady-state condition before the trace contaminant is spiked into the slurry, at known concentrations lower than solubility constraints. The change in contaminant concentration versus time in this pre-equilibrated system would likely be dominated by true adsorption processes. Such laboratory tests should be coordinated with detailed geochemical speciation and solubility calculations with computer codes such Geochemist Workbench or eSTOMP before and after adding the contaminant to the pre-equilibrated slurry to evaluate whether the slurry is close to equilibrium for macro constituents. A second approach is to develop detailed conceptual models and chemical reaction networks for waste form leachates contacting backfill and near-field sediments and then perform laboratory experiments to elucidate various hypotheses that can be generated from the predicted outcomes from the models/geochemical codes. If the results of such focused laboratory experiments agree with the hypotheses, adsorption/solubility processes would be partially verified (see Yabusaki et al. [2015] for further discussion).

Table 4.4. pH Data for Batch K_d Leachants (blanks) and Effluents

pH of IDF Pore Water Blanks versus Contact Time							pH of IDF Pore Water Effluents versus Contact Time					
Contact (days)	Tc	Cr	IO_3	I	Avg.	σ	Tc	Cr	IO_3	I	Avg.	σ
1	7.46	7.49	7.32	7.41	7.42	0.06	7.805	7.77	7.49	7.505	7.6425	0.15
3	7.46	7.97	7.38	7.44	7.56	0.24	7.75	7.765	7.65	7.665	7.71	0.05
7	7.53	7.81	7.36	7.48	7.55	0.17	7.695	7.62	7.625	7.77	7.68	0.06
14	7.6	7.36	7.42	7.46	7.46	0.09	7.75	7.695	7.68	7.725	7.71	0.03
28	7.65	7.62	7.48	7.4	7.54	0.10	7.805	7.685	7.67	7.74	7.73	0.05
				Overall Avg.	7.51	0.16				Overall Avg.	7.69	0.09
pH of Cast Stone Leachate Blanks versus Contact Time							pH of Cast Stone Leachate Effluents versus Contact Time					
Contact (days)	Tc	Cr	IO_3	I	Avg.	σ	Tc	Cr	IO_3	I	Avg.	σ
1	11.9	11.9	11.9	12	11.93	0.04	10.35	9.81	9.815	9.97	9.99	0.22
3	12	11.8	11.9	12	11.93	0.08	9.815	9.42	9.685	9.81	9.68	0.16
7	11.9	11.9	11.9	12	11.93	0.04	9.535	9.32	9.48	9.51	9.46	0.08
14	12	12	11.9	11.9	11.95	0.05	9.465	9.225	9.29	9.48	9.37	0.11
28	12	12	11.9	11.9	11.95	0.05	9.335	9.13	9.055	9.255	9.19	0.11
				Overall Avg.	11.94	0.06				Overall Avg.	9.54	0.32
pH of Glass Leachate Blanks versus Contact Time							pH of Glass Leachate Effluents versus Contact Time					
Contact (days)	Tc	Cr	IO_3	I	Avg.	σ	Tc	Cr	IO_3	I	Avg.	σ
1	8.62	8.75	8.58	8.58	8.63	0.07	7.99	7.98	7.81	7.775	7.89	0.10
3	8.67	8.73	8.62	8.6	8.66	0.05	8.005	7.97	7.97	7.965	7.98	0.02
7	8.62	8.63	8.62	8.61	8.62	0.01	7.95	7.915	7.965	7.995	7.96	0.03
14	8.65	8.7	8.58	8.59	8.63	0.05	7.935	8.005	7.925	7.895	7.94	0.04
28	8.6	8.67	8.59	8.6	8.62	0.03	7.755	8.01	7.875	7.965	7.90	0.10
				Overall Avg.	8.63	0.05				Overall Avg.	7.93	0.08

Table 4.5. Measured Aluminum Concentrations in Batch Test Solutions

Aluminum	mg/L	dl (mg/L)		Aluminum	mg/L	dl (mg/L)		Aluminum	mg/L	dl (mg/L)		Aluminum	mg/L	dl (mg/L)	
IDF PW				**IDF PW**				**IDF PW**				**IDF PW**			
Tc 1 day	485	0.49		Cr 1 day	475	0.981		I 1 day	456	0.336		IO3 1 day	455	0.336	
Tc 1 day DUP	487	0.49		Cr 1 day DUP	475	0.981		I 1 day DUP	459	0.336		IO3 1 day DUP	447	0.336	
Tc 3 day	474	0.49		Cr 3 day	464	0.981		I 3 day	442	0.336		IO3 3 day	423	0.336	
Tc 3 day DUP	486	0.49		Cr 3 day DUP	460	0.981		I 3 day DUP	461	0.336		IO3 day DUP	456	0.336	
Tc 7 day	485	0.49		Cr 7 day	462	0.981		I 7 day	433	0.336		IO3 7 day	444	0.336	
Tc 7 day DUP	482	0.49	**Effluent**	Cr 7 day DUP	462	0.981	**Effluent**	I 7 day DUP	435	0.336	**Effluent**	IO3 7 day DUP	450	0.336	**Effluent**
Tc 14 day	476	0.49	**Average**	Cr 14 day	474	0.981	**Average**	I 14 day	457	0.336	**Average**	IO3 14 day	451	0.336	**Average**
Tc 14 day DUP	482	0.49	**482.4**	Cr 14 day DUP	474	0.981	**465.4**	I 14 day DUP	460	0.336	**450.2**	IO3 14 day DUP	449	0.336	**447**
Tc 28 day	472	0.49	**σ**	Cr 28 day	462	0.981	**σ**	I 28 day	445	0.336	**σ**	IO3 28 day	442	0.336	**σ**
Tc 28 day DUP	495	0.49	**6.9**	Cr 28 day DUP	446	0.981	**9.3**	I 28 day DUP	454	0.336	**10.6**	IO3 28 day DUP	453	0.336	**9.5**
Tc 1 day Blank	498	0.49	**Blank**	Cr 1 day Blank	473	0.981	**Blank**	I 1 day Blank	444	0.336	**Blank**	IO3 1 day Blank	465	0.336	**Blank**
Tc 3 day Blank	478	0.49	**Average**	Cr 3 day Blank	475	0.981	**Average**	I 3 day Blank	469	0.336	**Average**	IO3 3 day Blank	478	0.336	**Average**
Tc 7 day Blank	496	0.49	**488.2**	Cr 7 day Blank	477	0.981	**481**	I 7 day Blank	473	0.336	**463**	IO3 7 day Blank	457	0.336	**460.2**
Tc14 day Blank	493	0.49	**σ**	Cr14 day Blank	496	0.981	**σ**	I 14 day Blank	463	0.336	**σ**	IO3 14 day Blank	457	0.336	**σ**
Tc 28 day Blank	476	0.49	**10.4**	Cr 28 day Blank	484	0.981	**9.4**	I 28 day Blank	466	0.336	**11.2**	IO3 28 day Blank	444	0.336	**12.5**
Aluminum	mg/L	dl (mg/L)		Aluminum	mg/L	dl (mg/L)		Aluminum	mg/L	dl (mg/L)		Aluminum	mg/L	dl (mg/L)	
Cast Stone Leachate				**Cast Stone Leachate**				**Cast Stone Leachate**				**Cast Stone Leachate**			
Tc 1 day	33.6	4.9		Cr 1 day	40.3	0.981		I 1 day	38	3.36		IO3 1 day	40.6	3.36	
Tc 1 day DUP	41.9	4.9		Cr 1 day DUP	38	0.981		I 1 day DUP	37.7	3.36		IO3 1 day DUP	39.9	3.36	
Tc 3 day	42.4	4.9		Cr 3 day	39.5	0.981		I 3 day	40.5	3.36		IO3 3 day	40.3	3.36	
Tc 3 day DUP	43.4	4.9		Cr 3 day DUP	38.3	0.981		I 3 day DUP	38	3.36		IO3 day DUP	40.6	3.36	
Tc 7 day	47	4.9		Cr 7 day	39.4	0.981		I 7 day	38.3	3.36		IO3 7 day	38.5	3.36	
Tc 7 day DUP	44.2	4.9	**Effluent**	Cr 7 day DUP	35.6	0.981	**Effluent**	I 7 day DUP	39.2	3.36	**Effluent**	IO3 7 day DUP	39.5	3.36	**Effluent**
Tc 14 day	41	4.9	**Average**	Cr 14 day	38.8	0.981	**Average**	I 14 day	36.3	3.36	**Average**	IO3 14 day	39.3	3.36	**Average**
Tc 14 day DUP	40.5	4.9	**41.71**	Cr 14 day DUP	40.8	0.981	**39.24**	I 14 day DUP	33.5	3.36	**36.7**	IO3 14 day DUP	38.7	3.36	**39.33**
Tc 28 day	42.9	4.9	**σ**	Cr 28 day	40.5	0.981	**σ**	I 28 day	30.7	3.36	**σ**	IO3 28 day	36.7	3.36	**σ**

Aluminum	mg/L	dl (mg/L)		Aluminum	mg/L	dl (mg/L)		Aluminum	mg/L	dl (mg/L)		Aluminum	mg/L	dl (mg/L)	
Cast Stone Leachate				**Cast Stone Leachate**				**Cast Stone Leachate**				**Cast Stone Leachate**			
Tc 28 day DUP	40.2	4.9	**3.5**	Cr 28 day DUP	41.2	0.981	**1.7**	I 28 day DUP	34.8	3.36	**2.9**	IO3 28 day DUP	39.2	3.36	**1.2**
Tc 1 day Blank	ND	4.9	**Blank**	Cr 1 day Blank	1	0.981	**Blank**	I 1 day Blank	ND	3.36	**Blank**	IO3 1 day Blank	ND	3.36	**Blank**
Tc 3 day Blank	ND	4.9	**Average**	Cr 3 day Blank	ND	0.981	**Average**	I 3 day Blank	ND	3.36	**Average**	IO3 3 day Blank	ND	3.36	**Average**
Tc 7 day Blank	ND	4.9	<4.9	Cr 7 day Blank	2.38	0.981	<0.981	I 7 day Blank	12.2	3.36	**<3,36**	IO3 7 day Blank	ND	3.36	<3.36
Tc 14 day Blank	ND	4.9	**σ**	Cr14 day Blank	ND	0.981	**σ**	I 14 day Blank	ND	3.36	**σ**	IO3 14 day Blank	ND	3.36	**σ**
Tc 28 day Blank	18.7	4.9	NA	Cr 28 day Blank	ND	0.981	**NA**	I 28 day Blank	ND	3.36	**NA**	IO3 28 day Blank	ND	3.36	**NA**
Aluminum	mg/L	dl (mg/L)		Aluminum	mg/L	dl (mg/L)		Aluminum	mg/L	dl (mg/L)		Aluminum	mg/L	dl (mg/L)	
Glass Leachate				**Glass Leachate**				**Glass Leachate**				**Glass Leachate**			
Tc 1 day	216	0.168		Cr 1 day	201	0.168		I 1 day	206	0.101		IO3 1 day	210	0.101	
Tc 1 day DUP	217	0.168		Cr 1 day DUP	200	0.168		I 1 day DUP	209	0.101		IO3 1 day DUP	211	0.101	
Tc 3 day	216	0.168		Cr 3 day	206	0.168		I 3 day	211	0.101		IO3 3 day	213	0.101	
Tc 3 day DUP	220	0.168		Cr 3 day DUP	202	0.168		I 3 day DUP	217	0.101		IO3 day DUP	212	0.101	
Tc 7 day	230	0.168		Cr 7 day	206	0.168		I 7 day	205	0.101		IO3 7 day	211	0.101	
Tc 7 day DUP	223	0.168	**Effluent**	Cr 7 day DUP	210	0.168	**Effluent**	I 7 day DUP	211	0.101	**Effluent**	IO3 7 day DUP	217	0.101	**Effluent**
Tc 14 day	217	0.168	**Average**	Cr 14 day	210	0.168	**Average**	I 14 day	217	0.101	**Average**	IO3 14 day	214	0.101	**Average**
Tc 14 day DUP	218	0.168	221.3	Cr 14 day DUP	209	0.168	206.4	I 14 day DUP	216	0.101	202.8	IO3 14 day DUP	210	0.101	212.5
Tc 28 day	226	0.168	**σ**	Cr 28 day	209	0.168	**σ**	I 28 day	206	0.101	**σ**	IO3 28 day	210	0.101	**σ**
Tc 28 day DUP	230	0.168	5.6	Cr 28 day DUP	211	0.168	4.1	I 28 day DUP	130	0.101	26.0	IO3 28 day DUP	217	0.101	2.7
Tc 1 day Blank	11.4	0.168	**Blank**	Cr 1 day Blank	9.98	0.168	**Blank**	I 1 day Blank	8.97	0.101	**Blank**	IO3 1 day Blank	9.44	0.101	**Blank**
Tc 3 day Blank	11.3	0.168	**Average**	Cr 3 day Blank	10.1	0.168	**Average**	I 3 day Blank	9	0.101	**Average**	IO3 3 day Blank	9.57	0.101	**Average**
Tc 7 day Blank	11.5	0.168	11.32	Cr 7 day Blank	10.2	0.168	10.1	I 7 day Blank	9.09	0.101	9.23	IO3 7 day Blank	9.73	0.101	9.56
Tc 14 day Blank	11.3	0.168	**σ**	Cr14 day Blank	10.1	0.168	**σ**	I 14 day Blank	10.3	0.101	**σ**	IO3 14 day Blank	9.46	0.101	**σ**
Tc 28 day Blank	11.1	0.168	0.15	Cr 28 day Blank	10	0.168	0.09	I 28 day Blank	8.8	0.101	0.61	IO3 28 day Blank	9.61	0.101	0.12

dl = detection limit; ND = not detected; NA = not applicable

Table 4.6. Measured Silicon Concentrations in Batch Test Solutions

Silicon	µg/L	dl (µg/L)		Silicon	µg/L	dl (µg/L)		Silicon	µg/L	dl (µg/L)		Silicon	µg/L	dl (µg/L)	
IDF PW				**IDF PW**				**IDF PW**				**IDF PW**			
Tc 1 day	10100	1310		Cr 1 day	7060	2620		I 1 day	10800	548		IO3 1 day	7610	548	
Tc 1 day DUP	**4630**	1310		Cr 1 day DUP	9110	2620		I 1 day DUP	10900	548		IO3 1 day DUP	7430	548	
Tc 3 day	11900	1310		Cr 3 day	13900	2620		I 3 day	12700	548		IO3 3 day	11700	548	
Tc 3 day DUP	12200	1310		Cr 3 day DUP	16200	2620		I 3 day DUP	13400	548		IO3 day DUP	13400	548	
Tc 7 day	13500	1310		Cr 7 day	15300	2620		I 7 day	13900	548		IO3 7 day	14500	548	
Tc 7 day DUP	13600	1310	**Effluent**	Cr 7 day DUP	15300	2620	**Effluent**	I 7 day DUP	14200	548	**Effluent**	IO3 7 day DUP	14500	548	**Effluent**
Tc 14 day	14800	1310	**Average**	Cr 14 day	13800	2620	**Average**	I 14 day	16700	548	**Average**	IO3 14 day	17700	548	**Average**
Tc 14 day DUP	14700	1310	**12703**	Cr 14 day DUP	13700	2620	**12857**	I 14 day DUP	16800	548	**14300**	IO3 14 day DUP	17100	548	**13744**
Tc 28 day	15800	1310	**σ**	Cr 28 day	12300	2620	**σ**	I 28 day	16300	548	**σ**	IO3 28 day	16200	548	**σ**
Tc 28 day DUP	15800	1310	**3364**	Cr 28 day DUP	11900	2620	**2880**	I 28 day DUP	17300	548	**2412**	IO3 28 day DUP	17300	548	**3779**
Tc 1 day Blank	ND	1310	**Blank**	Cr 1 day Blank	3620	2620	**Blank**	I 1 day Blank	ND	548	**Blank**	IO3 1 day Blank	ND	548	**Blank**
Tc 3 day Blank	ND	1310	**Average**	Cr 3 day Blank	ND	2620	**Average**	I 3 day Blank	ND	548	**Average**	IO3 3 day Blank	ND	548	**Average**
Tc 7 day Blank	ND	1310	**<1310**	Cr 7 day Blank	ND	2620	**<2620**	I 7 day Blank	ND	548	**<548**	IO3 7 day Blank	ND	548	**<548**
Tc14 day Blank	ND	1310	**σ**	Cr 14 day Blank	ND	2620	**σ**	I 14 day Blank	ND	548	**σ**	IO3 14 day Blank	ND	548	**σ**
Tc 28 day Blank	ND	1310	**NA**	Cr 28 day Blank	ND	2620	**NA**	I 28 day Blank	ND	548	**NA**	IO3 28 day Blank	ND	548	**NA**
Silicon	ug/L	dl (ug/L)		Silicon	ug/L	dl (ug/L)		Silicon	ug/L	dl (ug/L)		Silicon	ug/L	dl (ug/L)	
Cast Stone Leachate				**Cast Stone Leachate**				**Cast Stone Leachate**				**Cast Stone Leachate**			
Tc 1 day	23900	13100		Cr 1 day	13100	2620		I 1 day	15800	548		IO3 1 day	14700	548	
Tc 1 day DUP	42000	13100		Cr 1 day DUP	13800	2620		I 1 day DUP	16200	548		IO3 1 day DUP	15200	548	
Tc 3 day	ND	13100		Cr 3 day	11600	2620		I 3 day	13600	548		IO3 3 day	12800	548	
Tc 3 day DUP	ND	13100		Cr 3 day DUP	11400	2620		I 3 day DUP	13800	548		IO3 day DUP	12700	548	
Tc 7 day	ND	13100		Cr 7 day	10300	2620	**Effluent**	I 7 day	12200	548	**Effluent**	IO3 7 day	12100	548	**Effluent**
Tc 7 day DUP	ND	13100	**Effluent**	Cr 7 day DUP	9720	2620	**Average**	I 7 day DUP	12400	548	**Average**	IO3 7 day DUP	11900	548	**Average**
Tc 14 day	ND	13100	**Average**	Cr 14 day	9510	2620	**10612**	I 14 day	11800	548	**13320**	IO3 14 day	11400	548	**12400**
Tc 14 day DUP	17300	13100	**27733**	Cr 14 day DUP	9790	2620	**σ**	I 14 day DUP	12900	548	**σ**	IO3 14 day DUP	11400	548	**σ**
Tc 28 day	ND	13100	**σ**	Cr 28 day	8540	2620	**1829**	I 28 day	12300	548	**1550**	IO3 28 day	10600	548	**1506**

Silicon	µg/L	dl (µg/L)		Silicon	µg/L	dl (µg/L)		Silicon	µg/L	dl (µg/L)		Silicon	µg/L	dl (µg/L)	
Tc 28 day DUP	ND	13100	**12788**	Cr 28 day DUP	8360	2620	**Blank**	I 28 day DUP	12200	548	**Blank**	IO3 28 day DUP	11200	548	**Blank**
Cast Stone Leachate				**Cast Stone Leachate**				**Cast Stone Leachate**				**Cast Stone Leachate**			
Tc 1 day Blank	20100	13100	**Blank**	Cr 1 day Blank	19300	2620	**Average**	I 1 day Blank	19100	5480	**Average**	IO3 1 day Blank	18000	5480	**Average**
Tc 3 day Blank	19300	13100	**Average**	Cr 3 day Blank	19200	2620	**19280**	I 3 day Blank	18900	5480	**18800**	IO3 3 day Blank	18100	5480	**18280**
Tc 7 day Blank	18700	13100	**19300**	Cr 7 day Blank	19200	2620	**σ**	I 7 day Blank	19500	5480	**σ**	IO3 7 day Blank	18500	5480	**σ**
Tc 14 day Blank	19500	13100	**σ**	Cr 14 day Blank	19200	2620	**130.4**	I 14 day Blank	18500	5480	**574.5**	IO3 14 day Blank	18600	5480	**258.8**
Tc 28 day Blank	18900	13100	**547.7**	Cr 28 day Blank	19500	2620		I 28 day Blank	18000	5480		IO3 28 day Blank	18200	5480	
Silicon	ug/L	dl (ug/L)		Silicon	ug/L	dl (ug/L)		Silicon	ug/L	dl (ug/L)		Silicon	ug/L	dl (ug/L)	
Glass Leachate				**Glass Leachate**				**Glass Leachate**				**Glass Leachate**			
Tc 1 day	33700	274		Cr 1 day	41000	274		I 1 day	30200	164		IO3 1 day	26500	164	
Tc 1 day DUP	33700	274		Cr 1 day DUP	38000	274		I 1 day DUP	28900	164		IO3 1 day DUP	25600	164	
Tc 3 day	28900	274		Cr 3 day	33600	274		I 3 day	18400	164		IO3 3 day	21400	164	
Tc 3 day DUP	29400	274		Cr 3 day DUP	32800	274		I 3 day DUP	18800	164		IO3 day DUP	17500	164	
Tc 7 day	26400	274	**Effluent**	Cr 7 day	28300	274	**Effluent**	I 7 day	13500	164	**Effluent**	IO3 7 day	21500	164	**Effluent**
Tc 7 day DUP	26800	274	**Average**	Cr 7 day DUP	28900	274	**Average**	I 7 day DUP	14000	164	**Average**	IO3 7 day DUP	20900	164	**Average**
Tc 14 day	25300	274	**27360**	Cr 14 day	23500	274	**28680**	I 14 day	17300	164	**17767**	IO3 14 day	19900	164	**20700**
Tc 14 day DUP	24400	274	**σ**	Cr 14 day DUP	21400	274	**σ**	I 14 day DUP	15800	164	**σ**	IO3 14 day DUP	19100	164	**σ**
Tc 28 day	22700	274	**4062**	Cr 28 day	19600	274	**7623**	I 28 day	12700	164	**6962**	IO3 28 day	17300	164	**3255**
Tc 28 day DUP	22300	274	**Blank**	Cr 28 day DUP	19700	274	**Blank**	I 28 day DUP	8070	164	**Blank**	IO3 28 day DUP	17300	164	**Blank**
Tc 1 day Blank	68500	274	**Average**	Cr 1 day Blank	70600	274	**Average**	I 1 day Blank	65800	164	**Average**	IO3 1 day Blank	66100	164	**Average**
Tc 3 day Blank	74600	274	**71140**	Cr 3 day Blank	71600	274	**69980**	I 3 day Blank	65500	164	**64360**	IO3 3 day Blank	65900	164	**65340**
Tc 7 day Blank	71200	274	**σ**	Cr 7 day Blank	69900	274	**σ**	I 7 day Blank	64900	164	**σ**	IO3 7 day Blank	65200	164	**σ**
Tc 14 day Blank	70700	274	**2198**	Cr 14 day Blank	70000	274	**1394**	I14 day Blank	61800	164	**1623**	IO3 14 day Blank	64800	164	**635**
Tc 28 day Blank	70700	274		Cr 28 day Blank	67800	274		I 28 day Blank	63800	164		IO3 28 day Blank	64700	164	

dl = detection limit; ND = not detected; NA = not applicable.

Table 4.7. Measured Sodium Concentrations in Batch Test Solutions

Sodium	mg/L	dl (mg/L)		Sodium	mg/L	dl (mg/L)		Sodium	mg/L	dl (mg/L)		Sodium	mg/L	dl (mg/L)	
IDF PW				**IDF PW**				**IDF PW**				**IDF PW**			
Tc 1 day	137	0.447		Cr 1 day	127	0.894		I 1 day	127	0.447		IO3 1 day	130	0.447	
Tc 1 day DUP	134	0.447		Cr 1 day DUP	128	0.894		I 1 day DUP	131	0.447		IO3 1 day DUP	128	0.447	
Tc 3 day	135	0.447		Cr 3 day	129	0.894		I 3 day	122	0.447		IO3 3 day	120	0.447	
Tc 3 day DUP	138	0.447		Cr 3 day DUP	127	0.894		I 3 day DUP	129	0.447		IO3 day DUP	135	0.447	
Tc 7 day	137	0.447		Cr 7 day	128	0.894		I 7 day	126	0.447		IO3 7 day	127	0.447	
Tc 7 day DUP	138	0.447	**Effluent**	Cr 7 day DUP	129	0.894	**Effluent**	I 7 day DUP	121	0.447	**Effluent**	IO3 7 day DUP	129	0.447	**Effluent**
Tc 14 day	136	0.447	**Average**	Cr 14 day	132	0.894	**Average**	I 14 day	132	0.447	**Average**	IO3 14 day	130	0.447	**Average**
Tc 14 day DUP	138	0.447	**137.5**	Cr 14 day DUP	132	0.894	**129.2**	I 14 day DUP	130	0.447	**126.9**	IO3 14 day DUP	129	0.447	**128.6**
Tc 28 day	140	0.447	**σ**	Cr 28 day	132	0.894	**σ**	I 28 day	124	0.447	**σ**	IO3 28 day	127	0.447	**σ**
Tc 28 day DUP	142	0.447	**2.3**	Cr 28 day DUP	128	0.894	**2.0**	I 28 day DUP	127	0.447	**3.7**	IO3 28 day DUP	131	0.447	**3.8**
Tc 1 day Blank	132	0.447	**Blank**	Cr 1 day Blank	121	0.894	**Blank**	I 1 day Blank	117	0.447	**Blank**	IO3 1 day Blank	124	0.447	**Blank**
Tc 3 day Blank	128	0.447	**Average**	Cr 3 day Blank	122	0.894	**Average**	I 3 day Blank	122	0.447	**Average**	IO3 3 day Blank	129	0.447	**Average**
Tc 7 day Blank	131	0.447	**129.2**	Cr 7 day Blank	122	0.894	**123.2**	I 7 day Blank	127	0.447	**121.8**	IO3 7 day Blank	122	0.447	**123.4**
Tc14 day Blank	130	0.447	**σ**	Cr 14 day Blank	127	0.894	**σ**	I 14 day Blank	121	0.447	**σ**	IO3 14 day Blank	122	0.447	**σ**
Tc 28 day Blank	125	0.447	**2.8**	Cr 28 day Blank	124	0.894	**2.4**	I 28 day Blank	122	0.447	**3.6**	IO3 28 day Blank	120	0.447	**3.4**
Sodium	mg/L	dl (mg/L)		Sodium	mg/L	dl (mg/L)		Sodium	mg/L	dl (mg/L)		Sodium	mg/L	dl (mg/L)	
Cast Stone Leachate				**Cast Stone Leachate**				**Cast Stone Leachate**				**Cast Stone Leachate**			
Tc 1 day	1050	4.47		Cr 1 day	979	0.894		I 1 day	912	4.47		IO3 1 day	896	4.47	
Tc 1 day DUP	1010	4.47		Cr 1 day DUP	946	0.894		I 1 day DUP	931	4.47		IO3 1 day DUP	925	4.47	
Tc 3 day	1000	4.47		Cr 3 day	962	0.894		I 3 day	959	4.47		IO3 3 day	930	4.47	
Tc 3 day DUP	997	4.47		Cr 3 day DUP	931	0.894		I 3 day DUP	933	4.47		IO3 day DUP	955	4.47	
Tc 7 day	994	4.47		Cr 7 day	944	0.894	**Effluent**	I 7 day	914	4.47	**Effluent**	IO3 7 day	904	4.47	**Effluent**
Tc 7 day DUP	1010	4.47	**Effluent**	Cr 7 day DUP	872	0.894	**Average**	I 7 day DUP	929	4.47	**Average**	IO3 7 day DUP	913	4.47	**Average**
Tc 14 day	988	4.47	**Average**	Cr 14 day	938	0.894	**943.6**	I 14 day	918	4.47	**934**	IO3 14 day	975	4.47	**919.1**

Sodium	mg/L	dl (mg/L)		Sodium	mg/L	dl (mg/L)		Sodium	mg/L	dl (mg/L)		Sodium	mg/L	dl (mg/L)	
Cast Stone Leachate				**Cast Stone Leachate**				**Cast Stone Leachate**				**Cast Stone Leachate**			
Tc 14 day DUP	1000	4.47	**1004.9**	Cr 14 day DUP	972	0.894	**σ**	I 14 day DUP	951	4.47	**σ**	IO3 14 day DUP	897	4.47	**σ**
Tc 28 day	990	4.47	**σ**	Cr 28 day	924	0.894	**31.1**	I 28 day	933	4.47	**17.5**	IO3 28 day	880	4.47	**28.7**
Tc 28 day DUP	1010	4.47	**17.8**	Cr 28 day DUP	968	0.894	**Blank**	I 28 day DUP	960	4.47	**Blank**	IO3 28 day DUP	916	4.47	**Blank**
Tc 1 day Blank	1370	4.47	**Blank**	Cr 1 day Blank	1260	0.894	**Average**	I 1 day Blank	1240	4.47	**Average**	IO3 1 day Blank	1230	4.47	**Average**
Tc 3 day Blank	1370	4.47	**Average**	Cr 3 day Blank	1250	0.894	**1256**	I 3 day Blank	1290	4.47	**1260**	IO3 3 day Blank	1290	4.47	**1260**
Tc 7 day Blank	1360	4.47	**1364**	Cr 7 day Blank	1280	0.894	**σ**	I 7 day Blank	1260	4.47	**σ**	IO3 7 day Blank	1280	4.47	**σ**
Tc 14 day Blank	1370	4.47	**σ**	Cr 14 day Blank	1230	0.894	**18.2**	I 14 day Blank	1250	4.47	**18.7**	IO3 14 day Blank	1270	4.47	**28.3**
Tc 28 day Blank	1350	4.47	**8.9**	Cr 28 day Blank	1260	0.894		I 28 day Blank	1260	4.47		IO3 28 day Blank	1230	4.47	
Sodium	mg/L	dl (mg/L)		Sodium	mg/L	dl (mg/L)		Sodium	mg/L	dl (mg/L)		Sodium	mg/L	dl (mg/L)	
Glass Leachate				**Glass Leachate**				**Glass Leachate**				**Glass Leachate**			
Tc 1 day	2580	0.223		Cr 1 day	2420	0.223		I 1 day	NO DATA	NO DATA		IO3 1 day	NO DATA	NO DATA	
Tc 1 day DUP	2590	0.223		Cr 1 day DUP	2410	0.223		I 1 day DUP	NO DATA	NO DATA		IO3 1 day DUP	NO DATA	NO DATA	
Tc 3 day	2560	0.223		Cr 3 day	2440	0.223		I 3 day	NO DATA	NO DATA		IO3 3 day	NO DATA	NO DATA	
Tc 3 day DUP	missing			Cr 3 day DUP	2410	0.223		I 3 day DUP	NO DATA	NO DATA		IO3 day DUP	NO DATA	NO DATA	
Tc 7 day	2610	0.223		Cr 7 day	2490	0.223		I 7 day	NO DATA	NO DATA		IO3 7 day	NO DATA	NO DATA	
Tc 7 day DUP	2560	0.223	**Effluent**	Cr 7 day DUP	2500	0.223	**Effluent**	I 7 day DUP	NO DATA	NO DATA	**Effluent**	IO3 7 day DUP	NO DATA	NO DATA	**Effluent**
Tc 14 day	2510	0.223	**Average**	Cr 14 day	2480	0.223	**Average**	I 14 day	NO DATA	NO DATA	**Average**	IO3 14 day	NO DATA	NO DATA	**Average**
Tc 14 day DUP	2510	0.223	**2558**	Cr 14 day DUP	2450	0.223	**2452**	I 14 day DUP	NO DATA	NO DATA	**NO DATA**	IO3 14 day DUP	NO DATA	NO DATA	**NO DATA**
Tc 28 day	2530	0.223	**σ**	Cr 28 day	2460	0.223	**σ**	I 28 day	NO DATA	NO DATA	**σ**	IO3 28 day	NO DATA	NO DATA	**σ**
Tc 28 day DUP	2570	0.223	**34.9**	Cr 28 day DUP	2460	0.223	**32.2**	I 28 day DUP	NO DATA	NO DATA	**NA**	IO3 28 day DUP	NO DATA	NO DATA	**NA**
Tc 1 day Blank	2930	0.223	**Blank**	Cr 1 day Blank	2730	0.223	**Blank**	I 1 day Blank	NO DATA	NO DATA	**Blank**	IO3 1 day Blank	NO DATA	NO DATA	**Blank**

Sodium	mg/L	dl (mg/L)		Sodium	mg/L	dl (mg/L)		Sodium	mg/L	dl (mg/L)		Sodium	mg/L	dl (mg/L)	
Glass Leachate				**Glass Leachate**				**Glass Leachate**				**Glass Leachate**			
Tc 3 day Blank	2850	0.223	**Average**	Cr 3 day Blank	2770	0.223	**Average**	I 3 day Blank	NO DATA	NO DATA	**Average**	IO3 3 day Blank	NO DATA	NO DATA	**Average**
Tc 7 day Blank	2940	0.223	**2880**	Cr 7 day Blank	2820	0.223	**2778**	I 7 day Blank	NO DATA	NO DATA	**NO DATA**	IO3 7 day Blank	NO DATA	NO DATA	**NO DATA**
Tc 14 day Blank	2870	0.223	**σ**	Cr 14 day Blank	2800	0.223	**σ**	I 14 day Blank	NO DATA	NO DATA	**σ**	IO3 14 day Blank	NO DATA	NO DATA	**σ**
Tc 28 day Blank	2810	0.223	**54.8**	Cr 28 day Blank	2770	0.223	**34.2**	I 28 day Blank	NO DATA	NO DATA	**NA**	IO3 28 day Blank	NO DATA	NO DATA	**NA**

dl = detection limit; ND = not detected; NA = not applicable.

Table 4.8. Measured Calcium Concentrations in Batch Test Solutions

Calcium	mg/L	dl (mg/L)		Calcium	mg/L	dl (mg/L)		Calcium	mg/L	dl (mg/L)		Calcium	mg/L	dl (mg/L)	
IDF PW				**IDF PW**				**IDF PW**				**IDF PW**			
Tc 1 day	485	0.49		Cr 1 day	475	0.981		I 1 day	456	0.336		IO3 1 day	455	0.336	
Tc 1 day DUP	487	0.49		Cr 1 day DUP	475	0.981		I 1 day DUP	459	0.336		IO3 1 day DUP	447	0.336	
Tc 3 day	474	0.49		Cr 3 day	464	0.981		I 3 day	442	0.336		IO3 3 day	423	0.336	
Tc 3 day DUP	486	0.49		Cr 3 day DUP	460	0.981		I 3 day DUP	461	0.336		IO3 day DUP	456	0.336	
Tc 7 day	485	0.49		Cr 7 day	462	0.981		I 7 day	433	0.336		IO3 7 day	444	0.336	
Tc 7 day DUP	482	0.49	**Effluent**	Cr 7 day DUP	462	0.981	**Effluent**	I 7 day DUP	435	0.336	**Effluent**	IO3 7 day DUP	450	0.336	**Effluent**
Tc 14 day	476	0.49	**Average**	Cr 14 day	474	0.981	**Average**	I 14 day	457	0.336	**Average**	IO3 14 day	451	0.336	**Average**
Tc 14 day DUP	482	0.49	**482.4**	Cr 14 day DUP	474	0.981	**465.4**	I 14 day DUP	460	0.336	**450.2**	IO3 14 day DUP	449	0.336	**447**
Tc 28 day	472	0.49	**σ**	Cr 28 day	462	0.981	**σ**	I 28 day	445	0.336	**σ**	IO3 28 day	442	0.336	**σ**
Tc 28 day DUP	495	0.49	**6.9**	Cr 28 day DUP	446	0.981	**9.3**	I 28 day DUP	454	0.336	**10.6**	IO3 28 day DUP	453	0.336	**9.5**
Tc 1 day Blank	498	0.49	**Blank**	Cr 1 day Blank	473	0.981	**Blank**	I 1 day Blank	444	0.336	**Blank**	IO3 1 day Blank	465	0.336	**Blank**
Tc 3 day Blank	478	0.49	**Average**	Cr 3 day Blank	475	0.981	**Average**	I 3 day Blank	469	0.336	**Average**	IO3 3 day Blank	478	0.336	**Average**
Tc 7 day Blank	496	0.49	**488.2**	Cr 7 day Blank	477	0.981	**481**	I 7 day Blank	473	0.336	**463**	IO3 7 day Blank	457	0.336	**460.2**
Tc14 day Blank	493	0.49	**σ**	Cr 14 day Blank	496	0.981	**σ**	I 14 day Blank	463	0.336	**σ**	IO3 14 day Blank	457	0.336	**σ**
Tc 28 day Blank	476	0.49	**10.4**	Cr 28 day Blank	484	0.981	**9.4**	I 28 day Blank	466	0.336	**11.2**	IO3 28 day Blank	444	0.336	**12.5**

Calcium	mg/L	dl (mg/L)		Calcium	mg/L	dl (mg/L)		Calcium	mg/L	dl (mg/L)		Calcium	mg/L	dl (mg/L)	
Cast Stone Leachate				**Cast Stone Leachate**				**Cast Stone Leachate**				**Cast Stone Leachate**			
Tc 1 day	33.6	4.9		Cr 1 day	40.3	0.981		I 1 day	38	3.36		IO3 1 day	40.6	3.36	
Tc 1 day DUP	41.9	4.9		Cr 1 day DUP	38	0.981		I 1 day DUP	37.7	3.36		IO3 1 day DUP	39.9	3.36	
Tc 3 day	42.4	4.9		Cr 3 day	39.5	0.981		I 3 day	40.5	3.36		IO3 3 day	40.3	3.36	
Tc 3 day DUP	43.4	4.9		Cr 3 day DUP	38.3	0.981		I 3 day DUP	38	3.36		IO3 day DUP	40.6	3.36	
Tc 7 day	47	4.9		Cr 7 day	39.4	0.981		I 7 day	38.3	3.36		IO3 7 day	38.5	3.36	
Tc 7 day DUP	44.2	4.9	**Effluent**	Cr 7 day DUP	35.6	0.981	**Effluent**	I 7 day DUP	39.2	3.36	**Effluent**	IO3 7 day DUP	39.5	3.36	**Effluent**
Tc 14 day	41	4.9	**Average**	Cr 14 day	38.8	0.981	**Average**	I 14 day	36.3	3.36	**Average**	IO3 14 day	39.3	3.36	**Average**
Tc 14 day DUP	40.5	4.9	**41.71**	Cr 14 day DUP	40.8	0.981	**39.24**	I 14 day DUP	33.5	3.36	**36.7**	IO3 14 day DUP	38.7	3.36	**39.33**
Tc 28 day	42.9	4.9	**σ**	Cr 28 day	40.5	0.981	**σ**	I 28 day	30.7	3.36	**σ**	IO3 28 day	36.7	3.36	**σ**
Tc 28 day DUP	40.2	4.9	**3.5**	Cr 28 day DUP	41.2	0.981	**1.7**	I 28 day DUP	34.8	3.36	**2.9**	IO3 28 day DUP	39.2	3.36	**1.2**
Tc 1 day Blank	ND	4.9	**Blank**	Cr 1 day Blank	1	0.981	**Blank**	I 1 day Blank	ND	3.36	**Blank**	IO3 1 day Blank	ND	3.36	**Blank**
Tc 3 day Blank	ND	4.9	**Average**	Cr 3 day Blank	ND	0.981	**Average**	I 3 day Blank	ND	3.36	**Average**	IO3 3 day Blank	ND	3.36	**Average**
Tc 7 day Blank	ND	4.9	<4.9	Cr 7 day Blank	2.38	0.981	<0.981	I 7 day Blank	12.2	3.36	**<3.36**	IO3 7 day Blank	ND	3.36	<3.36
Tc 14 day Blank	ND	4.9	**σ**	Cr 14 day Blank	ND	0.981	**σ**	I 14 day Blank	ND	3.36	**σ**	IO3 14 day Blank	ND	3.36	**σ**
Tc 28 day Blank	18.7	4.9	NA	Cr 28 day Blank	ND	0.981	**NA**	I 28 day Blank	ND	3.36	**NA**	IO3 28 day Blank	ND	3.36	**NA**

Calcium	mg/L	dl (mg/L)		Calcium	mg/L	dl (mg/L)		Calcium	mg/L	dl (mg/L)		Calcium	mg/L	dl (mg/L)	
Glass Leachate				**Glass Leachate**				**Glass Leachate**				**Glass Leachate**			
Tc 1 day	216	0.168		Cr 1 day	201	0.168		I 1 day	206	0.101		IO3 1 day	210	0.101	
Tc 1 day DUP	217	0.168		Cr 1 day DUP	200	0.168		I 1 day DUP	209	0.101		IO3 1 day DUP	211	0.101	
Tc 3 day	216	0.168		Cr 3 day	206	0.168		I 3 day	211	0.101		IO3 3 day	213	0.101	
Tc 3 day DUP	220	0.168		Cr 3 day DUP	202	0.168		I 3 day DUP	217	0.101		IO3 day DUP	212	0.101	
Tc 7 day	230	0.168		Cr 7 day	206	0.168		I 7 day	205	0.101		IO3 7 day	211	0.101	
Tc 7 day DUP	223	0.168	**Effluent**	Cr 7 day DUP	210	0.168	**Effluent**	I 7 day DUP	211	0.101	**Effluent**	IO3 7 day DUP	217	0.101	**Effluent**
Tc 14 day	217	0.168	**Average**	Cr 14 day	210	0.168	**Average**	I 14 day	217	0.101	**Average**	IO3 14 day	214	0.101	**Average**
Tc 14 day DUP	218	0.168	221.3	Cr 14 day DUP	209	0.168	206.4	I 14 day DUP	216	0.101	202.8	IO3 14 day DUP	210	0.101	212.5
Tc 28 day	226	0.168	**σ**	Cr 28 day	209	0.168	**σ**	I 28 day	206	0.101	**σ**	IO3 28 day	210	0.101	**σ**

Calcium	mg/L	dl (mg/L)		Calcium	mg/L	dl (mg/L)		Calcium	mg/L	dl (mg/L)		Calcium	mg/L	dl (mg/L)	
Glass Leachate				**Glass Leachate**				**Glass Leachate**				**Glass Leachate**			
Tc 28 day DUP	230	0.168	5.6	Cr 28 day DUP	211	0.168	4.1	I 28 day DUP	130	0.101	26.0	IO3 28 day DUP	217	0.101	2.7
Tc 1 day Blank	11.4	0.168	**Blank**	Cr 1 day Blank	9.98	0.168	**Blank**	I 1 day Blank	8.97	0.101	**Blank**	IO3 1 day Blank	9.44	0.101	**Blank**
Tc 3 day Blank	11.3	0.168	**Average**	Cr 3 day Blank	10.1	0.168	**Average**	I 3 day Blank	9	0.101	**Average**	IO3 3 day Blank	9.57	0.101	**Average**
Tc 7 day Blank	11.5	0.168	11.32	Cr 7 day Blank	10.2	0.168	10.1	I 7 day Blank	9.09	0.101	9.23	IO3 7 day Blank	9.73	0.101	9.56
Tc 14 day Blank	11.3	0.168	**σ**	Cr 14 day Blank	10.1	0.168	**σ**	I 14 day Blank	10.3	0.101	**σ**	IO3 14 day Blank	9.46	0.101	**σ**
Tc 28 day Blank	11.1	0.168	0.15	Cr 28 day Blank	10	0.168	0.09	I 28 day Blank	8.8	0.101	0.61	IO3 28 day Blank	9.61	0.101	0.12

dl = detection limit; ND = not detected; NA = not applicable

4.5.2 Macro Chemistry of Column Influents and Effluents

The data for macro constituents (both cations and anions) from the flow-through column effluents exhibit similar reactions between the starting solutions (IDF vadose zone pore water, Cast Stone leachate, and glass leachate as described above for the batch tests). Two differences in the column versus batch test methods might cause some differences in the Al and Si reactions. First, the solid-to-solution ratio for the early portions of the column tests is much higher than the 1:2 ratio used in the batch tests; second, the residence time for solution in the flow-through columns is much shorter than the 1- to 28-day contact times used in the batch tests.

4.5.3 Iodine Speciation

Series II Quadrapole ICP-MS using an ESI FAST Autosampler system and Iodine Speciation Kit (proprietary anion exchange column) effluents from the batch K_d tests were "speciated" to ascertain whether there was any conversion of iodate or iodide to the other. Recall that separate batch K_d tests were run with solutions spiked with one of these two iodine species. Thus, for the iodide and iodate solutions, only one species was present at the start of the batch tests, and if there was any interconversion, the iodine speciation measurements would detect the amount of interconversion. Unfortunately, the iodine speciation data for the IDF pore water and Cast Stone leachate effluents from the batch K_d tests apparently contained interferents that caused poor separation of iodate and iodide within the proprietary anion exchange column. For the IDF pore water effluents, when run without dilution, the resulting chromatograms were misshapen and eluted at different times than those expected for iodate and iodide. Further, there was a high background signal between the misshapen peaks and poor washout of the column between sample injections. After several attempts to get useful separation using serial dilution, at a 50X dilution of the IDF pore water batch K_d effluents, we were able to see detectable iodate and iodide peaks right at their detection limits. Qualitatively, we did not see any definitive evidence of interconversion of iodate to iodide or vice versa. The limiting factor in this case was the very low concentrations of both species after sample dilution because the total iodine concentrations were so close to the detection limit.

The Cast Stone leachate effluents from the batch K_d tests also had far too many matrix issues to yield useable data. The resulting chromatograms showed misshapen and misplaced peaks as well as high background and poor washout of the column because of the nature of the sample matrix. Diluting these samples to an acceptable level for the column meant that the iodine concentrations were pushed below their detection limits and we could make no statement about species interconversion.

The glass leachate effluent solutions from the batch K_d gave the best chromatograms (Figure 4.17, Figure 4.18, and Figure 4.19). We were able to run these samples at a 10X dilution. While we are not able to report quantitative results for these samples due to QC being slightly outside our parameters, the glass leachate solutions do show qualitative signs of iodine species conversion. We observed a small amount of iodate converting to iodide. Figure 4.18 and Figure 4.19 suggest a small amount of iodate conversion to iodide in the glass leachate effluent from the batch K_d tests after contacting the IDF sediment. As noted in Figure 4.17, the 28-day control or blank glass leachate solution shows only the iodate peak at about 18 arbitrary time units on the X-axis, as one would expect if there was no species interconversion occurring. However, the two 28-day glass leachates that had been contacting the IDF sediment (Figure 4.18 and Figure 4.19) show both the iodate peak at 18 arbitrary time units as well as a

very small peak at 71 arbitrary time units on the X-axis. At this time, we do not believe that the interconversion of a small amount of iodate to iodide has any significance to future IDF PA calculations. We base this conclusion on the fact that the measured K_d values for iodide and iodate from both the batch and flow-through column laboratory tests are similar (essentially 0 mL/g). Thus, in a practical sense neither form of iodine is sorbing to Hanford sediment from any of the waste form leachates or the vadose zone pore water. Therefore, inter-conversion of the two species does not affect iodine sorption and transport through the IDF subsurface once released from the waste forms. This conclusion is valid as long as the concentrations of iodide and iodate in the leachates/pore waters is low (below any solubility constraints), which is likely true for the IDF subsurface.

As mentioned in Um et al. (2004), iodide is more thermodynamically stable and expected in the IDF subsurface geochemical conditions than iodate (see Figure 4.20). Thus, the interconversion of iodate to iodide does follow the available thermodynamic data.

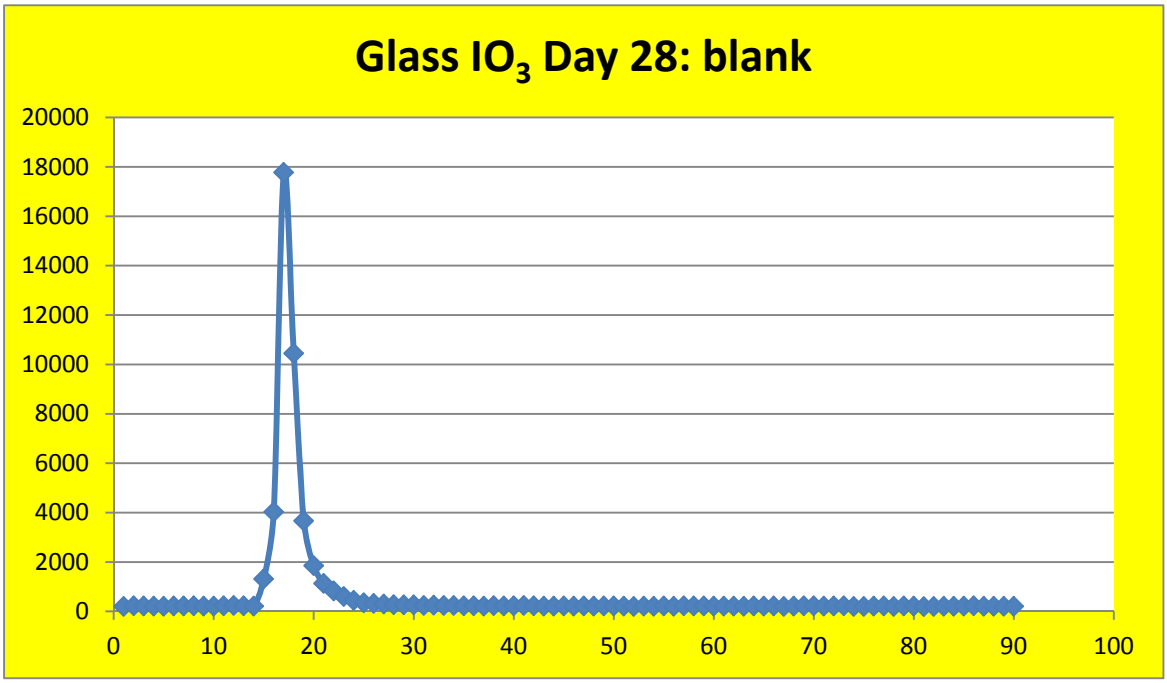

Figure 4.17. 28-day Blank, Glass Leachate, Iodate Chromatogram, Showing the Intensity in Counts Per Second (y-axis) versus Measurement Time Interval

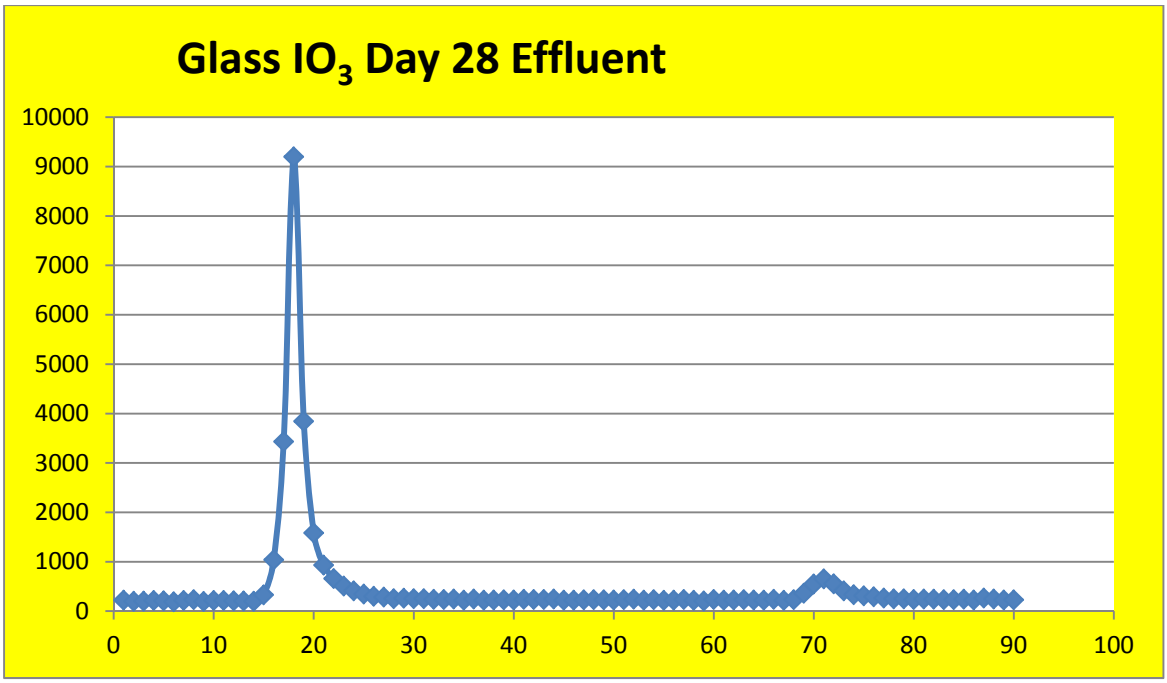

Figure 4.18. 28-day Glass Leachate Iodate Batch Effluent Chromatogram, Showing Slight Interconversion of Iodate to Iodide. The y-axis is intensity in counts per second and the x-axis is the measurement time interval.

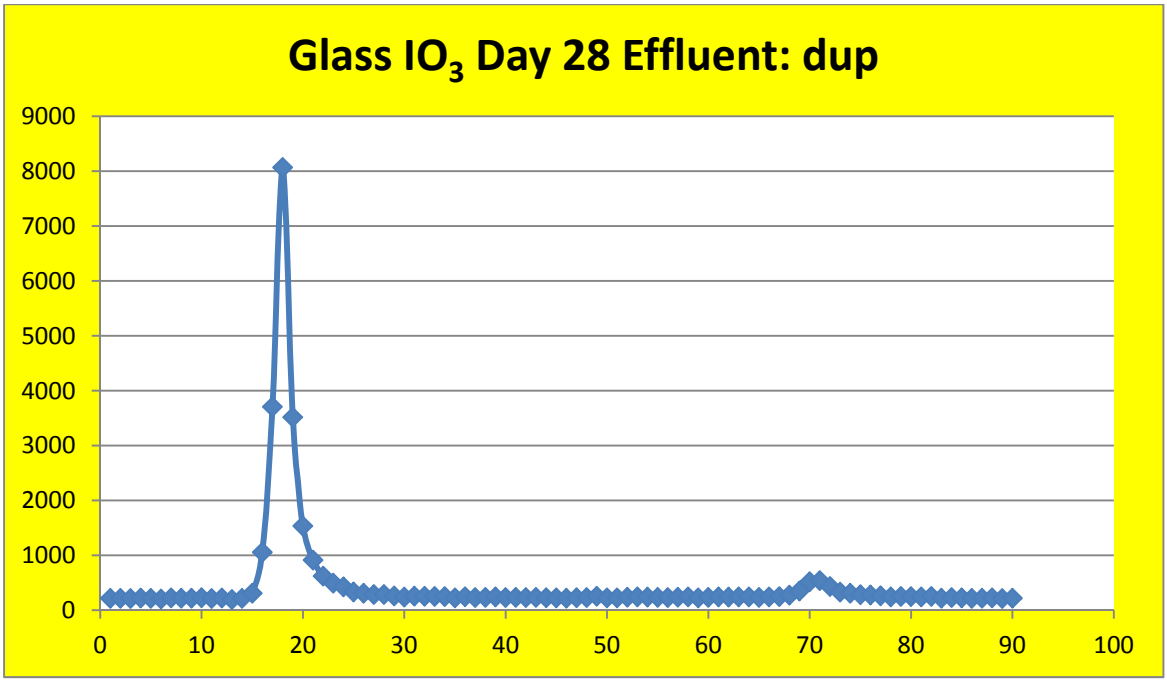

Figure 4.19. 28-day Glass Leachate Iodate Batch Duplicate Effluent Chromatogram, Showing Slight Interconversion of Iodate to Iodide. The y-axis is intensity in counts per second and the x-axis is the measurement time interval.

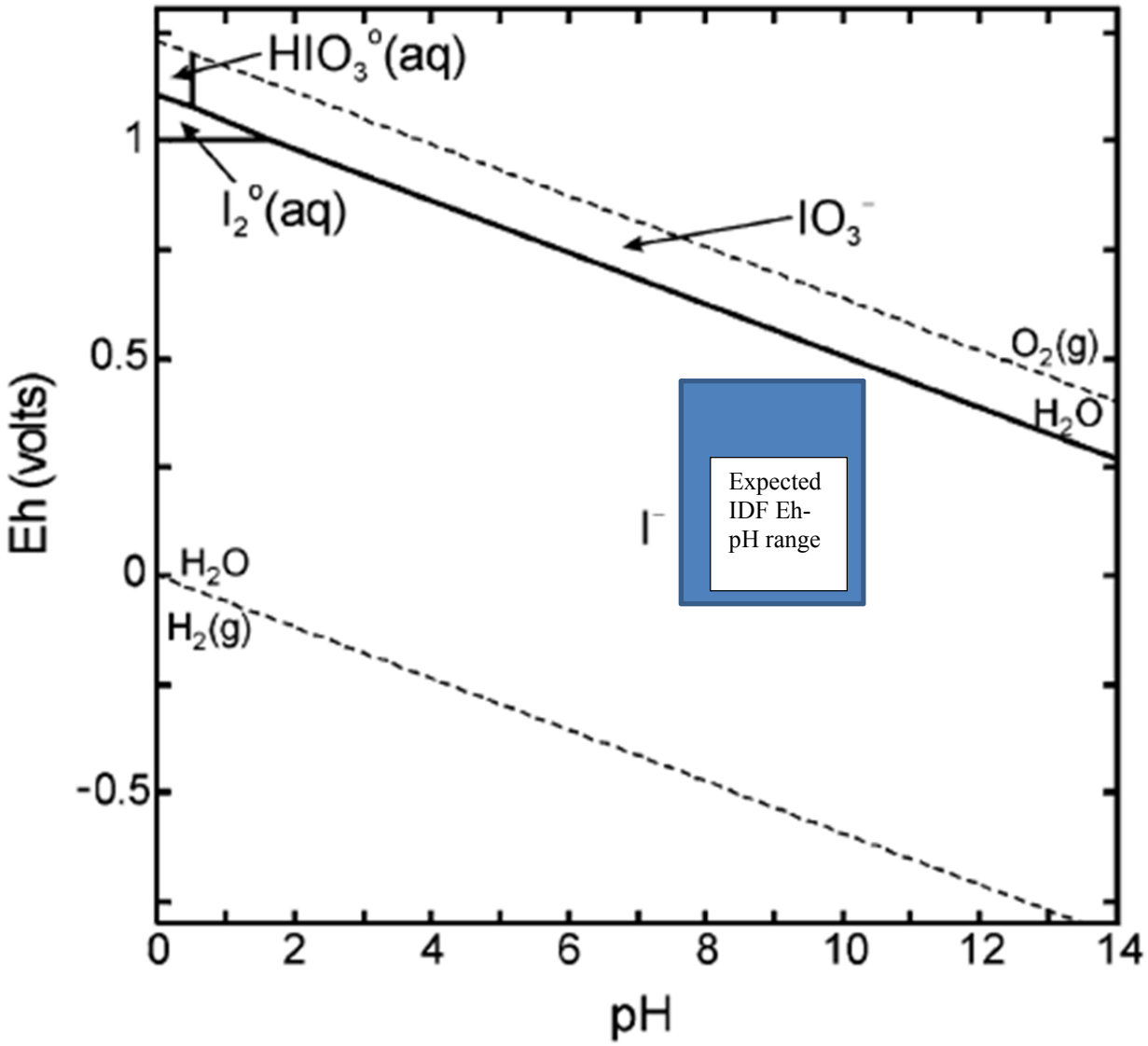

Figure 4.20. Eh-pH Stability Diagram for Dominant Iodine Aqueous Species at 25 °C, Based on a Total Concentration of 10^{-8} mol/L Dissolved Iodine. The dashed lines represent the boundaries for the thermodynamic stability of water. (Taken from Um et al. 2004).

4.6 Geochemical Modeling

Solution chemistry for IDF pore water, glass leachate, and Cast Stone leachate spiked with CrO_4^{2-}, I^-, and IO_3^- were simulated at 1 day using Geochemist Workbench spec8 and the thermo.com.v8.r6.dat database to determine if the solution was oversaturated with respect to secondary minerals that might form during these experiments. The results of the modeling showed that the IDF pore water was supersaturated with respect to dolomite and calcite. Both the Cast Stone leachate and glass leachate were supersaturated with respect to aragonite, calcite, and dolomite. Past research has shown that Cr (as chromate) can be incorporated into the structure of carbonate minerals, such as vaterite and calcite (Hua et al. 2006; Tang et al. 2007). A series of recent experiments at PNNL has also shown that chromate was

removed from the aqueous phase during calcium carbonate mineral precipitation (Sahajpal and Qafoku, personal communications). Co-precipitation of iodate with calcite has also been observed and reported in a recent study (Zhang et al. 2013). It is therefore possible that a portion of chromate and/or iodate may have been incorporated into calcium carbonate minerals during their precipitation.

5.0 Summary

Performance and risk assessments of ILAW and the IDF have shown that risks to groundwater can be quite sensitive to adsorption-desorption interactions. These interactions between the underlying sediments and the contaminants present in the leachates that descend from the buried glass, grouted secondary waste, and potentially Cast Stone waste packages have been represented in these assessments using the contaminant distribution coefficient (K_d) construct. Some contaminants (^{99}Tc, ^{129}I, and Cr) present in significant quantities in these wastes have low K_d values and tend to drive risk to public health and the environment. Small changes in the K_d value can result in relatively large changes in the retardation factor. Thus, even a small uncertainty in the K_d value for these key contaminants can result in a relatively large uncertainty in the risk determined through PA modeling.

The purpose of this study was to further reduce the uncertainty in K_d values for Tc (as $^{99}TcO_4^-$), iodine (as either iodide or iodate), and Cr (as chromate, CrO_4^{2-}) by conducting systematic adsorption-desorption experiments using actual sand-dominated Hanford formation sediments from beneath the IDF and solutions that closely mimic Hanford vadose zone pore water and leachates from Cast Stone and ILAW glass waste forms.

A total of 24 batch and 16 flow-through column experiments were conducted, contributing 256 measurements to improve understanding of Tc, Cr, iodide, and iodate transport of wastes disposed to the IDF. The 120 batch adsorption and 120 batch desorption K_d values are provided in Table 4.5 and Table 4.6, respectively. K_d values calculated from the 15 saturated and 1 unsaturated flow-through column tests are provided in Table 4.3. Table 5.1 summarizes these results. The bold, bracketed values are our best estimates from the experiments described in this report.

Table 5.1. Summary of K_d Results From the Batch and Column Experiments Conducted for This Study

Experiment	K_d Range (Number of Measurements) **[Best Estimate] (mL/g)**			
	Tc (as TcO_4^-)	Cr (as CrO_4^{2-})	Iodide (I^-)	Iodate (IO_3^-)
IDF Pore Water, Batch Adsorption	-0.1 to 0.1 (10) **[0]**	- 0.08 to 0.67 (10) **[0.14 to 0.67]**	-0.02 to -0.12 (10) **[0]**[(a)]	0.19 to 0.38 (10) **[0.21 to 0.36]**
IDF Pore Water, Batch Desorption[(b)]	-0.38 to 0.38 (10) **[0]**	0.67 to 9.8 (10) **[4.6 ± 3.1]**	-0.48 to 0.99 (10) **[NR]**	-0.24 to -0.49 (10) **[NR]**
IDF Pore Water, Sat. Column[(c)]	**[0]**	**[0.03]**	**[0]**	**[0.05]**
IDF Pore Water, Unsat. Column[(c)]	**[0]**	**---**	---	---
Glass Leachate, Batch Adsorption	0.00 to 0.02 (10) **[0 to 0.01]**	0.00 to 2.2 (10) **[0.02 to 2.1]**	-0.22 to 0.16 (10) **[NR]**	-0.11 to 1.5 (10) **[NR]**
Glass Leachate, Batch Desorption[(b)]	0.03 to 0.95 (10) **[0.09 ± 0.04]**	28 to 230 (10) **[79 ± 60]**	-0.68 to 0.69 (10) **[NR]**	-0.73 to 1.9 (10) **[NR]**
Glass Leachate, Sat. Column[(c)]	**[0]**	**[0]**	**[0]**	**[0.14]**
Cast Stone Leachate, Batch Adsorption	-0.08 to 0.04 (10) **[0]**	-0.18 to 0.64 (10) **[0.03 to 0.64]**	-0.05 to 0.04 (10) **[0]**	0.11 to 0.27 (10) **[0.11 to 0.27]**
Cast Stone Leachate, Batch Desorption[(b)]	-0.24 to 0.35 (10) **[0.00 ± 0.19]**	-0.36 to 2.4 (10) **[0.42 ± 1.05]**	-0.22 to 0.03 (10) **[NR]**	0.20 to 0.44 (10) **[NR]**
Cast Stone Leachate, Sat. Column[(c)]	**[0.01 to 0.03]**	**[0.04]**	**[0]**	**[0.01]**

(a) May have been impacted by anion exclusion.
(b) Some desorption results used parameters in the desorption equation that are not physically meaningful (negative mass sorbed on sediment). We do not recommend using these results directly in irreversibility transport predictions.
NR = none recommended
--- = not performed

Negative K_d values in the batch experiments should be considered as representing no significant adsorption, or K_d equal to zero. These negative values are caused by there being so little adsorption of these mobile contaminants that the concentrations of C_o and C_{eff} are nearly the same value, and the difference between the two is dominated by analytical variability. This, then, can lead to negative K_d values. A second cause of negative K_d values is anion exclusion, wherein anions are repelled away from wet sediments and thus concentrated in supernate above the sediments. It is supernate that is sampled in batch tests to measure C_{eff}. The relatively low volume of supernate solution above settled wet sediments in batch tests using a 2:1 ratio of solution to solids can readily be impacted by anions concentrating in it. In the flow-through column tests, bromide (Br^-) was used as the conservative tracer that was assigned a K_d value of 0 mL/g. The BTC curve of each contaminant was then compared to the Br^- BTC curve so that contaminant K_d values could be calculated. Because Br^- is also an anion similar to the four contaminants studied, anion exclusion effects are not accounted for in the flow-through column experiments. Some flow-through column test experimentalists use tritiated water as the conservative tracer, and because water is neutrally charged, anion exclusion has been observed for anions such as pertechnetate (Gee and

Campbell 1980). Tritiated water was not used in the flow-through tests described in this report because of new health and safety restrictions that designate tritium as a "hard to detect" radionuclide that requires extra (i.e., costly) laboratory protocols to be performed when using tritium. Such protocols were not required in 1980.

Although desorption K_d values for contaminants often are greater than adsorption K_d values, referred to as some element of irreversible sorption (see EPA 1999 and Um et al. 2004), the desorption batch data for all four contaminants studied may have been affected by a long hiatus between the end of the adsorption portion and the start of the desorption portion of the batch tests. These desorption data may be skewed towards higher K_d values. As noted in EPA [1999], the batch K_d methodology is not well suited for measuring K_d values for low-to-non-sorbing species; thus, even though the reported batch desorption K_d values in Table 5.1, especially for Tc and I, are not wholly inconsistent with the flow-through column K_d results, we do not recommend using the batch K_d adsorption or desorption data, except for sensitivity analyses.

The results from the flow-through column experiments described in this report should be considered for use in the next IDF PA. Table 5.2 summarizes these K_d values and compares and contrasts them with the last IDF-specific K_d values found in Krupka et al. (2004). The key differences in the new IDF-specific sediment K_d values (shown in red type) for Tc are that we now believe that there is very slight TcO_4^- sorption (K_d values ~0.00 to 0.01 mL/g) onto sediments contacting young and moderately aged (high and moderately alkaline pH, respectively) cementitious waste leachates. We also found non-zero K_d values (0.02 to 0.04 mL/g) for CrO_4^{2-} in cementitious waste leachates and vadose zone pore water contacting the IDF sand sediment. The current work was the first study using a simulated cementitious waste leachate spiked separately with iodide and iodate, and it appears that there is slight adsorption of IO_3^- from all three simulated solutions (vadose zone pore water, glass leachate, and cementitious waste leachate) onto the IDF-site specific sand. The only past iodine sorption tests using IDF site-specific sediments used iodide spiked into a glass leachate simulant that is no longer a preferred recipe. Table 5.3 shows which simulant sorption results are considered the best estimated K_d values for each of the Krupka et al. (2004) spatial/temporal zones along with some comments.

The iodine K_d values for cementitious near-field environments (zone 1b young, moderate, and aged cementitious waste reported in Krupka et al. [2004]) were taken from literature for sorption of iodide and iodate onto disaggregated cement paste and not sediments. It appears that cement has much higher sorption tendencies than IDF sediments and thus K_d values reported for zone 1b in Krupka et al. (2004) are not relevant for IDF sediments. The K_d values for zone 1b reported in Krupka et al. (2004) would be relevant for rubblized cement waste forms but not the backfill and Hanford formation sediments surrounding the weathered cementitious waste forms.

The recent tabulations of IDF sediment-specific recommend K_d values found in Last et al. (2006) (shown in Table 2.10) and Cantrell et al. (2007) (shown in Table 2.11) are generally consistent with the conservative, best estimate, and lower range of the new best estimate K_d values reported in Table 5.2. The new best estimate K_d value for iodide is 0 mL/g and the new best estimate K_d value for iodate ranges from 0.04 mL/g for sand-dominated sediments, regardless of whether leachates dominate the pore water chemistry. A value of 0.004 mL/g is arbitrarily chosen for the iodate K_d value in gravel-dominated sediments. The new range for iodide (0 to 0.04 mL/g) and iodate (0 to 0.3 mL/g) K_d values for IDF sand-dominated sediments has been reduced from 0 to 15 mL/g because none of the current work suggested iodine species adsorb to the IDF sand-dominated sediment with such a wide range.

It is uncertain which iodine species will dominate in actual ILAW glass or cementitious waste form leachates in the IDF disposal environment. As mentioned, thermodynamics (see Figure 4.20) predicts that iodide should dominate in the IDF subsurface. However, recent iodine speciation measurements on groundwaters in ^{129}I plumes suggest iodate predominates (Xu et al. 2014). We speculate that there might be a kinetic hindrance for iodate conversion to iodide in the highly oxidizing, hot nitric acid dissolved spent fuel waste stream that is the dominant source of ^{129}I in Hanford groundwater. Any iodine found in ILAW glass leachates and cementitious waste leachate emanating from IDF buried wastes likely will not originate as a highly oxidizing, hot nitric acid dissolved spent fuel waste stream, and thus the thermodynamically predicted iodide might prevail. Further, it is not apparent that using a "best estimate" K_d value of 0 or 0.04 mL/g for all iodine species in IDF subsurface pore waters will yield different groundwater risk predictions.

Table 5.2. New Technetium, Iodine, and Chromium K_d Values (red text) Compared to Krupka et al. (2004) by Spatial Zone

Geochemical Zone	Technetium			Iodine (as both I^- and IO_3^-)			Chromium (VI)		
	Conserv. K_d (mL/g)	Best Estimate K_d (mL/g)	K_d Range (mL/g)	Conserv. K_d (mL/g)	Best Estimate K_d (mL/g)	K_d Range (mL/g)	Conserv. K_d (mL/g)	Best Estimate K_d (mL/g)	K_d Range (mL/g)
Zone 1a – Near Field / Vitrified Waste	0 **0**	0 **0**	0 to 1 **0 to 0.02**	0.04 **0 (both)**	0.1 **0 (I^-)** **0.1 (IO_3^-)**	0.04 to 0.16 **0 to 0.2 (I-)** **0 to 1 (IO_3^-)**	0 **0**	0 **0**	0 to 1 **0 to 2**
Zone 1b – Near Field / Cementitious Waste (Young)	0 **0**	0 **0.01**	0 to 2 **0 to 0.04**	10 **0 (both)**	20 **0 (I^-)** **0.01 (IO_3^-)**	10 to 150 **0 to 0.04 (I-)** **0 to 0.3 (IO_3^-)**	0 **0**	0 **0.04**	0 to 2 **0 to 0.6**
Zone 1b – Near Field / Cementitious Waste (Mod. Aged)	0 **0**	0 **0.005**	0 to 2 **0 to 0.04**	5 **0 (both)**	8 **0 (I^-)** **0.01 (IO_3^-)**	5 to 15 **0 to 0.04 (I-)** **0 to 0.3 (IO_3^-)**	0 **0**	0 **0.02**	0 to 2 **0 to 0.6**
Zone 1b – Near Field / Cementitious Waste (Aged)	0 **0**	0 **0**	0 to 1 **0 to 0.02**	1 **0 (both)**	2 **0 (I^-)** **0.04 (IO_3^-)**	1 to 5 **0 to 0.04 (I-)** **0 to 0.3 (IO_3^-)**	0 **0**	0 **0.02**	0 to 1 **0 to 0.6**
Zone 2a – Chemically Impacted Far Field in Sand Sequence	0 **0**	0 **0**	0 to 0.1 **0 to 0.02**	0 **0 (both)**	0.1 **0 (I^-)** **0.04 (IO_3^-)**	0 to 0.2 **0 to 0.04 (I-)** **0 to 0.3 (IO_3^-)**	0 **0**	0 **0.02**	0 to 0.1 **0 to 0.6**
Zone 2b – Far Field in Sand Sequence (no impact from wastes)	0 **0**	0 **0**	0 to 0.6 **0 to 0.02**	0 **0 (both)**	0.25 **0 (I^-)** **0.04 (IO_3^-)**	0.0 to 15 **0 to 0.04 (I-)** **0 to 0.3 (IO_3^-)**	0 **0**	0 **0.02**	0 to 0.6 **0 to 0.6**
Zone 3a – Chemically Impacted Far Field in Gravel Sequence[(a)]	0 **0**	0 **0**	0 to 0.01 **0 to 0.01**	0 **0 (both)**	0 **0 (I^-)** **0.004 (IO_3^-)**	0 to 0.02 **0 to 0.004 (I-)** **0 to 0.03 (IO_3^-)**	0 **0**	0 **0.002**	0 to 0.01 **0 to 0.006**
Zone 3b and 4 – Far Field in Gravel Sequence[(a)]	0 **0**	0 **0**	0 to 0.06 **0 to 0.01**	0 **0 (both)**	0.02 **0 (I^-)** **0.004 (IO_3^-)**	0 to 1.5 **0 to 0.004 (I-)** **0 to 0.03 (IO_3^-)**	0 **0**	0 **0.002**	0 to 0.06 **0 to 0.006**
Zone 5 – Unconfined Far Field Aquifer	0 **0**	0 **0**	0 to 0.6 **0 to 0.1**	0 **0 (both)**	0.25 **0 (I^-)** **0.04 (IO_3^-)**	0.0 to 15 **0 to 0.04 (I-)** **0 to 0.3 (IO_3^-)**	0 **0**	0 **0**	0 to 0.6 **0 to 0.6**

(a) Corrected for gravel content.
(b) Red type are new K_d values based on lab tests described herein.

Table 5.3. Cross Walk Between Krupka et al. (2004) Spatial/Temporal Zones and Simulant Sorption Data in Current Work

Spatial/Temporal Zone from Krupka et al. (2004)	Simulated Leachate Sorption Data (this report)	Comments
Zone 1a – Near Field / Vitrified Waste	Glass Leachate Sorption Results	New glass leachate simulant moderate pH at all times
Zone 1b – Near Field / Cementitious Waste (Young)	Cast Stone Leachate Sorption Results	pH above 10
Zone 1b – Near Field / Cementitious Waste (Mod. Aged)	Cast Stone Leachate Sorption Results	pH ~10 down to 8.5; there is so little sorption from young cement assume new data for Cast Stone leachate covers this category too
Zone 1b – Near Field / Cementitious Waste (Aged)	Vadose Zone Pore Water Sorption Results	pH 7 to 8.5; there is so little sorption from Cast Stone leachate assume that VZ pore water data is appropriate for this category
Zone 2a – Chemically Impacted Far Field in Sand Sequence	Combination of Glass Leachate and Cast Stone Leachate Sorption Results	Somewhat arbitrary; need to consider % of impacted pore water coming from glass vs. grouts leachates when disposal details become available
Zone 2b – Far Field in Sand Sequence (no impact from wastes)	Vadose Zone Pore Water Sorption Results	VZ pore water is proper choice for this zone
Zone 3a – Chemically Impacted Far Field in Gravel Sequence[(a)]	1/10th Combination of Glass Leachate and Cast Stone Leachate Sorption Results	Arbitrary use of 10%; same as past recommendations
Zone 3b and 4 – Far Field in Gravel Sequence	1/10th Vadose Zone Pore Water Sorption Results	Arbitrary use of 10%; same as past recommendations
Zone 5 – Unconfined Far Field Aquifer	Vadose Zone Pore Water Sorption Results	We did not use any IDF aquifer sediments or groundwater simulants in this new work. Arbitrary decision to use vadose zone pore water results except for best estimate CrO_4^{2-}, which was set to 0 mL/g. Effectively we are reducing best estimate K_d for iodine species and range of K_d values compared to Krupka et al. 2004.

6.0 References

Bacon DH and BP McGrail. 2005. *Waste Form Release Calculations for the 2005 Integrated Disposal Facility Performance Assessment*. PNNL-15198, Pacific Northwest National Laboratory, Richland, Washington.

Brown CF, KN Geiszler, and TS Vickerman. 2005. "Extraction and Quantitative Analysis of Iodine in Solid and Solution Matrixes." *Analytical Chemistry* 77(21):7062-7066. doi:10.1021/ac050972v.

Brown CF, KN Geiszler, and MJ Lindberg. 2007. "Analysis of ^{129}I in Groundwater Samples: Direct and Quantitative Results below the Drinking Water Standard." *Applied Geochemistry* 22(3):648-655. doi:10.1016/j.apgeochem.2006.12.010.

Cantrell KJ, RJ Serne, and GV Last. 2003. *Hanford Contaminant Distribution Coefficient Database and Users Guide*. PNNL-13895, Rev. 1, Pacific Northwest National Laboratory, Richland, Washington.

Cantrell KJ, JM Zachara, PE Dresel, KM Krupka and RJ Serne. 2007. *Geochemical Processes Data Package for the Vadose Zone in the Single-Shell Tank Waste Management Areas at the Hanford Site*. PNNL-16663, Pacific Northwest National Laboratory, Richland, Washington.

Cantrell KJ, CF Brown, RJ Serne, and KM Krupka. 2008. *Geochemical Characterization Data Package for the Vadose Zone in the Single-Shell Tank Waste Management Areas at the Hanford Site*. PNNL-17154, Pacific Northwest National Laboratory, Richland, Washington.

DOE O 435.1. 2001. *Radioactive Waste Management*. DOE O 435.1, Approved 7-09-99, Review 7-9-01, U.S. Department of Energy, Washington, D.C.

DOE M 435.1-1. 2007. *Radioactive Waste Management Manual*. DOE M 435.1-1, Change 1: 6-19-01; Certified 1-9-07, U.S. Department of Energy, Washington, D.C.

DOE. 2012. *Final Tank Closure and Waste Management Environmental Impact Statement for the Hanford Site, Richland, Washington*. DOE/EIS-0391, U.S. Department of Energy, Richland, Washington.

EPA. 1999. *Understanding Variation in Partition Coefficient, Kd, Values: Volume I. The Kd Model, Methods of Measurement, and Application of Chemical Reaction Codes*. EPA 402-R-99-004A, U.S. Environmental Protection Agency, Washington, D.C. Prepared by KM Krupka, DI Kaplan, G Whelan, RJ Serne, and SV Mattigod at Pacific Northwest National Laboratory, Richland, Washington.

EPA. 2007. EPA-846: Test Method 6010C, Revision 3: *Inductively Coupled Plasma-Atomic Emission Spectrometry*. U.S. Environmental Protection Agency, Washington, D.C.

Gee GW and AC Campbell. 1980. *Monitoring and Physical Characterization of Unsaturated Zone Transport---Laboratory Analysis*. PNL-3304, Pacific Northwest Laboratory, Richland, Washington.

Horton DG, HT Schaef, RJ Serne, CF Brown, MM Valenta, TS Vickerman, IV Kutnyakov, SR Baum, KN Geiszler, and KE Parker. 2003. *Geochemistry of Samples from Borehole C3177 (299-E24-21)*. PNNL-14289, Pacific Northwest National Laboratory, Richland, Washington.

Hua B, B Deng, EC Thornton, J Yang, and JE Amonette. 2006. "Incorporation of Chromate into Calcium Carbonate Structure During Coprecipitation." *Water, Air, and Soil Pollution* 179(1-4):381-390. doi:10.1007/s11270-006-9242-7.

Kaplan DI and RJ Serne. 1995. *Distribution Coefficient Values Describing Iodine, Neptunium, Selenium, Technetium, and Uranium Sorption to Hanford Sediments*. PNL-10379, SUP.1, Pacific Northwest Laboratory, Richland, Washington.

Kaplan, DI, RJ Serne, AT Owen, J Conca, TW Wietsma, and TL Gervais. 1996. *Radionuclide Adsorption Distribution Coefficients Measured in Hanford Sediments for the Low Level Waste Performance Assessment Project.* PNNL-11485, Pacific Northwest National Laboratory, Richland, Washington.

Kaplan DI, KE Parker, and RD Orr. 1998a. *Effects of high pH and high Ionic Strength Groundwater on Iodide, Pertechnetate, and Selenite Sorption to Hanford Sediments: Final Report for Subtask 3a*. PNNL-11964, Pacific Northwest National Laboratory, Richland, Washington.

Kaplan DI, KE Parker, and IV Kutnyakov. 1998b. *Radionuclide Distribution Coefficients for Sediments Collected from Borehole 299-E17-21: Final Report for Subtask 1a*. PNNL-11966, Pacific Northwest National Laboratory, Richland, Washington.

Kaplan DI and RJ Serne. 2000. *Geochemical Data Package for the Hanford Immobilized Low-Activity Tank Waste Performance Assessment (ILAW PA)*. PNNL-13037, Rev. 1, Pacific Northwest National Laboratory, Richland, Washington.

Kaplan DI, RJ Serne, HT Shaef, CW Lindenmeier, KE Parker, AT Owen, DE McCready, and JS Young. 2003. *The Influence of Glass Leachate on the Hydraulic, Physical, Mineralogical and Sorptive Properties of Hanford Sediment*. PNNL-14325, Pacific Northwest National Laboratory, Richland, Washington.

Khaleel R. 1999. *Far-Field Hydrology Data Package for Immobilized Low Activity Tank Waste Performance Assessment*. HNF-4769, Rev. 1, Fluor Daniel Northwest, Inc., Richland, Washington.

Khaleel R. 2004. *Far-Field Hydrology Data Package for Integrated Disposal Facility Performance Assessment*. RPP-20621, Rev. 0, CH2M Hill Hanford Group, Richland, Washington.

Krupka KM, RJ Serne, and DI Kaplan. 2004. *Geochemical Data Package for the 2005 Hanford Integrated Disposal Facility Performance Assessment*. PNNL-13037, Rev. 2, Pacific Northwest National Laboratory, Richland, Washington.

Langton CA. 1988. "Challenging Applications for Hydrated and Chemical Reacted Ceramics." DP-MS-88-163, presentation given at American Ceramic Society Meeting, Sydney, Australia, July 12, 1988.

Last GV, EJ Freeman, KJ Cantrell, MJ Fayer, GW Gee, WE Nichols, BN Bjornstad, and DG Horton. 2006. *Vadose Zone Hydrogeology Data Package for Hanford Assessments*. PNNL-14702, Rev. 1, Pacific Northwest National Laboratory, Richland, Washington.

Mann FM, CR Eiholzer, AH Lu, PD Rittmann, NW Kline, Y Chen, and BP McGrail. 1998. *Hanford Low-Activity Tank Waste Performance Assessment*. DOE/RL-97-69, Rev. 0, U.S. Department of Energy, Richland, Washington.

Mann FM, KC Burgard, WR Root, RJ Puigh, SH Finfrock, R Khaleel, DH Bacon, EJ Freeman, BP McGrail, SK Wurstner, and PE LaMont. 2001. *Hanford Immobilized Low-Activity Waste Performance Assessment: 2001 Version*. DOE/ORP-2000-24, Rev. 0, Office of River Protection, U.S. Department of Energy, Richland, Washington.

Mann FM, RJ Puigh, SH Finfrock, R Khaleel, and MI Wood. 2003a. *Integrated Disposal Facility Risk Assessment*. RPP-15834, Rev. 0, CH2M Hill Hanford Group, Inc., Richland, Washington.

Mann FM, RJ Puigh, R Khaleel, S Finfrock, BP McGrail, DH Bacon, and RJ Serne. 2003b. *Risk Assessment Supporting the Decision on the Initial Selection of Supplemental ILAW Technologies*. RPP-17675, Rev. 0, CH2M Hill Hanford Group, Inc., Richland, Washington.

Meyer PD and RJ Serne. 1999. *Near Field Hydrology Data Package for the Immobilized Low-Activity Waste 2001 Performance Assessment*. PNNL-13035, Pacific Northwest National Laboratory, Richland, Washington.

NQA-1-2000, *Quality Assurance Requirements for Nuclear Facility Applications.* American Society Mechanical Engineers, New York, New York.

NQA-1-2008, Quality Assurance Requirements for Nuclear Facility Applications. American Society Mechanical Engineers, New York, New York.

NQA-1a-2009, *Addenda to ASME NQA-1-2008 Quality Assurance Requirements for Nuclear Facility Applications*. American Society Mechanical Engineers, New York, New York.

Parker JC and MT van Genuchten. 1984. Determining Transport Parameters From Laboratory And Field Tracer Experiments. *Virginia Agricultural Experiment Station Bulletin*, 1-96.

Qafoku NP, CC Ainsworth, JE Szecsody, and OS Qafoku. 2003. "Effect of Coupled Dissolution and Redox Reactions on $Cr(VI)_{aq}$ Attenuation during Transport in the Sediments under Hyperalkaline Conditions." *Environ Science and Technology* 37:3640-3646.

Qafoku NP, CC Ainsworth, JE Szecsody, and OS Qafoku. 2004. "Transport-controlled kinetics of dissolution and precipitation in the sediment under alkaline and saline conditions." *Geochemica et Cosmochimica Acta* 68(14):2981-2995.

Qafoku NP, PE Dresel, JP McKinley, C Liu, SM Heald, CC Ainsworth, JL Philips, and JS Fruchter. 2009. "Pathways of Aqueous Cr(VI) Attenuation in a Slightly Alkaline Oxic Subsurface." *Environ. Sci. Technol*. 2009, 43:1071-1077.

Reidel SP, KD Reynolds, and DG Horton. 1998. *Immobilized Low-Activity Waste Site Borehole 299-E17-21*. PNNL-11957, Pacific Northwest National Laboratory, Richland, Washington.

Reidel SP, DG Horton, and MM Valenta. 2001. *Geologic and Wireline Borehole Summary from the Second ILAW Borehole (299-E24-21)*. PNNL-13652, Pacific Northwest National Laboratory, Richland, Washington.

Reidel SP. 2005. *Geologic Data Package for 2005 Integrated Disposal Facility Performance Assessment*. PNNL-14586, Rev. 1, Pacific Northwest National Laboratory, Richland, Washington.

Relyea JF, RJ Serne, and D Rai. 1980. *Methods for Determining Radionuclide Retardation Factors: Status Report*. PNL-3349, Pacific Northwest Laboratory, Richland, Washington.

Serne RJ, JH Westsik, Jr, BD Williams, HB Jung, and G Wang. 2015. *Extended Leach Testing of Simulated LAW Cast Stone Monoliths.* PNNL-24297, Pacific Northwest National Laboratory, Richland, Washington.

Serne RJ, WJ Martin, RO Lokken, VL LeGore, CW Lindenmeier, and PFC Martin. 1989. *Leach and EP Toxicity Tests on Grouted Waste From Tank 106-AN*. PNL-6960, Pacific Northwest Laboratory, Richland, Washington.

Stumm W and JJ Morgan. 1981. *Aquatic Chemistry: An Introduction Emphasizing Chemical Equilibria in Natural Waters*. Wiley, New York.

Tang Y, EJ Elzinga, Y Jae Lee, and RJ Reeder. 2007. "Coprecipitation of chromate with calcite: Batch experiments and X-ray absorption spectroscopy." *Geochimica et Cosmochimica Acta* 71(6):1480-1493. doi:10.1016/j.gca.2006.12.010.

Toride N, FJ Leij, and MT van Genuchten. 1999. The CXTFIT Code for Estimating Transport Parameters from Laboratory or Field Tracer Experiments. U.S. Salinity Laboratory, U.S. Department of Agriculture, Riverside, California.

Um W and RJ Serne. 2005. "Sorption and Transport Behavior of Radionuclides in the Proposed Low-Level Radioactive Waste Facility at the Hanford Site, Washington." *Radiochimica Acta* 93:57-63.

Um W, RJ Serne, and KM Krupka. 2004. "Linearity and Reversibility of Iodide Adsorption on Sediments from Hanford, Washington Under Water Saturated Conditions." *Water Research* 38(8):2009-2016.

Um W, RJ Serne, and KM Krupka. 2007. "Surface Complexation Modeling of U(VI) Sorption to Hanford Sediment with Varying Geochemical Conditions." *Environ. Sci. Technol*. 2007, 41:3587-3592.

Van Genuchten MT and PJ Wierenga. 1976. "Mass transfer studies in sorbing porous media: I. Analytical solutions." *Soil Sci. Soc. Am.* 40:473.

Westsik JH and RJ Serne. 2012. *Secondary Waste Cast Stone Waste Form Qualification Testing Plan*. PNNL-21656, Rev. 1, Pacific Northwest National Laboratory, Richland, Washington.

Xu C, DI Kaplan, S Zhang, M Athon, YF Ho, YF Ho, HP Li, CM Yeager, KA Schwehr, R Grandbois, D Wellman, and PH Santschi. 2014. "Radioiodine sorption/desorption and speciation transformation by subsurface sediments from the Hanford Site." *Journal of Environmental Radioactivity* 139:43-55.

Yabusaki SB, RJ Serne, ML Rockhold, G Wang, and JH Westsik, Jr. 2015. *Technical Approach for Determining Key Parameters Needed for Modeling the Performance of Cast Stone for the Integrated Disposal Facility Performance Assessment*. PNNL-24022, Pacific Northwest National Laboratory, Richland, Washington.

Zachara JM, GE Brown, Jr., CC Ainsworth, S Traina, JP McKinley, J Catalano, O Qafoku, JE Szecsody, and SC Smith. 2003. "Chromium speciation and mobility in a high level nuclear waste plume." *Geochim. Cosmochim. Acta* 68(1):13-30.

Zhang S, C Xu, D Creeley, YF Ho, HP Li, R Grandbois, KA Schwehr, DI Kaplan, CM Yeager, D Wellman, and PH Santschi. 2013. "Iodine-129 and iodine-127 speciation in groundwater at the Hanford site, US: iodate incorporation into calcite." *Environ Sci Technol* 47(17):9635-42. doi:10.1021/es401816e.

Distribution*

OFFSITE

Energy Solutions
I Joseph

Intera
R Andrews

Oak Ridge National Laboratory
EM Pierce

Savannah River National Laboratory
AD Cozzi
KM Fox
DI Kaplan
CA Langton
DJ McCabe

U.S. Department of Energy
Office of River Protection
AA Kruger
GL Pyles

Vitreous State Laboratory
H Gan
W Kot
I Muller
IL Pegg

Washington River Protection Solutions
EE Brown
PA Cavanah
SE Kelly
KP Lee (AREVA)
WG Ramsey
KH Subramanian
DJ Swanberg
LE Thompson
WRPS Documents – TOCVND@rl.gov

ONSITE

Pacific Northwest National Laboratory

DH Bacon
VL Freedman
GV Last
II Leavy
J Neeway
NP Qafoku
ML Rockhold
RJ Serne
GL Smith
MMV Snyder
JE Stephenson
CE Strickland
W Um
JH Westsik, Jr.

*All distribution will be made electronically.

Pacific Northwest
NATIONAL LABORATORY

Proudly Operated by **Battelle** *Since 1965*

U.S. DEPARTMENT OF
ENERGY

902 Battelle Boulevard
P.O. Box 999
Richland, WA 99352
1-888-375-PNNL (7665)

www.pnnl.gov